Alma Mater Studiorum – Università di Bologna

DOTTORATO DI RICERCA IN

Scienze Ambientali: Tutela e Gestione Delle Risorse Naturali

Ciclo XXVI

Settore Concorsuale di afferenza: 03/A1 – CHIMICA ANALITICA

Settore Scientifico disciplinare: CHIM/12 - CHIMICA DELL'AMBIENTE E DEI BENI CULTURALI

TITOLO TESI

CHEMISTRY OF AEROSOL PARTICLES AND FOG DROPLETS DURING FALL - WINTER SEASON IN THE PO VALLEY

Presentata da: Dott.ssa Lara Giulianelli

Coordinatore Dottorato

Prof. Enrico Dinelli

Tutore

Prof. Emilio Tagliavini

Relatore

Dott.ssa M. Cristina Facchini

Esame finale anno 2014

Summary

Abstract

Air quality represents a key issue in the so-called pollution “hot spots”: environments in which anthropogenic sources are concentrated and dispersion of pollutants is limited. One of these environments, the Po Valley, normally experiences exceedances of PM10 and PM2.5 concentration limits, especially in winter when the ventilation of the lower layers of the atmosphere is reduced.

This thesis provides a highlight of the chemical properties of particulate matter and fog droplets in the Po Valley during the cold season, when fog occurrence is very frequent. Fog-particles interactions were investigated with the aim to determine their impact on the regional air quality.

Size-segregated aerosol samples were collected in Bologna, urban site, and San Pietro Capofiume (SPC), rural site, during two campaigns (November 2011; February 2013) in the frame of Supersito project. The comparison between particles size-distribution and chemical composition in both sites showed the relevant contribution of the regional background and secondary processes in determining the Po Valley aerosol concentration.

Occurrence of fog in November 2011 campaign in SPC allowed to investigate the role of fog formation and fog chemistry in the formation, processing and deposition of PM10. Nucleation scavenging was investigated with relation to the size and the chemical composition of particles. We found that PM1 concentration is reduced up to 60% because of fog scavenging. Furthermore, aqueous-phase secondary aerosol formation mechanisms were investigated through time-resolved measurements.

In SPC fog samples have been systematically collected and analysed since the nineties; a 20 years long database has been assembled. This thesis reports for the first time the results of this long time series of measurements, showing a decrease of sulphate and nitrate concentration and an increase of pH that reached values close to neutrality. A detailed discussion about the occurred changes in fog water composition over two decades is presented.

Papers on the international refereed literature originating from this thesis:

- Gilardoni, S., Massoli, P., Giulianelli, L., Rinaldi, M., Paglione, M., Pollini, F., Lanconelli, C., Poluzzi, V., Carbone, S., Hillamo, R., Russell, L. M., Facchini, M. C. and Fuzzi, S. (2014). Fog Scavenging of Organic and Inorganic Aerosol in the Po Valley. *Atmospheric Chemistry and Physics Discussion* 14, 4787-4826.

- Giulianelli L., Tarozzi L., Gilardoni S., Rinaldi M., Decesari S., Carbone C., Facchini M.C., Fuzzi S. Fog occurrence and chemical composition in the Po Valley over the last twenty years (to be submitted).

1. Introduction

Air pollution represents a real threat to human health in Europe. Air quality is a key issue of the European environmental policy to guarantee a sufficient level of protection against air pollutants, such as particulate matter, whose harmful effect has been reported in numerous recent studies (Brunekreef, 2013; Fuzzi and Gilardoni, 2013).

This doctoral thesis set the objective to highlight the properties of particulate matter and fog droplets in fall and winter in the Po Valley, where fog occurrence is very frequent during the cold season. The interactions between particles and fog droplets will be also investigated with the aim to determine their impact on the air quality of this region.

The following sections will introduce the general definitions of aerosol particles and fog droplets as well as a brief illustration of their physical and chemical properties. Sections 1.4 and 1.5 will describe the specific field of this study and its principal purposes.

1.1 Tropospheric aerosol

An aerosol is properly defined as a suspension of fine solid or liquid particles in a gas, even though in atmospheric science common usage refers to the aerosol as the solid or deliquesced (concentrated liquid) particulate component only, while specific terms are used for the liquid or ice particles in fogs and clouds (droplets, drops, crystals, hydrometeors etc.) (Seinfeld and Pandis, 1998).

Atmospheric aerosol particles consist of a large variety of species, arising from natural sources such as volcanoes, sea spray, plant evapotranspiration or soil erosion and from anthropogenic activities like agricultural practises, industrial and combustion processes.

Particulate matter can be classified also as primary and secondary aerosol. Primary particles are directly emitted into the atmosphere, from sources such as incomplete combustion of fossil fuels, biomass burning, mechanical erosion of dry soils, resuspension of particles by vehicular traffic, sea spray, volcanic eruptions and biological debris (pollen, spores, plant fragments, etc.). By contrast, secondary particles are formed in the atmosphere by the

transformation of reactive gases into particulate matter through chemical reactions and condensation processes (gas-to-particle conversion).

Particles are removed from the atmosphere by gravitational settling and diffusion to Earth surfaces (dry deposition) and by incorporation of particles into cloud droplets during the formation of precipitation (wet deposition). These removal mechanisms lead to relatively short residence times of aerosol particles in the troposphere, ranging from a few hours to a couple of weeks. Due to their short residence times and to the non-homogeneous distribution of the sources, tropospheric aerosols composition and concentration are temporally and spatially highly variable.

1.1.1 Aerosol size distribution

The aerodynamic diameter (D_a) is usually used in order to classify particles according to their size. It is defined as the diameter of a spherical particle with density = 1 g cm^{-3} having the same gravitational settling velocity as the particle in question.

The atmospheric aerosol particles size distribution ranges from a few nanometres to about a hundred micrometres, even if particles with aerodynamic diameters smaller than 10 μm account for most of the total aerosol particles (on both number and mass basis). The atmospheric aerosol size distribution is characterized by modes, corresponding to different populations of particles, classified as nucleation (D_a < 0.01 μm), Aitken mode (0.01 μm < D_a < 0.1 μm); accumulation (0. 1 μm < D_a < 1 μm) and coarse mode (D_a > 1 μm) (Fig.1.1). The first three modes, that is particles with D_a < 1 μm, are also referred to as fine aerosol.

A fundamental distinction between fine and coarse aerosol has to be found in the source mechanisms of particles production. For this reason, the experimental work of this thesis is discussed separating particles according to their size.

Coarse particles are formed mainly by mechanical processes such as dust suspension and resuspension, and sea spray. They never account for more than a few percent of the particles by number concentration, even if they can account for a large fraction of particulate mass.

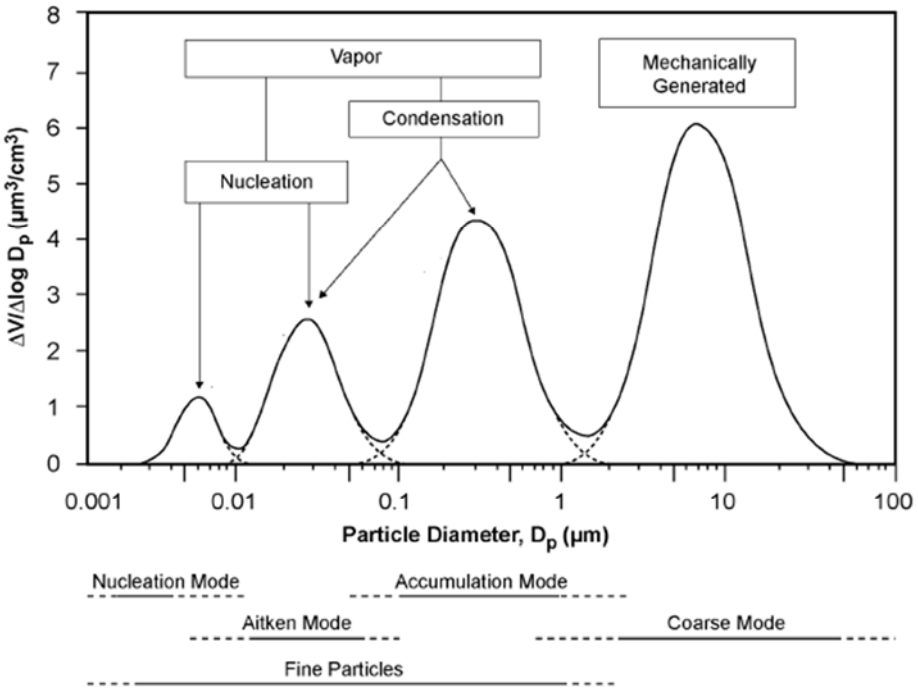

Figure 1.1: ideal size distribution with their four principal modes. The diagram also shows the main mechanisms of formation of particles acting in the various size ranges.

Fine particles are mainly produced by combustion processes (open burning, vehicular emissions, etc.) and by secondary processes such as gas-to-particle conversion mechanisms. More in detail, the nucleation mode arises from nucleation of new particles from rapid gas condensation, the Aitken mode results from condensation of vapours onto nucleation mode particles and from their coagulation, as well as from primary combustion emissions. Finally, the accumulation mode particles usually form from prolonged (several hours to days) condensation of vapours on Aitken particles and from the formation of particles by chemical reactions in non-precipitating cloud droplets.

1.1.2 Aerosol sources and chemical composition

Due to the relative low residence time in atmosphere, tropospheric aerosol exhibits a chemical composition characterized by a great spatial and temporal variability, reflecting the variety of

sources, transformation, and removal processes. That is why the chemical composition of tropospheric aerosol is usually referred to a specific environment and size interval.

In general, aerosol particles consist of complex mixtures of inorganic water-soluble salts such as sulphates, nitrates, ammonium salts and sea salt, soluble and insoluble carbonaceous material (organic species, black carbon, carbonates) and insoluble inorganic compounds including mineral soil particles and combustion ash.

The submicron inorganic mass fraction is prevalently composed by species derived from gas-to-particle conversion processes, as in the case of sulphate, produced in the atmosphere by the oxidation of sulphur dioxide (SO_2). Sulphuric acid (H_2SO_4) produced by the oxidation of SO_2 can further react with ammonia (NH_3) to produce ammonium bisulphate (NH_4HSO_4) and ammonium sulphate $(NH_4)_2SO_4$ (Hazi et al., 2003).

Similarly, nitrogen oxides (NO_x) are oxidized in the atmosphere to nitric acid (HNO_3) which can form both non-volatile and semivolatile salts in the aerosol phase. Most common semivolatile nitrate salts, such as NH_4NO_3, exist in the troposphere in a dynamic equilibrium with the gas phase precursors and the actual partitioning between the gas and the aerosol phases can change continuously following the diurnal cycle of temperature and relative humidity. Since the fine fraction of the aerosol is more rich in acidic species (e.g., ammonium bisulfate) than the coarse fraction where conversely alkaline species may occur (sea salt, calcium carbonate), nitric acid often partitions efficiently into coarse particles.

Organic compounds are produced by both anthropogenic and natural sources (Fuzzi, et al., 2006) and represent a relevant fraction of atmospheric fine particles, accounting for 20-90% of aerosol mass in the lower troposphere (Kanakidou et al., 2005). In the fine fraction, organic aerosol originates either from primary emissions due to combustion processes at high temperature, or from the oxidation of volatile organic compounds (VOC) and gas-to-particle conversion mechanisms (Kroll and Seinfeld, 2008; Zhang et al., 2007). In the coarse fraction, it can result also from biological debris (Jaenicke, 2005).

Black carbon (BC) accounts for insoluble carbonaceous material showing absorbance across all the spectrum of visible light. It overlaps with the so called elemental carbon (EC), characterized by very low hydrogen and oxygen contents, and which is refractory at temperatures below 350 °C. BC in the fine fraction is typically emitted by high-temperature

combustion processes (traffic, open combustion, etc.). In the coarse mode, BC can originate by resuspended dust containing soot.

Sea salt mass is mainly distributed in the coarse fraction and is produced by the mechanical mechanisms at the sea surface (breaking waves and whitecaps) (Blanchard, 1983).

Mineral dust is produced by natural weathering processes, and is enriched in the coarse aerosol mode.

1.2 Fog

Fog is physically a cloud that forms close to the ground or in contact with it and is associated with visibility lower than 1km. Fogs are classified according to their formation process. Some continental areas, such as the Po Valley, are usually affected in the cold season by phenomena named “radiation fogs”. This type of fog forms at night under clear sky and stagnant air conditions. Nightly, heat absorbed by the earth during the day is radiated back to space cooling the air close to the surface. In presence of moisture, humidity will soon reach 100% allowing condensation and fog to occur.

Another type of fog is advection fog. It is also the result of condensation, but occurs when warm moist air passes over a cold surface and is cooled down to the dew point. Typical examples are sea fogs that form when warm air drifts over a cool oceanic current. Advection fog may also form when moist maritime air drifts over a cold inland area. Other types of fog are upslope fog, ice fog, evaporation fog, but a detailed description of their characteristics is beyond the purpose if this thesis.

1.2.1 Fog formation

Fog droplets, as well as clouds, are formed in the atmosphere by the condensation of water vapour on aerosol particles when the relative humidity (RH) exceeds 100% and a slight degree of supersaturation (typically $\leq$ 1%) is achieved. Not all particles will grow to real droplets. Particles that enable droplets to form at supersaturation levels found in the atmosphere are called cloud condensation nuclei (CCN).

Condensation of water vapour on aerosol particles is described by the Köhler theory (Köhler, 1936). It is expressed by an equation composed of two terms: one taking into account the influence of the curvature of the droplet, the "Kelvin effect", and the other accounting for the solute effect (Raoult's law). The resulting curves are reported in Fig.1.2.

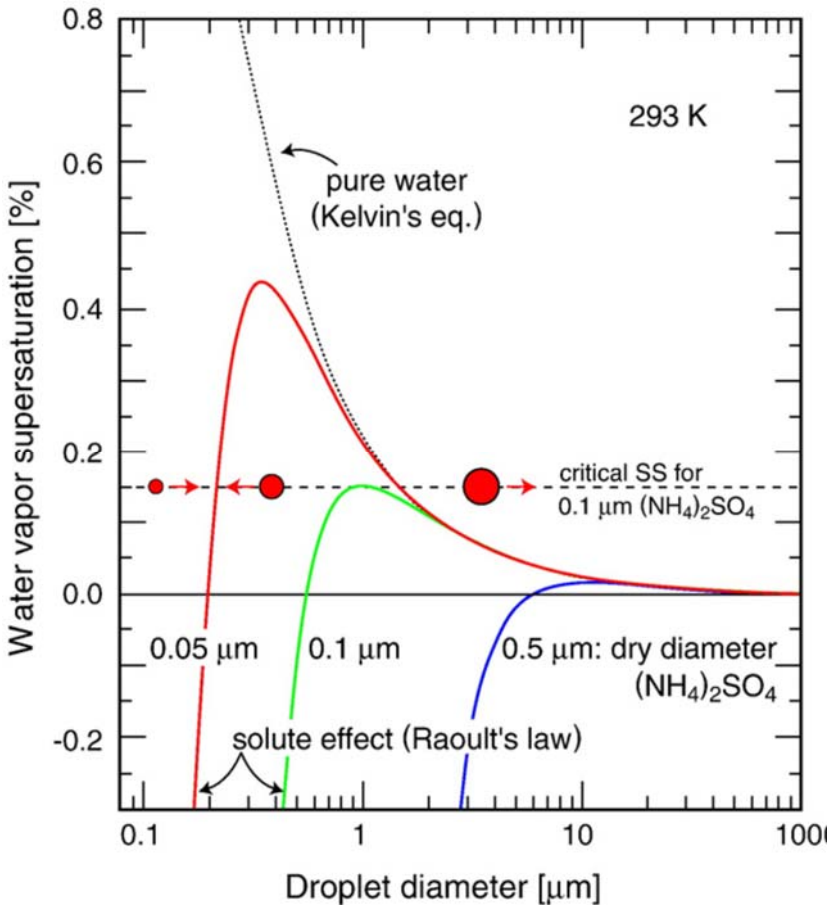

Figure 1.2. Köhler curves showing the equilibrium water vapour supersaturation at 293 K for droplets of pure water (dotted curve) and for droplets containing various masses of dissolved $(NH_4)_2SO_4$ (solid curves) vs. diameter of the droplet (Seinfeld and Pandis, 1998). In the indicated example, an ambient water vapor supersaturation (S) of 0.15% (dashed line) exceeds the critical value for all ammonium sulfate aerosols with dry diameter ≥0.1 µm. These aerosols will therefore activate and grow into cloud droplets, whereas smaller aerosols remain as un-activated haze particles. Droplets below their corresponding equilibrium curve will shrink by evaporation whereas those above will grow by condensation (the indicated droplets correspond, for example, to a dry diameter of 0.05 µm). (From Andreae and Rosenfeld, 2008).

With increasing RH, the particle will absorb water and grow until saturation is reached. If the air becomes enough supersaturated to enable the particle to reach a diameter just beyond the maximum (critical supersaturation), the particle enters a region of instability and grows continuously limited only by the availability of water vapour and by the kinetic of diffusion: the particle has been activated to a real cloud (or fog) droplet. The supersaturation required for aerosol activation depends on the size and the composition of the particle. As a large amount of the supersaturated water vapour concentration is used for the growth of the droplets originated by the first-nucleated particles, the supersaturation level will decrease rapidly unless it is compensated by the cooling rate. Particles which have not yet grown above their critical diameter will then re-evaporate to dimensions where the Raoult effect prevails over the Kelvin term and the aerosol liquid water content is in equilibrium with the ambient RH. The non-activated particles form the so-called "interstitial aerosol". Large sizes and large water solubility correspond to lower critical supersaturations that is a better attitude for the particles to act as CCN. Since ambient aerosols are very often polydisperse with respect to size and composition, nucleation scavenging is a very selective process, and only a fraction of the total number of aerosol particles present in the air is able to serve as CCN (Arends, 1996; Fuzzi, 1994).

1.2.2 Fog chemical composition

The initial composition of fog droplets depends mainly on the nature of the particles that acted as CCN. During the fog lifetime, many concurrent physical and chemical processes take place that will cause change in the fog droplets composition, such as the dissolution of trace gases into droplets, chemical reactions within fog droplets and the capture of interstitial aerosol particles by droplets, although this is expected to be of minor importance (Fuzzi et al., 2002).

Fog chemical composition reflects the chemical properties of the air in which it forms, therefore is highly variable in time and space. In general, the major compounds of fog droplets are soluble inorganic species like sulphate (SO_4^{2-}), nitrate (NO_3^-), chloride (Cl^-), ammonium (NH_4^+), sodium (Na^+), potassium (K^+), magnesium (Mg^{2+}) and calcium (Ca^{2+}). Sodium and chloride are major compounds especially in marine areas, because sea-salt particles are very efficient CCN. Also the presence of K^+, Ca^{2+} and Mg^{2+} ions can originate from marine sources

(Keene et al., 1986), but it mostly depends on the mineral component of aerosol particles originating from soil dust. NH_4^+, NO_3^- and SO_4^{2-} derive both from the incorporation of atmospheric aerosol and from the scavenging of gaseous ammonia (NH_3), nitric acid (HNO_3) and sulphur dioxide (SO_2). H_2SO_4 and HNO_3 produced from the oxidation of SO_2 and NO_x are the dominant strong acids in fog water, while NH_3 is the only alkaline gaseous species in the atmosphere. NH_3 is therefore the main buffering agent of fog acidity. The balance between acid and basic components scavenged from the air or produced within the droplets determines the actual pH of fog water (Fuzzi, 1994). However, since the Henry coefficients of nitric acid and of sulphuric acid are much greater than that of ammonia, alkaline pH are rarely found in fog water, while strong acidic pH values have been recorded in some polluted areas (Fuzzi et al., 1985; Hileman, 1983).

Although inorganic ions account for the major fraction of fog water chemical components, organic matter concentrations are by no means negligible, accounting for up to more than 30% of the total solute mass (Fuzzi et al., 2002). Organic concentrations show a great variability depending on the environment, as shown in Fig.1.3. As expected, the highest values are found in polluted urbanized areas and the lowest in marine fogs. However, organic matter concentrations can be fairly high also at continental rural sites because of the scavenging of biogenic organic particles and gases (Herckes et al., 2013).

It should be noticed that, contrary to the chemistry of fog inorganic constituents is relatively well known, especially in respect to the species involved in the acid-base equilibria, the current knowledge of fog organic components is based on a rather sparse literature (Herckes et al., 2013). In our study, we will present one of the longest measurement record of fog dissolved organic carbon concentrations currently available.

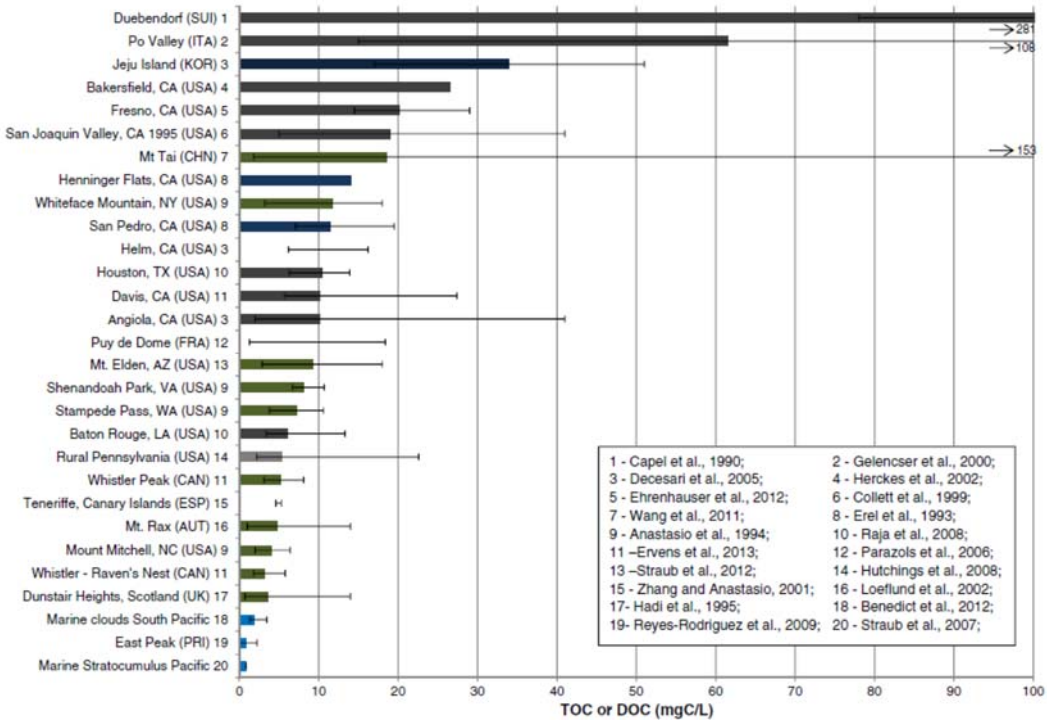

Figure 1.3. Dissolved organic carbon (DOC) mg C/L concentrations reported for fogs and ground based clouds. Bars represent average values, while the error bars represent the range of observations (min–max). Absence of a solid bar means no average/median was provided. Marine clouds and fogs are depicted in blue, hill or mountain intercepted clouds in green (except if heavily marine influenced, then in dark blue), radiation fogs or polluted urban fogs in grey (Herckes et al., 2013).

1.3 Aerosol/clouds interactions

1.3.1 Effects of aerosol on cloud properties

For a given cloud liquid water content and cloud depth, an increase in aerosol particle number concentration (hence in CCN) leads to an increase in cloud droplet number concentration, and a concurrent reduction of droplet diameter, which can cause an increase of cloud albedo. Such effect is generally referred to as first indirect effect of aerosol on climate. The increase in cloud albedo would lead to cooling and partially counteract the warming due to greenhouse gases. A second indirect effect of aerosol particles concerns the increase in clouds lifetime and extent: for a given liquid water content, the increase in cloud droplet number concentration produces smaller droplets, therefore reducing the probability that droplets collide to form precipitating droplets. Since precipitations are hindered, cloud lifetime is prolonged and

clouds are more abundant. Additional feedback mechanisms potentially responsible for the uncertainty in the prediction of the indirect effects, include changes in precipitation regimes and in increases or decreases in cloud cover due to pollution and smoke aerosol (Kaufman and Koren, 2006; Rosenfeld et al., 2008).

This indirect aerosol effect is presently considered the most uncertain of the known forcing mechanisms in the prediction of climate change over the industrial period. Due to the scales involved, it is one of the major challenges in understanding and predicting the indirect radiative effect of aerosols: while the effect itself is global, the processes causing it occur on spatial scales as small as micrometres and temporal scales as short as seconds. Thus, the global-scale phenomenon cannot be understood and predicted quantitatively without adequate understanding of the microscale processes.

1.3.2 Effects of clouds on aerosol composition and lifecycle

Nucleation scavenging is the process by which CCN particles activate to form cloud/fog droplets. Once the droplet are formed, interstitial particles can be incorporated into the droplet by in-cloud scavenging due to Brownian diffusion, inertial impaction and phoretic effects, but their contribution in terms of mass is generally small (Flossmann et al., 1985). By contrast, gas absorption and chemical reactions in the aqueous phase can affect substantially the chemical composition of fog solutes. In-cloud aqueous phase reactions play a major role in the atmospheric cycling of many trace gases. For example, gas phase SO_2 oxidation reactions are much slower than corresponding reactions in the liquid phase (Calvert et al., 1986; Hoffmann, 1986). Eventually, the evaporation of cloud and fog droplets produces aerosol particles with different chemical and physical characteristics compared to the original particles, which acted as CCN for cloud/fog droplets. Such effects are generally referred to as *cloud (or fog) processing*. Since submicron aerosols account for the greatest fraction of CCN number concentrations, most of the material that is produced by aqueous-phase reactions increased fine particle mass (Collett et al., 1993; Fuzzi et al., 1992a; Wobrock et al., 1994).

Since the eighties, many studies investigated the effects of cloud processing on aerosol particles. For example, (Laj et al., 1997) reported a significant increase in sulphate concentration in an aerosol population passing through a cloud. The increase in sulphur (IV)

oxidation was promoted by the radicals produced by peroxides (H_2O_2) dissolved in the cloud droplets. Eventually, the uptake of NH_3 from the gas phase led to evaporating cloud drops forming aerosol particles enriched in ammonium sulphate. Clearly, by modifying the dimension of the particles and the content of soluble inorganic salts, cloud processing can impact the hygroscopic properties of the aerosols, and consequently their CCN efficiency (Hallberg et al., 1992; Svenningsson et al., 1992).

Clouds and fog also determine the residence time of particles in the atmosphere through "wet deposition" processes. It should be noticed that, beside the removal of aerosol particles via incorporation in raindrops, the deposition of fog and low-level cloud droplets to the ground and other surfaces can also occur in the absence of precipitations. This process is often referred to as "occult deposition" (Dollard et al., 1983). Deposition occurs both due to the settling of large droplets and to turbulent impaction on surfaces. This removal mechanism can be relevant in certain areas where the amount of water deposited through cloud water interception was found to be comparable or even larger than the amount deposited by precipitation. This is especially true in the case of forested mountain areas where vegetation is an efficient collector of cloud water. (Waldman and Hoffmann, 1987); (Fuzzi, 1994; Fuzzi et al., 1992a; Fuzzi et al., 1985).

Fogs and clouds cause changes in airborne particle concentrations, with different effects depending on aerosol size distribution. During a fog cycle, big particles are more efficiently scavenged then the smaller ones, and, upon evaporation, their average size is even greater than the original one because of the accretion caused by the sulphates and the other components formed by aqueous phase reactions. Consequently, fog cycles tend to generate bimodal aerosol size distributions by exacerbating the difference in size between the big particles which undergo a progressive growth and the smaller, interstitial particles, left untouched. However, the growth of "droplet mode" particles is limited by the enhanced dry and wet deposition. In fact, depositional losses of aerosol particles are much more effective in the large size fraction of the aerosol distribution (Pandis et al., 1990).

Finally, (Fuzzi et al., 1997a), reported the influence of fog on biological particles. They observed an enrichment of the concentration of bacteria and yeasts in air in foggy conditions compared to clear air conditions: acting as culture media for viable particles, fog droplets represent an atmospheric source of secondary biological aerosol particles. These findings are

relevant for the possibility of transmission of pathogenic airborne microorganisms and also for the possible impact on the atmospheric CCN population (Casareto et al., 1996).

1.4 Fogs in polluted environments

Many studies investigated the effects of aerosol-clouds interactions and the related impacts on the ecosystems and human health (Fowler et al., 2009; Isaksen et al., 2009). This thesis work wants to focus the attention on aerosol interactions with fog droplets, which play a major role in the frame of air quality, being formed close to the Earth's surface.

The interest on fog and aerosol interaction began in the middle of the XX century (Houghton, 1955), but raised in the eighties, after the discovery of the acid fog (Waldman et al., 1982). In those years, the research was mainly focused on fog and cloud acidification, especially in the industrialized northern hemisphere (Barrie, 1985; Hoffmann, 1986; Munger et al., 1983). Many studies investigated the deposition processes of water and the environmental consequences on interception of cloud-borne solutes by vegetation (Fuzzi et al., 1985; Lovett, 1984; Schemenauer, 1986; Waldman et al., 1985). Soon it became clear that fogs are characterized by a much higher solute concentration compared to precipitations, and therefore understanding the chemistry of wet depositions is particularly important in geographical regions characterized by high fog occurrence and high level of pollutants in the atmosphere.

During the nineties, the research was extended to the investigation of aerosol processing by clouds and fog. (Facchini et al., 1999) reported a study regarding the highly polluted environment of the Po Valley (Italy), where they showed how fog can act as an efficient separator for carbonaceous species, with polar water-soluble compounds efficiently scavenged into fog, while water-insoluble carbonaceous species preferentially remain in the interstitial particles.

During the 2000s, the development of modern analytical techniques for trace-level organic compound determination allowed to face the challenging issue of the chemical characterization of organic matter in cloud and fog water. Specifically, many studies have focused on the formation of secondary organic aerosol species through fog and cloud

processing of volatile organic precursors (Ervens et al., 2011; Herckes et al., 2013; Lim et al., 2013; Tan et al., 2012).

All these studies show how atmospheric pollutants are affected by the presence of fogs. The processes responsible for the formation and transformation of aerosol constituents and soluble trace gases must be studied in connection with the chemistry of cloud and fog water in order to adopt effective pollution abatement strategies at the regional scale. This is particularly true for many continental areas at the mid-latitudes, where air pollutants typically show peak concentrations in wintertime, when fogs occur.

1.5 Aerosol composition in wintertime in continental areas

Composition and concentration of aerosol particles change from place to place and differences can occur from season to season within the same observation site. In this section, I present an overview of field studies focusing on wintertime aerosol in mid-latitude continental areas, which is the type of aerosol we are interested in within this doctoral thesis, being it impacted by radiation fog occurrence to the greatest extent.

In winter, high pressure conditions in continental areas are characterised by temperatures frequently dropping below the dew point, stagnant air and a reduced height of the Planetary Boundary Layer (PBL). Winter season is the period in which the most serious particulate matter (PM) pollution episodes (PM10 > 50 mg m^{-3}) occur. In these cases nitrate becomes the main contributor to PM10 and PM2.5 together with organic matter (OM) in sites affected by local emissions. Anthropogenic sources of NO_x lead to the formation of nitrate, whose condensation in the particulate phase as NH_4NO_3 is favoured in cold conditions (Ge et al., 2012; Putaud et al., 2004; Watson and Chow, 2002).

Organic aerosol (OA) is composed by both primary organic particulate (POA) and secondary organic particulate (SOA). Primary emission sources of OA in this period of the year include mainly vehicular traffic and domestic heating. Wood combustion as domestic heating can be the most important source for particulate matter at rural location (Puxbaum et al., 2007; Weimer et al., 2009). The transport of wood burning particles also impact air quality in the cities (Favez, et al., 2010). Contribution of ~20%, ~30% and ~40% of wood combustion to total

organic carbon were measured in in Vienna (Austria), Oslo (Norway) and Zürich (Switzerland), respectively (Caseiro et al., 2009); (Yttri et al., 2009) (Szidat et al., 2006).

A revision of the European emission inventories for POA performed in the frame of the project EUCAARI (European Aerosol Cloud Climate and Air Quality Interactions) has shown that the emission of organic carbon in the fine fraction of aerosol particles in Europe is dominated by the residential combustion of wood and coal. Transport (diesel use) and residential combustion also represent the largest sources of submicron elemental carbon (EC) (Kulmala et al., 2011). Organic aerosol originating from biomass burning is rich in carcinogenetic compounds, such as polycyclic aromatic hydrocarbons (Ge et al., 2012; Lewtas, 2007). It also has a significant climate impact, representing a significant source of light-absorbing carbonaceous aerosols (Andreae and Gelencser, 2006).

Even though in winter conditions most of OA is of primary origin, a non-negligible amount of SOA can be produced. Low mixing height and stagnant conditions favour the accumulation of SOA precursors and despite the low photochemical activity, low temperatures and high relative humidity favour the partitioning of the gaseous precursors to the particle phase (Chen et al., 2010; Ge et al., 2012). In addition, the occurrence of fog events in cold season may enhance SOA production via aqueous-phase reactions. (Ge et al., 2012) reported a positive correlation between SOA and sulphate, suggesting that aqueous-phase reactions, which are known to regulate the production of sulphate, also affect the formation of organic particles.

1.6 Air quality and fogs in the Po Valley, Italy

The Po Valley is located in Northern Italy and represents the largest flat region of Italy and one of the most extended in the Mediterranean Europe. It is surrounded by mountains on three sides, the Alps in the North and West sides and the Apennines in the South, only the East side is delimited by the Adriatic Sea (Fig.1.4).

Figure 1.4. *Satellite view of haze in the Po Valley (Credit: Jeff Schmaltz). MODIS NASA*

Together with the Rhine-Ruhr (Germany), the region has been included into the list of European "megacities", owning megacity features (population $\geq$ 10 millions), even if it can be better described as an urban conglomeration rather than as a single metropolitan area.

Po Valley is the most industrialised area of the peninsula and it is also characterised by intensive livestock and agricultural activities. The Po Valley suffers bad air quality conditions, with frequent exceedances of the PM10 concentration limits in the cold season, mainly because of the strong anthropogenic sources of VOC and aerosols and of the adverse meteorological conditions. In wintertime, the low mixing layer heights and the weak atmospheric circulation promote stagnation of air masses at the low altitudes, and does not allow to the pollutants to disperse in the atmosphere, favouring the development of critical pollution episodes.

For these reasons, despite the application of legislation pointed to air pollution control, the Po valley has been identified as an area in Europe where pollutant levels are expected to remain problematic in the years to come(Pernigotti et al., 2012).

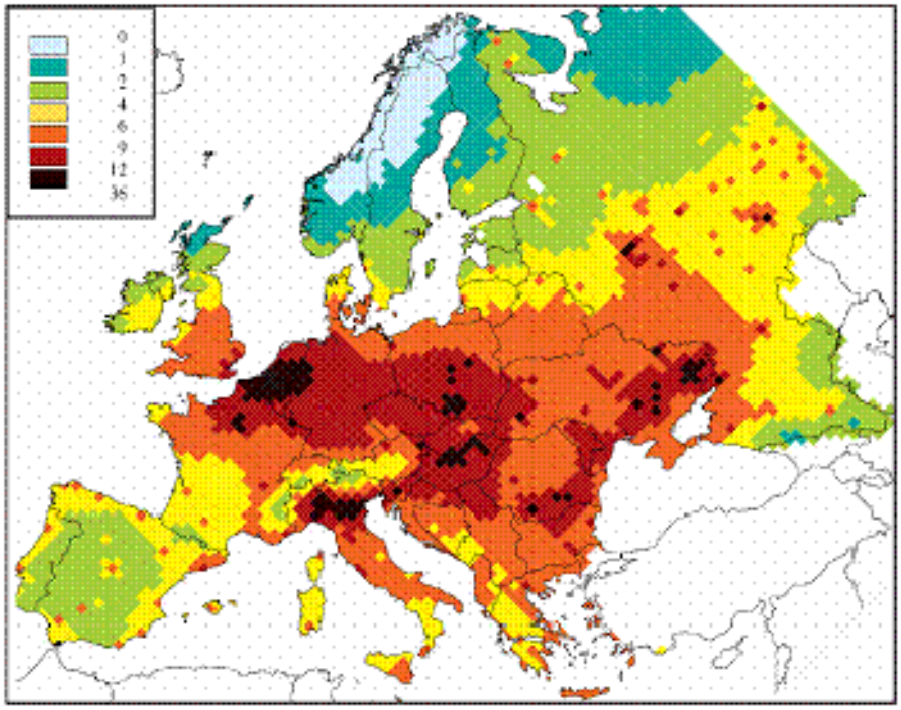

Figure 1.5. Loss in life expectancy (months) attributable to exposure to anthropogenic PM2.5 for year 2000 emissions (Source: EC, IIASA).

Air quality is therefore one of the most urgent and challenging problem to solve in this region, considering the consequences of pollution on people health (Fig.1.5). Within the complex issue of air quality in the Po Valley, this thesis aims to strengthen the knowledge of processes involving atmospheric pollutants. Among these processes, interactions between aerosol particles and fog droplets play a relevant role in the Po Valley, because of the high frequency of fog events during the cold season. These interactions will be investigated in the following chapters, to better clarify their effects on air pollutants.

Furthermore, a long time series of data regarding fog chemical and physical properties will be presented in chapter 4. Long time series represent a useful tool to appreciate the effectiveness of the adopted environmental policy strategies.

A more detailed scientific knowledge and a deeper comprehension of atmospheric chemistry and processes is fundamental to support the legislation in making effective choices pointed to the abatement of pollutants.

2. Experimental setup

The present thesis work reports data from two field campaigns set up in the Po Valley during the fall-winter season by CNR-ISAC, in collaboration with ARPA Emilia Romagna (within the Supersito project, see chapter 3), with the purpose of getting an insight into atmospheric particulate matter physico-chemical properties. Data from routine sampling and analysis of Po Valley fog water, in the period November - March, will be also presented and discussed. The Po Valley fog sampling and characterization activity has been carried out since the nineties and the results of this long-term database will be also discussed in the following chapters.

Sampling sites description and analytical protocols of both aerosol particles and fog droplets analysis will be reported in the following sections.

2.1 Sampling sites

Samples have been collected in two different sites: Bologna and San Pietro Capofiume (Molinella).

Bologna is a city located in the south-eastern part of the Po Valley, at the foot of the Tosco-Emiliano Apennines. The inhabitants are approximately 380.000 in an urban area of 140.000 km^2, even though the whole metropolitan area reaches roughly 980.000 inhabitants. The sampling was carried out at the Institute of Atmospheric Sciences and Climate (ISAC) building, in the northern outskirts, 3.5 km far away from the city centre.

The Meteorological station Giorgio Fea in San Pietro Capofiume (Fig.2.1), is located in a flat rural area of the Eastern Po Valley. The closest cities are Bologna (35 km south-west) and Ferrara (25 km north) and the Adriatic Sea is about 60 km in the east direction. According to EMEP (European Monitoring and Evaluation Programme under the Convention on Long-range Transboundary Air Pollution) conventions, it can be classified as a rural background site, although during the winter season, in condition of reduced aerosol dispersion, it behaves more as an urban background.

Figure 2.1. *Measurement station of San Pietro Capofiume (BO) during a foggy winter day.*

2.2 Aerosol sampling

Size segregated aerosol particles were sampled by a five-stage Berner impactor (flow rate 80 L min^{-1}) with 50% size cut-offs at 0.14, 0.42, 1.2, 3.5, and 10 µm aerodynamic diameter (D_a) (Fig.2.2). Samples were collected contemporary on Tedlar and aluminium foils: they were put together on the impaction plate each covering one half of the impaction surface (Fig.2.3). Contemporary sampling on Tedlar and aluminium foils allows to analyse the same samples by analytical techniques requiring different substrates (Matta et al., 2003). The aluminium half was used to carry out analysis of Total Carbon (TC), while the half Tedlar foil was an excellent substrate for water-soluble aerosol material analysis, due to the very low blank values for both inorganic and organic species.

Figure 2.2. *Five-stages Berner impactor at the San Pietro Capofiume measurement station.*

Before sampling, Tedlar foils were washed three times with Milli-Q water (deionised water by Millipore, resistivity 18.2 MΩ cm), sonicated for 30 minutes, rinsed again with Milli-Q and let drying under a laminar flow cap located in a clean room for 24h. Aluminum foils were pre-fired at 500 °C for 4h. These procedures were carried out in order to reduce blank values for both inorganic and organic analysis.

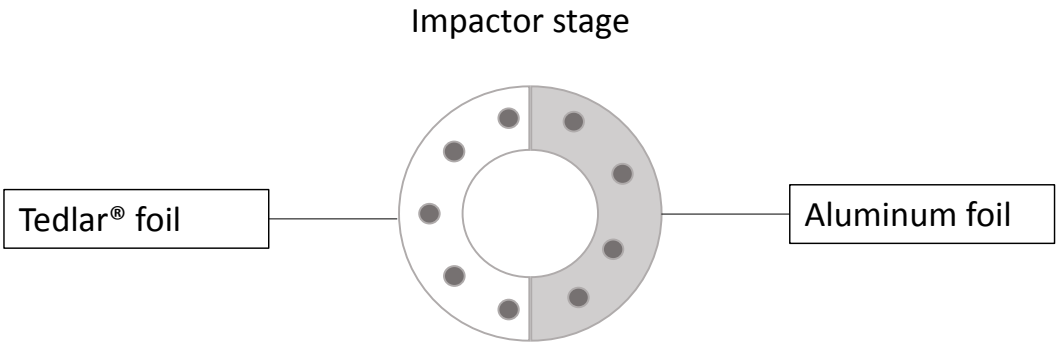

Figure 2.3. *Double tedlar/aluminum sampling substrate scheme.*

Simultaneously with Berner impactor sampling, aerosol particles were also collected with a dichotomous high volume sampler from MSP Corporation (Universal Air Sampler, model 310) working at a constant nominal airflow rate of 300 L/min. The dichotomous sampler allowed the collection of atmospheric aerosols in their PM1 (particles with D_a < 1 µm) and PM1-10 (particles with 1 µm < D_a < 10 µm) fractions. PALL quartz-fibre filters were used as substrates. To reduce their blank values, filters for fine fraction were washed with 500 mL of Milli-Q water and then fired at 800 °C for 1 h. Filters for the collection of the coarse fraction were only fired at 800°C for 1h. Samples collected by the dichotomous sampler were addressed to ^{1}H-NMR analysis for the characterization of the water-soluble organic fraction.

2.3 Fog sampling

Fog was sampled using an automated, computer driven active string collector (Fig.2.4). It consists of a system in which a fan located at the rear part of a short wind tunnel creates an air stream containing fog droplets that impact on a series of strings, initially made of teflon. The collected droplets coalesce with each other and drain off the strings into a funnel and the sampling bottle. The fog collector was modified in 1997 to allow fog water analysis of organic compounds and all parts coming into contact with the fog droplets, including the sampling strings, were made out of stainless steel to avoid problems of artefact formation and adsorption on the surfaces for these compounds (Fuzzi et al., 1997b). A Particulate Volume Monitor PVM-100, used to determine fog liquid water content (LWC) with a time resolution of 1 min, was used to activate the string collector. A LWC threshold of 0.08 g m^{-3} was chosen for the activation. Even if there is no direct physical relationship between LWC and visibility, empirical tests showed that this threshold usually corresponds to ca. 200 m visibility. Both instruments are located at the field station of San Pietro Capofiume and stand outside for the whole fall-winter season (November – March). The LWC threshold of 0.08 g m^{-3} was chosen in order to avoid interferences in data recording, due to the presence of external factors, as for example spider webs.

Figure 2.4. *Fog string collector and PVM in the background.*

2.4 Analytical methods

2.4.1 Sample handling

Size segregated aerosol samples from the Berner impactors were put in Petri dishes and stored in freezer at -15°C until analysis were performed. Quartz filters were stored in freezer as well.

Before analysis, both quartz-fibre filters and tedlar foils were extracted in 10 mL Milli-Q deionised water and sonicated for 30 minutes. Liquid extract of quartz-fibre filters was filtered before analysis in order to remove quartz residues. A summary of the analytical procedure performed on aerosol samples is shown in Fig.2.5.

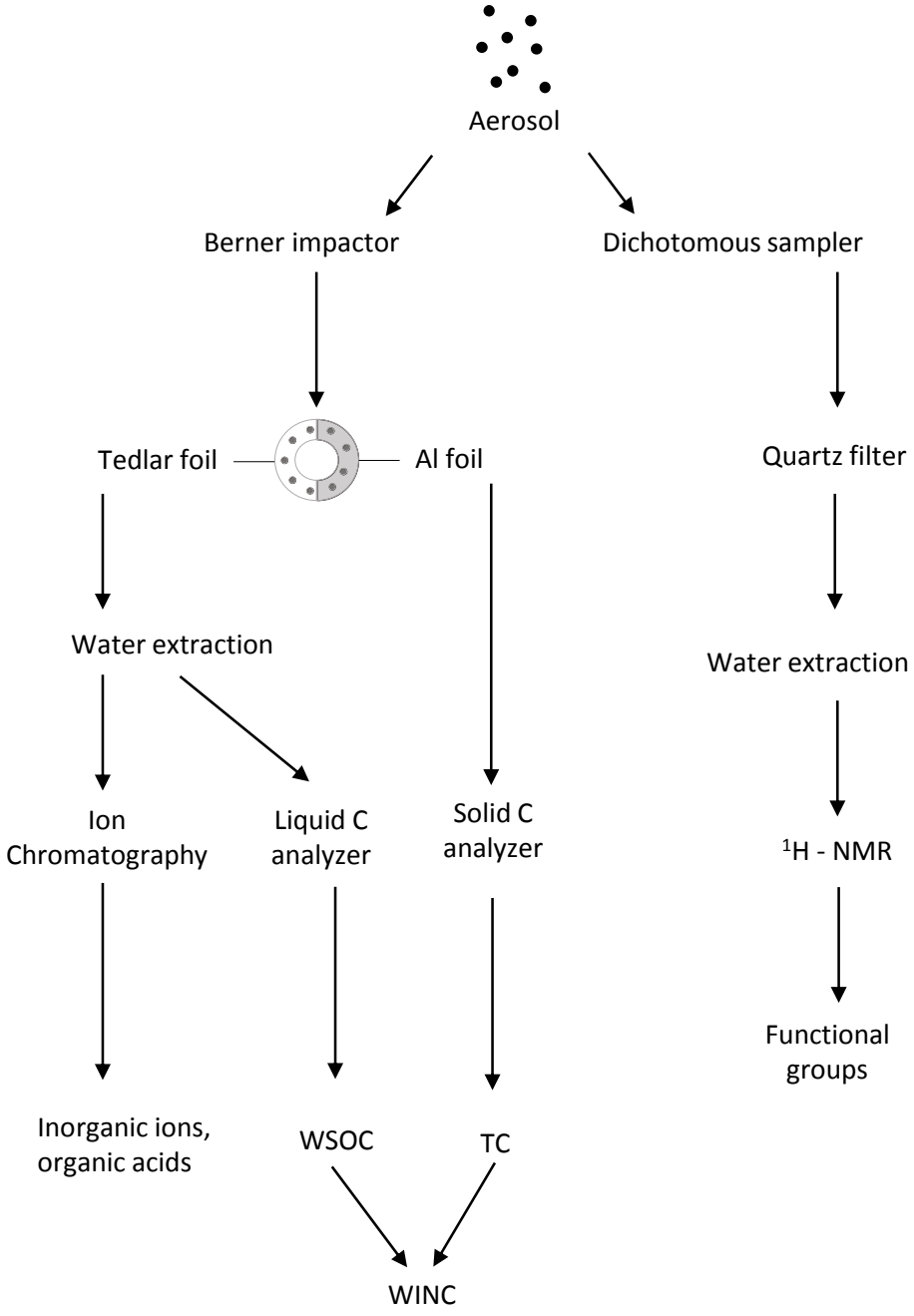

Figure 2.5. *Scheme of analytical procedure performed on aerosol samples.*

Fog water samples were filtered on 47 mm quartz-fibre filters (Whatman, QMA grade) within a few hours after collection to remove suspended particulate and conductivity and pH measurements were carried out immediately. The samples were then stored frozen until analysis. A schematic summary of the analytical procedure performed on fog samples is shown in Fig.2.6.

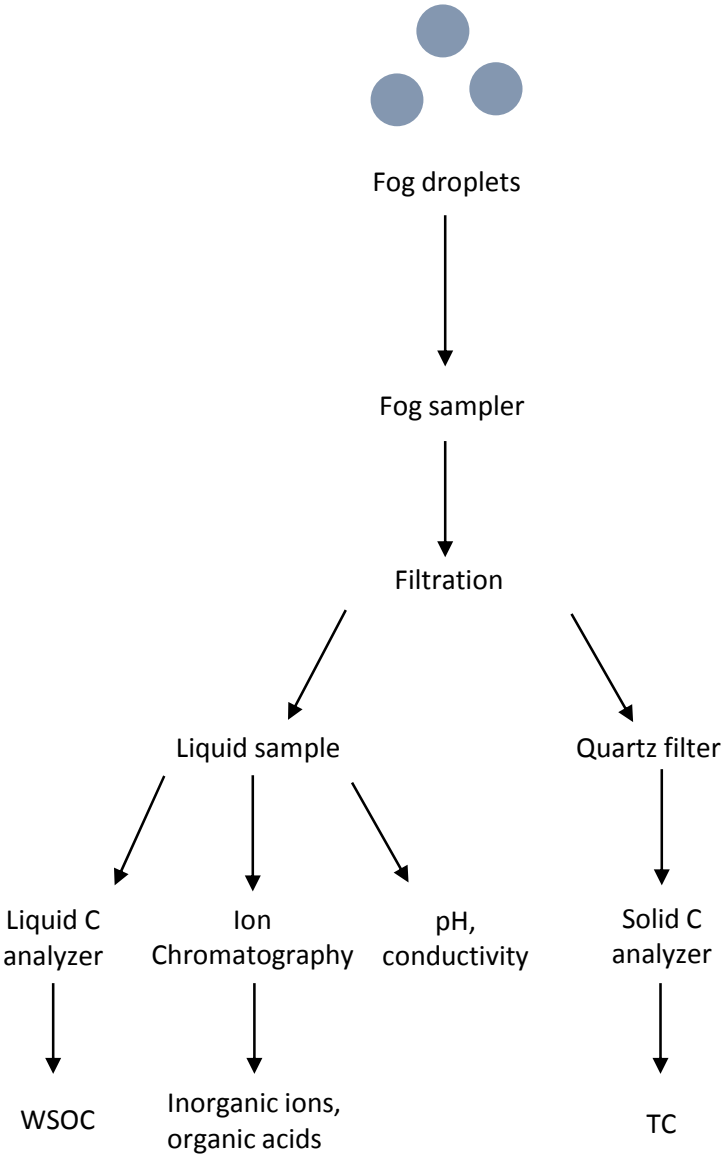

Figure 2.6 *Scheme of analytical procedure performed on fog samples.*

2.4.2 Ion Chromatography

To determine the samples ionic content two Dionex ICS_2000 ion chromatographs were used. For anions detection and quantification, the ion chromatograph was equipped with an IonPac AG11 2x50 mm Dionex guard column, IonPac AS11 2x250 mm Dionex separation column and ASRS 300 self-regenerating suppressor. A solution of KOH was used as eluent. Its

concentration increased from 0.8 mM to 38 mM, in a 35 minutes long run (0.8 mM for 10 min, 5 mM reached at 15 min, 10 mM at 20 min and 38 mM at 35 min). The flow rate was 0.25 mL/min. The chromatographic equipment for cation analysis consisted of an IonPac CG16 3x50 mm Dionex guard column, IonPac CS16 3x250 mm Dionex separation column and CSRS 300 self-regenerating suppressor. The analysis were performed using a solution of MSA as eluent with a flow rate of 0.36 mL/min. The following separation method was used: initial eluent concentration 6 mM, increase to 15 mM in 20 minutes, then 30 mM reached at 30 min and 50 mM from 31 min until 42 min. This program allows to separate both inorganic cations (sodium, ammonium, potassium, magnesium, calcium) and methyl-, dimethyl-, trimethyl-, ethyl- and diethylammonium.

2.4.3 Water-soluble organic carbon (WSOC)

Two instruments were used to determine the WSOC content in fog and aerosol samples: a carbon analyser Shimadzu TOC-5000A and a nitrogen/carbon analyser Analitik Jena Multi N/C 2100S. The two instruments follow the same analysis procedure: parallel measurements of inorganic carbon (IC) and total soluble carbon (TSC) are carried out. The measurement of the TSC is performed by catalytic high temperature combustion (800 °C, in presence of a Pt catalyst) in a pure carrier gas (oxygen for the Analitik Jena and air for the Shimadzu) and an Infrared Detector (NDIR) to measure the evolved CO_2. IC content is provided acidifying the solution and measuring the generated CO_2. WSOC is determined by difference (WSOC = TSC – IC) (Rinaldi et al., 2007).

Standard calibration curves obtained with potassium hydrogen phthalate and with a mixture of sodium carbonate and sodium hydrogen carbonate were used to quantify TSC and IC respectively. Replicate measurements of standard solutions showed a reproducibility within 5% for concentration range typically encountered in samples extracts.

2.4.4 Total Carbon (TC)

The total carbon (TC) content of the samples was determined by the Analitik Jena Multi N/C 2100S analyser equipped with a furnace for solid analysis. A small portion (about 1 cm^2) of

aluminium foils (for aerosol samples) or quartz filters (for fog samples) is introduced into the furnace where it is exposed to a constant temperature 950 °C in a pure oxygen atmosphere, in presence of a catalyst (CeO_2). All the carbonaceous matter (both organic, carbonate and elemental carbon) evolves in CO_2 under these conditions. A non-dispersive infrared detector (NDIR) is used to measure the evolved CO_2. The instrument was calibrated using pre-muffled quartz filter or aluminium foils soaked with different volumes of potassium hydrogen phthalate 100 or 1000 ppm solution. The instrumental detection limit is 0.2 μg of carbon and the accuracy of the TC measurement resulted better than 5% for 1 μg of carbon.

By subtracting WSOC from TC the water-insoluble carbon (WINC) content of the collected aerosol samples was calculated.

2.4.5 WSOC characterization by Proton Nuclear Magnetic Resonance (^{1}H-NMR) spectroscopy

Proton Nuclear Magnetic Resonance (^{1}H-NMR) spectroscopy was applied to quantify the functional groups of WSOC, following the procedure described in Decesari et al. 2000. ^{1}H-NMR spectroscopy provides information about main structural units and it is able to identify individual compounds. Another important characteristic of NMR spectroscopy is that quantitative analysis is straightforward, since the integrated area of the spectra is proportional to the moles of organic hydrogen atoms present in the sample (Derome, 1987); (Braun et al., 1998) . Aliquots of fog water samples and quartz filters extracts were vacuum dried and redissolved in 650 μL D_2O in order to be subjected to the analyses; sodium 3-trimethylsilyl-(2,2,3,3-d_4) propionate ($TSPd_4$) was added to the solution as internal standard. ^{1}HNMR spectra were acquired by a Varian MERCURY 400 spectrometer working at 400 MHz in a 5 mm probe. In order to obtain a good signal-to-noise ratio, the carbon content of the analysed aliquot should not be lower than 80 μgC.

2.4.6 On-line aerosol chemical characterization

Besides the previously described off-line analysis of collected filters, aerosol chemical composition and size distribution of chemical constituents were characterized on-line by a

High Resolution Time of Flight Aerosol Mass Spectrometer (HR-ToF-AMS). Even though HR-ToF-AMS measurements are not the main topic of this thesis, it is worth to provide here a general information on the AMS set up, because AMS measurements accompanied filter sampling during all the field campaigns described in this study and some results are reported in chapter 5 to support off-line analysis data.

A detailed description of the HR-ToF-AMS can be found in (DeCarlo et al., 2006). Briefly, the instrument provides size resolved atmospheric concentrations of the non-refractory fraction of PM1 particles, i.e., sulphate, nitrate, ammonium, chloride, and organics, with a time resolution of the order of 5 minutes. The AMS has an effective 50% cut-off for particle sizes below 80 and above 600 nm in vacuum aerodynamic diameter, D_{va}, as determined by the transmission characteristics of the standard aerodynamic lens (Zhang et al., 2002; Zhang et al., 2004). All the AMS data were analysed using standard AMS software (SQUIRREL v1.51 and PIKA v1.10) within Igor Pro 6.2.1 (WaveMetrics, Lake Oswego, OR) (DeCarlo et al., 2006). To obtain PM1 mass closure HR-ToF-AMS analysis were integrated with online black carbon (BC) measurements, carried out by a Soot Particle Aerosol Mass Spectrometer (SP-AMS). The SP-AMS provide measurements of the refractory component of the submicron aerosol, nominally rBC, and of the non-refractory coating material associated with it (Onasch et al., 2012).

2.4.7 Evaluation of the random uncertainties associated to the measurements

The random uncertainty associated to each aerosol component atmospheric concentration and each size range was computed using the standard procedure for error propagation, considering:

1. the uncertainty in the sampled air volume (± 3% for Berner impactor and ± 10% for high volume sampler);
2. the precision of the extraction water volume (± 0.04 mL);
3. the uncertainties in ion chromatography, WSOC and TC measurements (± 5%);
4. the uncertainty associated to the blank variability, in order to take into account the error due to the subtraction of an average blank value.

The random uncertainties associated to the concentration of each fog water component was assumed as high as the instrumental uncertainty, being the concentrations measured in the field blanks absolutely negligible as compared to the sampled fog.

The overall mean relative random uncertainties for each aerosol and fog component are reported in Table 2.1.

Table 2.1. *Overall mean relative random uncertainties for each aerosol component; uncertainties are given as percentages.*

size range (µm)	Cl^-	NO_3^-	SO_4^{2-}	Na^+	NH_4^+	K^+	Mg^{2+}	Ca^+	WSOC	WINC
0.05-0.14	21	9	5	60	6	9	100	46	13	27
0.14-0.42	8	7	5	19	5	5	182	34	8	21
0.42-1.2	5	5	5	7	5	5	52	20	6	10
1.2-3.5	6	5	5	11	5	7	38	13	7	15
3.5-10	12	10	5	8	10	18	43	16	19	21
fog droplet	5	5	5	5	5	5	5	9	5	5

The uncertainty associated with ^{1}H-NMR analysis is about 15% for the aliphatic functional group concentrations (in µmolH/m^3), and up to 20-30% for the band of aromatic proton.

3. Aerosol chemical composition in the Po Valley

"Supersito" is a project promoted by Emilia Romagna region and coordinate by the Regional Environmental Agency of Emilia Romagna (ARPA-EMR). The goal of the project is to furnish complete and detailed observations of physical, chemical and toxicological atmospheric parameters and integrating environmental and health data. Numerous recent studies demonstrate a correlation between high concentration of particulate matter and health effects (Brunekreef, 2013; Pope and Dockery, 2006). The project aspires to reach a deeper knowledge about primary and secondary aerosol particles, their chemical composition and their formation mechanisms, in order to drive the governance towards incisive policies for the environmental and health protection.

Within this project, the Institute of Atmospheric Science and Climate (ISAC) – CNR of Bologna participates investigating chemical composition of aerosol particles. Online measurements and samples are collected during Intensive Observation Period (IOP) scheduled over the three years of experimental work (2011-2014).

Five different places located all over the region have been chosen as sampling and measurement sites. The study reported in this chapter deals with data recorded during two intensive field campaigns in the frame of Supersito project carried out in Bologna and San Pietro Capofiume. A detailed description of both sites is reported in chapter 2. Bologna (BO) represents the Main Site of the project. Due to the high population of the Bologna urban area, it is representative and significative for future epidemiological studies. In the frame of the project, San Pietro Capofiume (SPC) has been classified as Rural Satellite site.

The interest of this Ph.D. thesis is focused on the characterization of atmospheric chemistry during the fall-winter season in the Po Valley. For this purpose November 2011 and February 2013 field campaigns were chosen to be analysed.

3.1 November 2011 field campaign

In November 2011 the first Intensive Observation Period (IOP) of the Supersito project was scheduled both in Main Site and San Pietro Capofiume field station. In Bologna, samples have been collected starting from 17 November until 7 December, while in SPC sampling started on 15 November and ended on 1 December. In both sites, size segregated aerosol particles were sampled using a 5-stage Berner impactor. Every day two samples were collected: daytime sample from 9:00 to 17:00 and night-time sample from 17:00 to 9:00 of the following day. Daytime and night-time conditions were established based on the evolution of the Planetary Boundary Layer (PBL), according to CALMET meteorological pre-processor (Deserti et al., 2001). In Table 3.1 and Table 3.2 an overview of the samples collected during the campaigns is presented.

A total of 36 samples was collected in Bologna and 37 in SPC on both aluminium and tedlar foils. A series of samples was selected, removing samples which encountered technical problems and favouring those sampled contemporary to other measurements, and analysed according to the procedure described in chapter 2.

Temperature, relative humidity and wind speed registered during the campaign in both sites are reported in Fig. 3.1. The meteorological parameters in Fig.3.1 describe the typical Po Valley autumn-winter atmospheric stability condition that favours the accumulation of pollutants. Slightly higher temperatures were recorded in Bologna during the night as well as lower relative humidity, both night-time and daytime. The lowest temperature recorded in Bologna was -0.7 °C and -1.4 °C in SPC, while highest values are very similar: 12.6 °C and 12.8 °C in Bologna and SPC, respectively. As it can be seen from Fig 3.1, San Pietro Capofiume was affected by fog presence almost every night during the campaign. On 15/11/2011 and 20/11/2011 RH was close to 94% also in daytime. Winds were very weak or absent, especially in Bologna. Wind speed never exceeded 5 m s^{-1}.

Table 3.1. *Aerosol sampling schedule at Main Site. * = local time. ** = analysed samples.*

Bologna

Sample	Classification	Start date*	Stop date*	Time of sampling (min)
BO171111_D**	day	17/11/2011 12.31	17/11/2011 17.01	270
BO171111_N**	night	17/11/2011 17.05	18/11/2011 09.01	956
BO181111_D**	day	18/11/2011 09.07	18/11/2011 17.00	473
BO181111_N**	night	18/11/2011 22.45	19/11/2011 09.00	615
BO191111_D	day	19/11/2011 09.03	19/11/2011 17.00	477
BO191111_N	night	19/11/2011 17.40	20/11/2011 09.00	920
BO201111_D	day	20/11/2011 09.45	20/11/2011 17.14	449
BO201111_N	night	20/11/2011 18.03	21/11/2011 09.05	902
BO211111_D	day	21/11/2011 09.08	21/11/2011 17.01	473
BO211111_N	night	21/11/2011 17.04	22/11/2011 09.00	956
BO221111_D	day	22/11/2011 09.04	22/11/2011 17.00	476
BO221111_N	night	22/11/2011 18.00	23/11/2011 09.00	900
BO231111_D	day	23/11/2011 09.06	23/11/2011 16.59	473
BO231111_N	night	23/11/2011 17.30	24/11/2011 09.05	935
BO241111_D	day	24/11/2011 09.07	24/11/2011 17.00	473
BO241111_N	night	24/11/2011 17.34	25/11/2011 09.00	926
BO251111_D**	day	25/11/2011 09.03	25/11/2011 17.03	480
BO251111_N**	night	25/11/2011 17.47	26/11/2011 09.02	915
BO261111_D**	day	26/11/2011 09.07	26/11/2011 17.02	475
BO261111_N**	night	26/11/2011 17.34	27/11/2011 09.00	926
BO271111_D**	day	27/11/2011 09.04	27/11/2011 17.04	480
BO271111_N**	night	27/11/2011 17.33	28/11/2011 09.00	927
BO281111_D**	day	28/11/2011 09.03	28/11/2011 17.00	477
BO281111_N**	night	28/11/2011 17.35	29/11/2011 09.00	925
BO291111_D**	day	29/11/2011 09.03	29/11/2011 17.00	477
BO291111_N**	night	29/11/2011 17.33	30/11/2011 09.03	930
BO301111_D**	day	30/11/2011 09.05	30/11/2011 17.00	475
BO301111_N**	night	30/11/2011 17.28	01/12/2011 09.00	932
BO011211_D**	day	01/12/2011 09.03	01/12/2011 17.00	477
BO011211_N**	night	01/12/2011 17.38	02/12/2011 09.03	925
BO021211_D**	day	02/12/2011 09.06	02/12/2011 17.04	478
BO051211_D**	day	05/12/2011 09.07	05/12/2011 17.00	473
BO051211_N**	night	05/12/2011 17.28	06/12/2011 09.00	932
BO061211_D**	day	06/12/2011 09.03	06/12/2011 17.00	477
BO061211_N**	night	06/12/2011 17.00	07/12/2011 09.02	962
BO071211_D**	day	07/12/2011 09.06	07/12/2011 17.00	474

Table 3.2. *Aerosol sampling schedule at San Pietro Capofiume field station. * = local time. ** = analysed samples.*

San Pietro Capofiume				
Sample	Classification	Start date *	Stop date *	Time of sampling (min)
SPC151111_D**	day	15/11/2011 09.23	15/11/2011 17.00	457
SPC151111_Na**	night	15/11/2011 18.03	15/11/2011 22.03	240
SPC151111_Nb**	night	15/11/2011 22.40	16/11/2011 02.40	240
SPC151111_Nc**	night	16/11/2011 03.15	16/11/2011 07.15	240
SPC151111_Nd**	night	16/11/2011 07.35	16/11/2011 11.18	223
SPC161111_D**	day	16/11/2011 11.46	16/11/2011 16.55	309
SPC161111_N**	night	16/11/2011 18.12	17/11/2011 09.00	888
SPC171111_D**	day	17/11/2011 09.33	17/11/2011 17.00	447
SPC171111_Na**	night	17/11/2011 17.25	17/11/2011 21.25	240
SPC171111_Nb**	night	17/11/2011 21.47	18/11/2011 01.47	240
SPC171111_Nc**	night	18/11/2011 02.07	18/11/2011 05.50	223
SPC181111_D**	day	18/11/2011 09.25	18/11/2011 17.00	455
SPC181111_N**	night	18/11/2011 17.45	19/11/2011 08.35	890
SPC191111_D	day	19/11/2011 09.10	19/11/2011 17.00	470
SPC191111_N	night	19/11/2011 17.37	20/11/2011 08.30	893
SPC201111_D	day	20/11/2011 09.00	20/11/2011 17.06	486
SPC201111_N	night	20/11/2011 18.02	21/11/2011 09.00	898
SPC211111_D	day	21/11/2011 09.28	21/11/2011 17.00	452
SPC211111_N	night	21/11/2011 17.31	22/11/2011 08.54	923
SPC221111_D	day	22/11/2011 09.26	22/11/2011 17.00	454
SPC221111_N	night	22/11/2011 17.48	23/11/2011 09.00	912
SPC231111_D	day	23/11/2011 09.20	23/11/2011 17.00	460
SPC231111_N	night	23/11/2011 17.35	24/11/2011 09.07	932
SPC241111_D	day	24/11/2011 09.42	24/11/2011 17.00	438
SPC241111_N	night	24/11/2011 17.38	25/11/2011 08.27	889
SPC251111_D**	day	25/11/2011 09.00	25/11/2011 16.59	479
SPC251111_N**	night	25/11/2011 17.59	26/11/2011 09.18	919
SPC261111_D**	day	26/11/2011 09.45	26/11/2011 16.59	434
SPC261111_N**	night	26/11/2011 17.29	27/11/2011 09.02	933
SPC271111_D**	day	27/11/2011 09.33	27/11/2011 17.01	448
SPC271111_N**	night	27/11/2011 17.28	28/11/2011 09.12	944
SPC281111_D**	day	28/11/2011 09.55	28/11/2011 17.00	425
SPC281111_N**	night	28/11/2011 17.41	29/11/2011 09.10	929
SPC291111_D**	day	29/11/2011 09.33	29/11/2011 16.59	446
SPC291111_N**	night	29/11/2011 17.31	30/11/2011 09.18	947
SPC301111_D**	day	30/11/2011 09.52	30/11/2011 17.00	428
SPC301111_N**	night	30/11/2011 17.32	01/12/2011 09.00	928

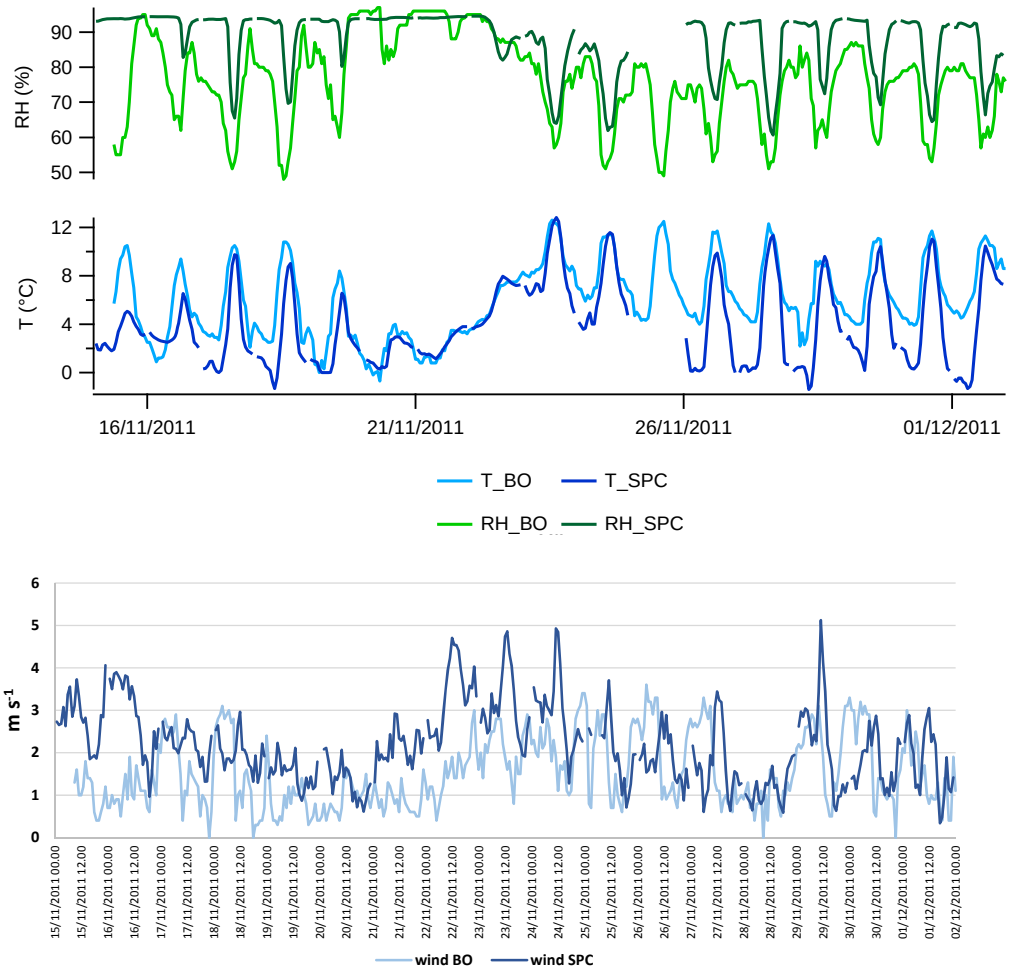

Figure 3.1. *Meteorological parameters recorded during in Bologna and in San Pietro Capofiume from 15/11/2011 to 02/12/2011.*

3.2 February 2013 field campaign

Another field campaign was scheduled in Bologna and San Pietro Capofiume in February 2013. In both sites samples have been collected starting from 4 until 15 February. As for the previous campaign, size segregated aerosol particles were sampled using a 5-stage Berner impactor twice a day (9:00 - 18:00, 18:00 - 9:00 of the following day). In Table 3.3 and Table 3.4 an overview of the samples collected during the campaigns is presented.

Table 3.3. *Aerosol sampling schedule at Main Site. * = local time. ** = analysed samples.*

Bologna

Sample	Classification	Start date *	Stop date *	Time of sampling (min)
BO040213_D	day	04/02/2013 09.28	04/02/2013 18.00	512
BO040213_N**	night	04/02/2013 18.18	05/02/2013 09.00	882
BO050213_D**	day	05/02/2013 09.04	05/02/2013 18.00	536
BO050213_N**	night	05/02/2013 18.22	06/02/2013 08.55	873
BO060213_D	day	06/02/2013 09.21	06/02/2013 17.57	516
BO060213_N	night	06/02/2013 18.20	07/02/2013 09.00	880
BO070213_D	day	07/02/2013 09.18	07/02/2013 18.01	523
BO070213_N**	night	07/02/2013 18.03	08/02/2013 09.00	897
BO080213_D**	day	08/02/2013 09.20	08/02/2013 17.58	518
BO080213_N	night	08/02/2013 18.21	09/02/2013 09.00	879
BO110213_D	day	11/02/2013 09.28	11/02/2013 18.00	512
BO110213_N	night	11/02/2013 ???	12/02/2013 09.05	n.a.
BO120213_D**	day	12/02/2013 09.06	12/02/2013 18.00	534
BO120213_N**	night	12/02/2013 18.19	13/02/2013 09.00	881
BO130213_D**	day	13/02/2013 09.27	13/02/2013 18.00	513
BO130213_N**	night	13/02/2013 18.23	14/02/2013 09.00	877
BO140213_D**	day	14/02/2013 09.20	14/02/2013 18.07	527
BO140213_N**	night	14/02/2013 18.10	15/02/2013 09.00	890
BO150213_D**	day	15/02/2013 09.20	15/02/2013 18.00	520
BO150213_N	night	15/02/2013 18.23	16/02/2013 09.01	878

Table3.4. *Aerosol sampling schedule at San Pietro Capofiume field station. * = local time. ** = analysed samples.*

San Pietro Capofiume				
Sample	Classification	Start date *	Stop date *	Time of sampling (min)
SPC040213_D	day	04/02/2013 09.00	04/02/2013 18.00	540
SPC040213_N**	night	04/02/2013 18.00	05/02/2013 09.00	900
SPC050213_D**	day	05/02/2013 09.00	05/02/2013 18.00	540
SPC050213_N**	night	05/02/2013 18.00	06/02/2013 09.00	900
SPC060213_D	day	06/02/2013 09.14	06/02/2013 18.00	526
SPC060213_N	night	06/02/2013 18.00	07/02/2013 09.00	900
SPC070213_D	day	07/02/2013 09.07	07/02/2013 18.00	533
SPC070213_N**	night	07/02/2013 18.00	08/02/2013 09.00	900
SPC080213_D**	day	08/02/2013 09.05	08/02/2013 18.00	535
SPC080213_N	night	08/02/2013 18.00	09/02/2013 09.00	900
SPC110213_D	day	11/02/2013 09.05	11/02/2013 18.00	535
SPC110213_N	night	11/02/2013 18.00	12/02/2013 09.00	900
SPC120213_D**	day	12/02/2013 09.02	12/02/2013 18.00	538
SPC120213_N**	night	12/02/2013 18.00	13/02/2013 09.00	900
SPC130213_D**	day	13/02/2013 09.02	13/02/2013 18.00	538
SPC130213_N**	night	13/02/2013 18.00	14/02/2013 09.00	900
SPC140213_D**	day	14/02/2013 09.00	14/02/2013 18.00	540
SPC140213_N**	night	14/02/2013 18.00	15/02/2013 09.00	900
SPC150213_D**	day	15/02/2013 09.02	15/02/2013 18.00	538
SPC150213_N	night	15/02/2013 18.03	16/02/2013 09.03	900

Fig.3.2 shows meteorological parameters (T, RH and wind speed) of the two sites during the campaign. Conditions met during this campaign are more variable than in November 2011, with low pressure systems bringing occasional rain over the sampling sites. Temperature are similar in the two sites with values ranging from -1.3 °C to 12.2 °C in Bologna and from -0.7°C to 12.3 °C in SPC. Trend of RH is the same for both sites, with values usually slightly lower in Bologna. Red circles indicate rainy periods in both sites: 06/02/2013 6:00 – 9:00, 11/02/2013 9:00 – 12/02/2013 15:00 and 13/02/2013 21:00 – 22:00 in Bologna and 06/02/2013 06:00 – 08:00, 11/02/2013 09:00 –23:00 and 13/02/2013 21:00 – 22:00 in SPC. In this campaign, winds are weaker in SPC and are slightly faster than the previous campaign, with values reaching 12 m s^{-1} in Bologna on 11/02/2013.

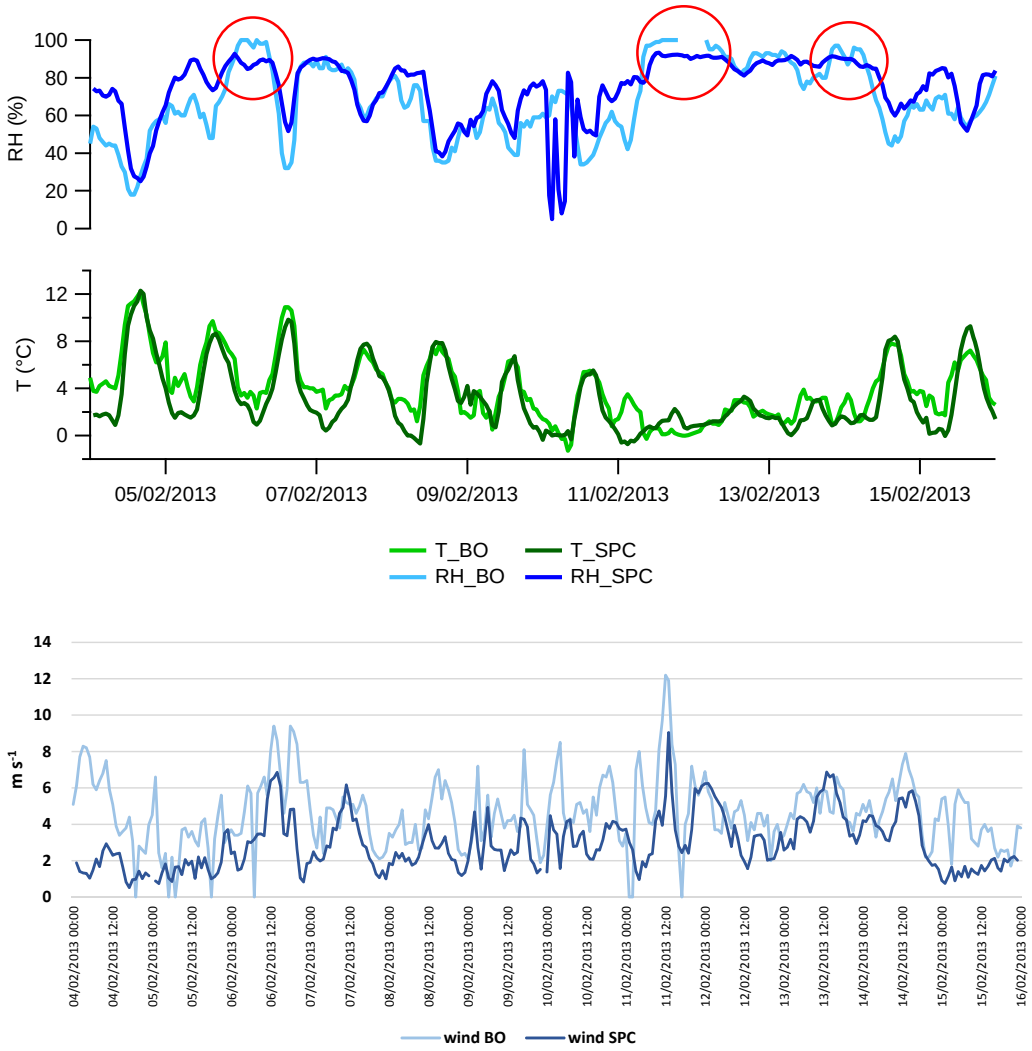

Figure 3.2. *Meteorological parameters recorded during in Bologna and in San Pietro Capofiume from 04/02/2013 to 16/02/2013. Red circles indicate rainy periods.*

3.3 Size segregated chemical characterization of aerosol particles

This paragraph presents a detailed description of the chemical composition of the water-soluble fraction of size segregated aerosol particles collected during the two field campaigns. Water-soluble fraction was reconstructed adding together the inorganic fraction analysed by ion chromatography and the water-soluble organic carbon (WSOC) content measured by a carbon analyser (see chapter 2). Because of technical problems, water-insoluble carbon (WINC) was measured only for samples collected in SPC during the November field campaign.

Therefore, data are not included in the following discussion and will be presented in detail in chapter 5.

Fig.3.3 shows the concentration of water-soluble compounds of PM10 collected in the two campaigns. Total mass concentrations are obtained summing up the five Berner stages.

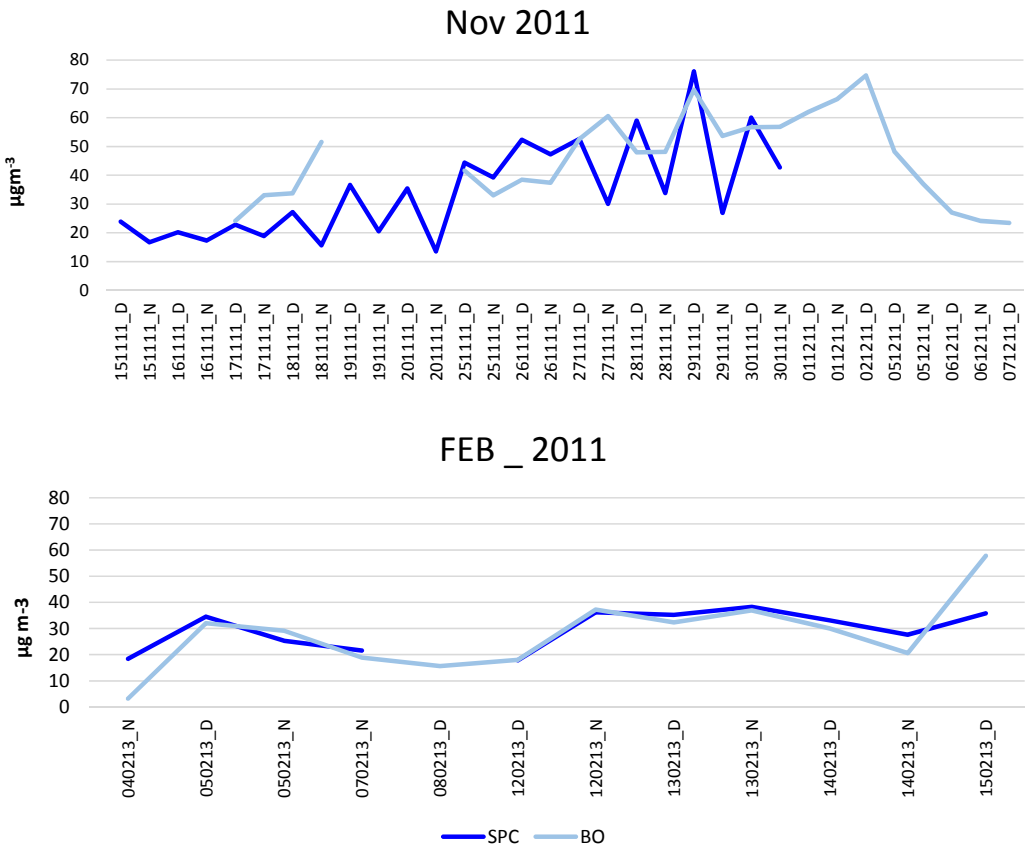

Figure 3.3. *Concentration of PM10 water-soluble fraction during the November 2011 and February 2013 campaigns.*

In November2011, PM10 water-soluble fraction concentration is comparable between San Pietro Capofiume and Bologna. Soluble mass showed low concentrations in the first period, then particles accumulated at the end of November and at the beginning of December (in December data are available only for Bologna). Concentrations range between 24 – 75 µgm^{-3} in Bologna and 14 – 76 µg m^{-3} in SPC. These values do not account for the insoluble matter

present in aerosol particles that was not analysed. Nevertheless, in the second half of the campaign PM10 soluble fraction concentrations exceed the 50 μg m^{-3} PM10 threshold.

In February 2013 concentrations are also very similar between the two sites and are comparable to those measured in the first half of November 2011, with values ranging between 3.2 - 58 μg m^{-3} in Bologna and 18 – 38 μg m^{-3} in San Pietro Capofiume.

Soluble mass concentration remains almost constant all over the measuring period, without any daily trend, as it is expected, given the scarce evolution of the PBL during daytime in winter (Carbone et al., 2010). Conversely, for the November campaign, a clear diurnal trend is observed, especially for samples collected in SPC: PM10 concentration decreases during the night and increases again during the day. This trend is linked with the presence of fog in night hours and will be further discussed in chapter 5.

We expected higher particles concentration in an urban site compared to a rural background, while similar concentrations are observed in the two sites. The water-soluble fraction is the most influenced by secondary processes and less affected by local source emissions as traffic and domestic heating (Seinfeld and Pandis, 1998). The above data indicate that concentrations of secondary aerosol particles is rather homogeneous across the region. We expect that adding the water-insoluble components (especially elemental carbon and water-insoluble organic carbon), mass concentrations will be higher in Bologna, according to what reported in literature. Carbone et al. (2010) showed that aerosol collected in Milan (Po Valley urban site) differed from the rural site of SPC for the larger amount of water insoluble carbonaceous matter (WINCM), and its enrichment in small particles confirms the important role of domestic heating and traffic-related sources at the urban site.

In November, fine particles (PM1.2) account on average for 86 (±8) % and 86 (±5) % of the total water-soluble mass in Bologna in daytime and night-time conditions, respectively. In SPC they contribute for 79 (±21) % and 49 (±13) %. In February, PM1.2 accounts on average for 89 (±4) % and 81 (±7) % in Bologna, while in SPC on average for 86 (±11) % and 79 (±12) %. Fine concentrations are obtained summing up stage 1, 2 and 3 of Berner impactor (size range 0.05-1.2 μm). Hereafter in the chapter, I will refer to fine particles as particles in the size range between 0.05 and 1.2 μm and coarse particles will be those in the size range between 1.2 and 10 μm (the sum of stage 4 and 5).

A detailed size segregated average chemical composition of aerosol particles collected in November 2011 and February 2013 in the two sites is reported in Fig.3.4, and Fig.3.5, respectively.

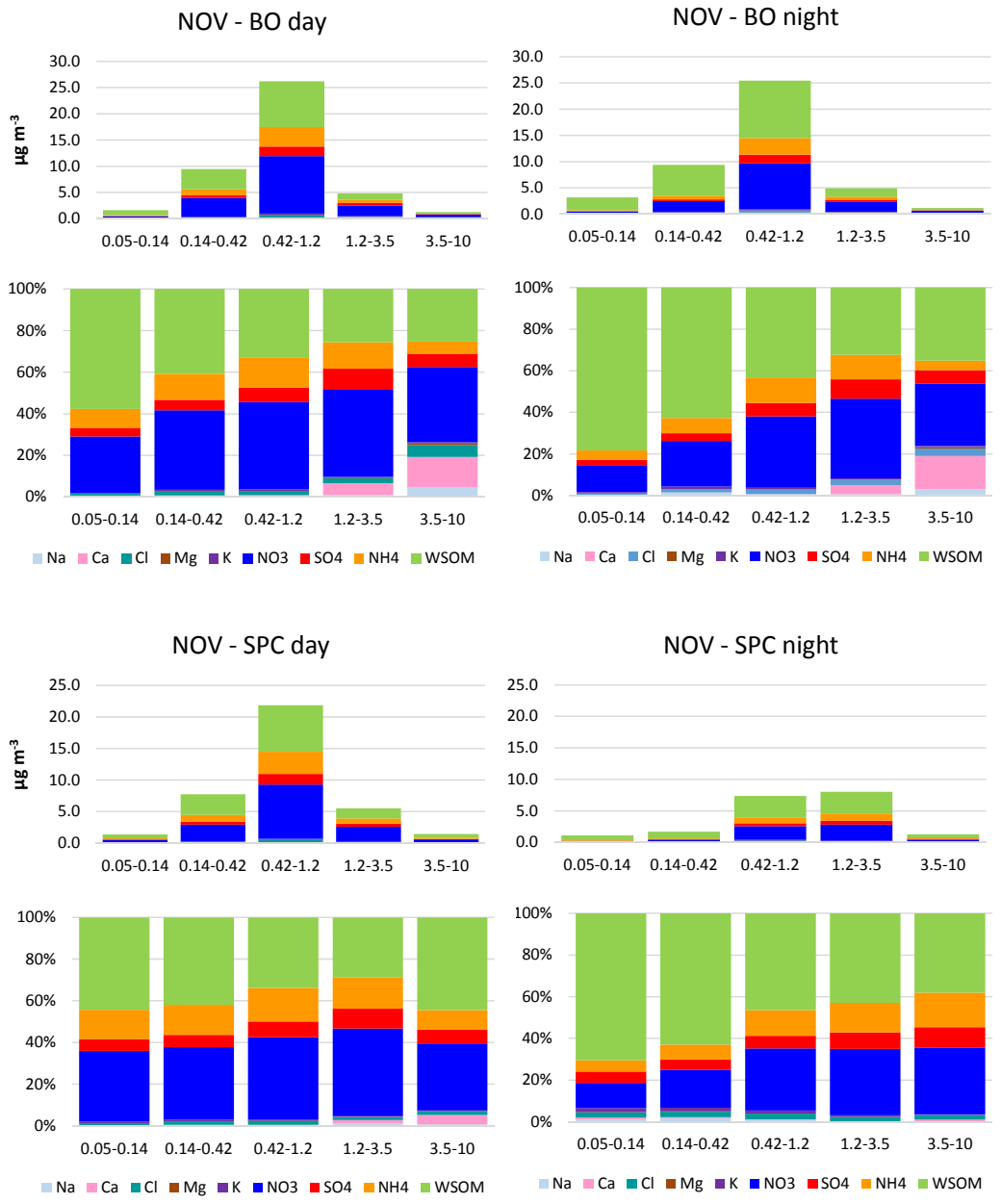

Figure 3.4. *Average size segregated absolute and relative chemical composition of aerosol particles collected in November 2011 in Bologna and San Pietro Capofiume. Samples have been divided between nocturnal and diurnal.*

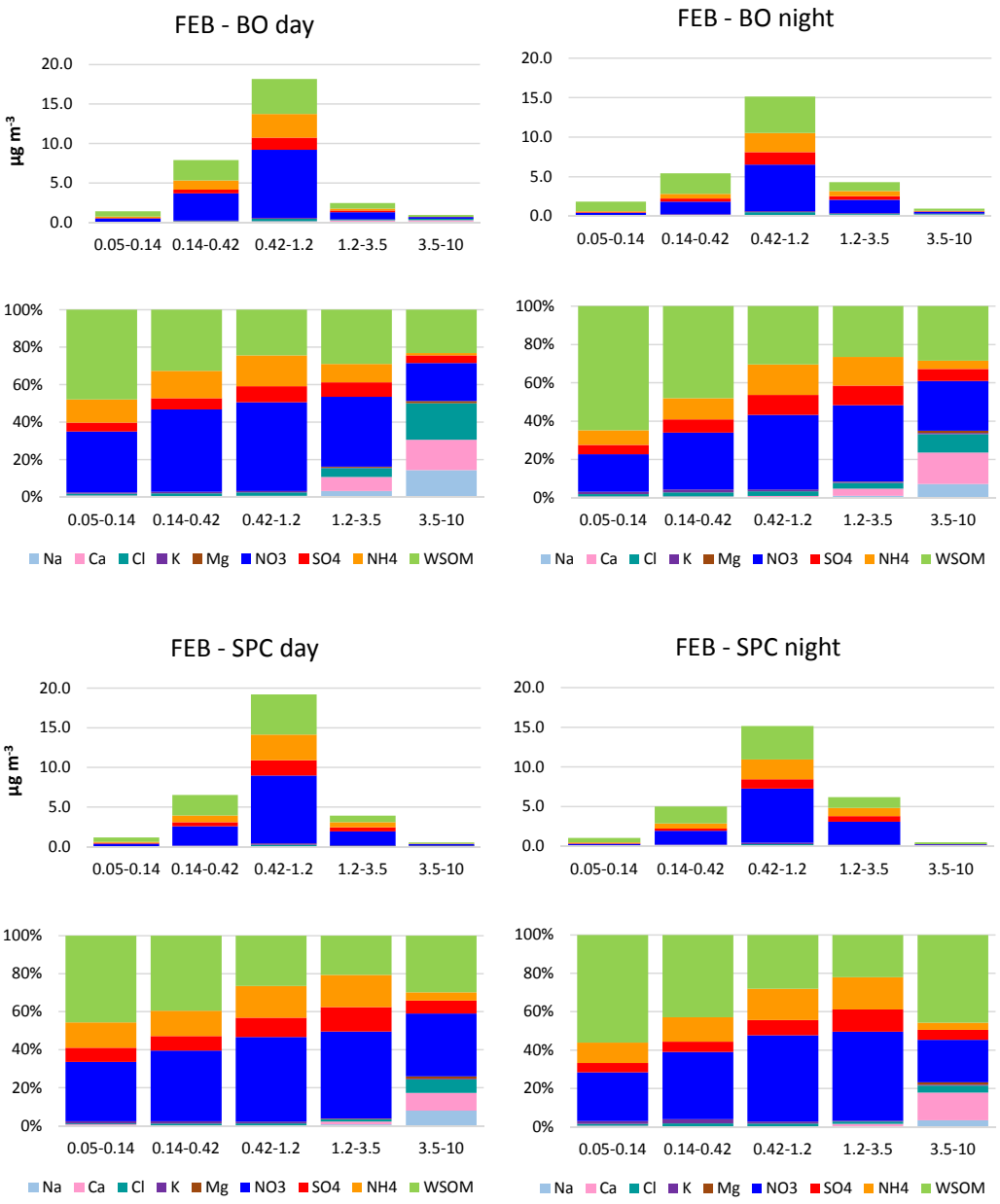

Figure 3.5. *Average size segregated absolute and relative chemical composition of aerosol particles collected in February 2013 in Bologna and San Pietro Capofiume. Samples have been divided between nocturnal and diurnal.*

The size range between 0.42 and 1.2 µm is always the most abundant in terms of mass, except for one case: nocturnal samples collected in SPC in Nov 2011. As stated above, this campaign was characterised by the occurrence of fog during the night. Fog scavenging depleted fine particles ($0.14 < D_a < 1.2$ µm), thus affecting aerosol mass size distribution. Average concentration of the third stage of Berner impactor reached a value close to that of fourth

stage. The effects of fog droplets and aerosol particles interaction will be discussed in detail in chapter 5.

Chemical composition of fine fraction is very similar in Bologna and San Pietro Capofiume, confirming that the water-soluble fraction of particulate matter over the Po Valley is mainly related to regional sources. Inorganic species in the fine fraction are dominated by nitrate, sulphate and ammonium that, in November, account together for 50 (±10) % and 51 (±9) % of the total soluble mass in Bologna and SPC, respectively. In February they account on average for 63 (±14) % and 65 (±10) % in BO and SPC. These three species are mainly distributed in the fine fraction peaking in the accumulation mode (0.14 μm < D_a <1.2 μm). These ionic species accumulate into fine particles in the form of ammonium salts. This is confirmed by the high correlation between the sum of nitrate and sulphate with ammonium: R^2 = 0.98 and R^2 = 0.99 in BO and SPC November samples, respectively, and R^2 = 0.95 and R^2 = 0.98 in BO and SPC February samples. Furthermore, this hypothesis is supported by the ionic balance (Fig.3.6), showing that ammonium is fully neutralised by the sum of nitrate and sulphate.

Ammonium nitrate dominates the chemical composition of fine aerosol in the fall winter season, in agreement with previous studies carried out in the Po Valley (Carbone et al., 2010; Lonati et al., 2007; Putaud et al., 2004; Rodriguez et al., 2007).

Water-soluble organic matter constitutes a significant fraction of fine particles soluble mass, in November accounting on average for 42 (±11) % and 44 (±10) % in BO and SPC, and in February 33 (±13) % and 32 (±9) % in BO and SPC. The homogeneous distribution of WSOM between BO and SPC is indicative of secondary processes as the main source of WSOM over the Po Valley during the investigated period. Finest particles in the size range between 0.05 and 0.14 μm are the most enriched in organic compounds, with WSOM accounting up to 86% of the total soluble mass.

Aerosol mass concentration of coarse fraction is much lower than fine fraction, accounting for 14 (±7) % and 33 (±21) % of the total soluble mass in November BO and SPC samples, and 15 (±7) % and 18 (±12) % in February BO and SPC samples.

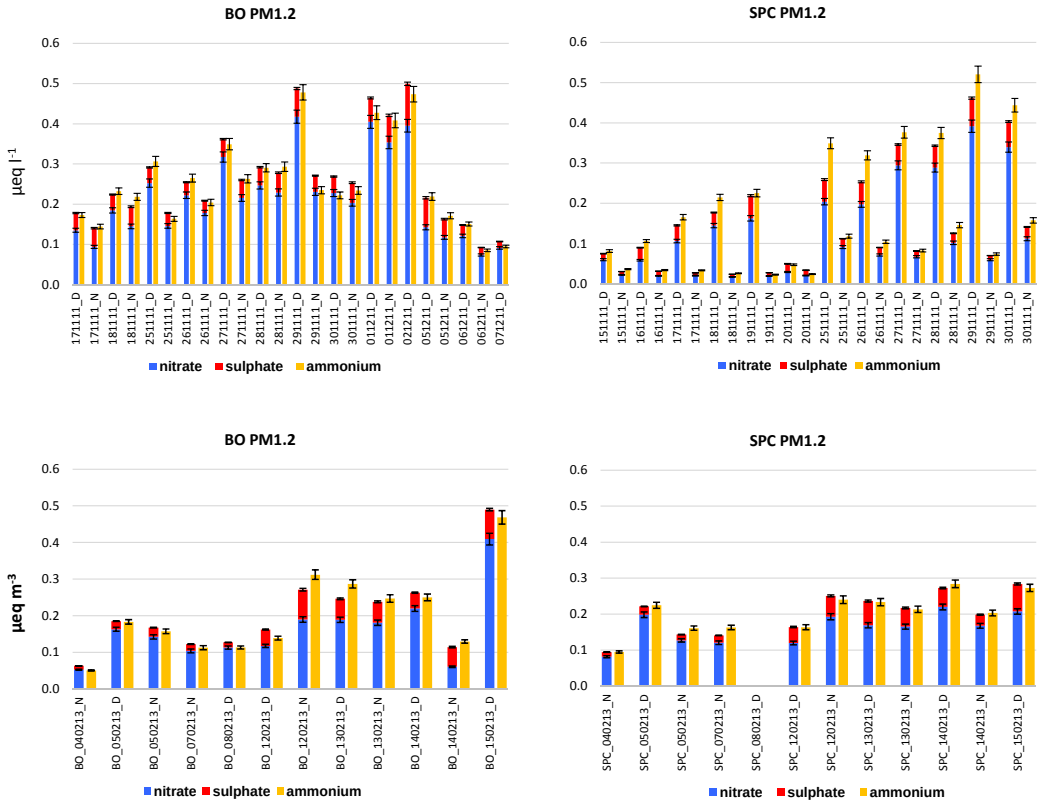

Figure 3.6. *Atmospheric concentration of the main inorganic species in fine particles (PM1.2), expressed as µeq m^{-3}, during the November 2011 (top panels) and February 2013 (bottom panels) campaigns. Error bars refer to the measurements uncertainties described in chapter 2.*

Chemical composition of coarse particles is characterized by a higher amount of Ca^{2+}, especially in samples collected in Bologna. In November, Ca^{2+} accounts for 6 (±3) % and 16 (±4) % in particles collected in Bologna with D_a in the range 1.2 - 3.5 µm and 3.5 - 10 µm respectively, and decreases to 1 (±2) % and 6 (±6) % in SPC samples. In February, Ca^{2+} accounts for 8 (±7) % and 15 (±7) % in particles collected in Bologna with D_a in the size intervals 1.2 - 3.5 µm and 3.5 - 10 µm respectively, and 3 (±3) % and 10 (±6) % in SPC samples. Calcium is generally originated from soil mineral particles (Putaud et al., 2004; Zhang et al., 2008) and its mass size distribution shows a peak in the size range 1.2 - 3.5 µm. The enrichment in calcium in Bologna samples is attributable to resuspension of soil particles caused by vehicular traffic. Aerosol sampler in SPC are located in the middle of a field, far from traffic related sources.

WSOM contribution is significant also in the coarse fraction, accounting in November for 29 (±5) % and 35 (±10) % in Bologna and SPC respectively, and in February for 30 (±8) % and 29 (±11) % in Bologna and SPC.

In February, the chemical composition of aerosol samples does not present any diurnal cycle, neither in Bologna nor in San Pietro Capofiume. The same behaviour can be observed in Bologna in November. On the contrary, samples collected in November in SPC show an evident difference between daytime and night-time composition due to the presence of fog, as will be explained in detail in chapter 5.

A detailed description of particles average chemical composition is reported in Table 3.5 and Table 3.6.

Table3.5. *November 2011*

µg m^{-3}	**NO_3^-**			**SO_4^{2-}**			**NH_4^+**			**other ions**			**WSOM**		
PM1.2	**average**	**max**	**min**	**average**	**max**	**min**	**average**	**max**	**min**	**average**	**max**	**min**	**average**	**max**	**m**
BO_D	15 ± 7	26	5.7	2.3 ± 1.1	5.0	0.87	5.1 ± 2.2	8.6	1.7	3.9 ± 5.1	20	0.5	14 ± 5	22	7.
BO_N	11 ± 5	22	4.6	2.1 ± 0.6	3.2	0.9	4.0 ± 1.5	7.4	1.5	2.8 ± 2.0	8.1	0.9	19 ± 6	32	1.
SPC_D	12 ± 7	24	1.8	2.9 ± 0.8	3.4	0.7	4.8 ± 2.7	9.4	0.9	0.9 ± 0.7	2.1	0.1	11 ± 7	25	3.
SPC_N	2.7 ± 2.1	7.0	0.8	0.6 ± 0.3	1.4	0.2	1.1 ± 0.8	2.8	0.3	0.6 ± 0.4	1.2	0.1	5.1 ± 4.0	16	1.
PM1.2-10	**average**	**max**	**min**	**average**	**max**	**min**	**average**	**max**	**min**	**average**	**max**	**min**	**average**	**max**	**m**
BO_D	2.5 ± 1.6	6.8	0.9	0.6 ± 0.8	3.1	0.2	0.7 ± 0.7	3.0	0.17	0.8 ± 0.3	1.2	0.3	1.5 ± 1.1	4.8	0.
BO_N	2.2 ± 1.0	4.4	1.3	0.5 ± 0.3	1.1	0.6	0.6 ± 0.4	1.4	0.2	0.7 ± 0.2	1.2	0.26	2.0 ± 0.8	3.5	0.
SPC_D	2.8 ± 2.8	11	0.6	0.6 ± 0.5	2.1	0.2	1.0 ± 1.0	3.8	0.2	0.4 ± 0.2	0.9	0.15	2.0 ± 1.9	6.8	0.
SPC_N	2.9 ± 1.1	4.7	1.2	0.7 ± 0.3	1.6	0.3	1.3 ± 0.4	1.9	0.59	0.3 ± 0.1	0.5	0.0	3.7 ± 2.5	12.4	1.

Table3.6. *February 2013*

µg m^{-3}	NO_3^-			SO_4^{2-}			NH_4^+			other ions			WSOM		
PM1.2	**average**	**max**	**min**	**average**	**max**	**min**	**average**	**max**	**min**	**average**	**max**	**min**	**average**	**max**	**min**
BO_D	13 ± 7	25	7.0	2.1 ± 1.2	3.9	0.7	4.3 ± 2.3	8.4	2.0	0.9 ± 0.6	1.7	0.3	7.7 ± 3.8	13	3.5
BO_N	7.6 ± 3.7	12	3.3	2.0 ± 1.3	3.9	0.5	3.0 ± 1.7	5.6	0.9	0.9 ± 0.2	1.3	0.6	7.8 ± 2.4	10	3.3
SPC_D	11 ± 2	14	7.4	2.5 ± 1.0	3.7	1.1	4.2 ± 0.9	5.1	2.9	0.6 ± 0.4	1.2	0.2	8.2 ± 3.8	13	3.7
SPC_N	8.8 ± 2.4	12	5.1	1.5 ± 0.9	2.8	0.6	3.2 ± 0.9	4.3	1.7	0.7 ± 0.2	0.9	0.3	7.0 ± 1.2	8.3	5.7
PM1.2-10	**average**	**max**	**min**	**average**	**max**	**min**	**average**	**max**	**min**	**average**	**max**	**min**	**average**	**max**	**min**
BO_D	1.1 ± 0.8	2.4	0.2	0.2 ± 0.2	0.5	0.1	0.3 ± 0.3	0.8	0.0	0.9 ± 0.6	1.7	0.2	0.9 ± 0.5	1.7	0.4
BO_N	2.0 ± 1.7	4.3	0.3	0.5 ± 0.5	1.2	0.1	0.7 ± 0.8	2.0	0.0	0.7 ± 0.4	1.4	0.4	1.4 ± 0.7	2.3	0.9
SPC_D	2.0 ± 2.2	5.9	0.6	0.5 ± 0.7	1.7	0.1	0.7 ± 1.0	2.4	0.2	0.3 ± 0.2	0.5	0.1	1.0 ± 0.5	1.7	0.4
SPC_N	3.0 ± 2.9	7.6	0.5	0.7 ± 0.9	2.3	0.06	1.1 ± 1.2	2.9	0.0	0.3 ± 0.1	0.5	0.1	1.6 ± 0.6	2.5	1.0

In wintertime, soluble species represent the main compounds of aerosol particles in the Po Valley, especially for the fine fraction. In (Matta et al., 2003) they account for more than 70% of PM10 mass and in (Carbone et al., 2010) their contribution ranges from 40 to 70% of submicron aerosol mass. Our results show a rather homogeneous chemical composition of this fraction in both urban and rural site, confirming the dominant role of regional secondary processes in particles formation under typical winter conditions. Sources of secondary aerosol in the whole area of the Po Valley, together with long-range transport processes (Alves et al., 2012; Maurizi et al., 2013) should be taken into account in order to adopt effective pollution abatement strategies.

4. Fog chemical composition in the Po Valley

In the Po Valley (northern Italy), the occurrence of radiation fog episodes is very frequent during the fall-winter season in condition of stagnation of air masses. These meteorological conditions together with the low mixing layer heights favour the development of critical pollution episodes. The interaction between fog droplets and the pollutants emitted in the atmosphere may have an important impact on the local environment, on the agriculture and on the human health.

For this reason, the study of the chemical composition of fog droplets in the Po Valley is a very interesting topic. At the field station of San Pietro Capofiume, the first fog sampling activities date back to the beginning of the '80s. Initially fog water was sampled only during scheduled field campaigns. Starting from 1989, a systematic activity of fog sampling was established. During the fall-winter season (from November to March) each episode of dense fog was recorded and fog droplets were sampled and then analysed. Within a few hours from collection, samples were filtered on 47 mm quartz-fibre filters. A few millilitres of solution were used immediately for pH and conductivity measurements. Some aliquots of filtered fog water were stored in freezer and later analysed to determine the ionic chemical composition by ion chromatography and the water-soluble organic carbon content. The same procedure is still ongoing and all the data collected since 1989 enabled to build an over twenty years long database of fog water chemical composition, pH, conductivity and liquid water content (LWC). This chapter will focus on the trend of fog occurrence in the Po Valley over the years, and on the description of fog chemical composition and observation of possible time trends of the measured parameters.

4.1 Fog frequency

A decrease of the frequency and persistence of fog throughout Europe over the last decades was described by (Vautard et al., 2009). These authors report that the frequency of low-visibility conditions such as fog, mist and haze has declined in Europe over the past 30 years, for all seasons and all visibility ranges between distances of 0 and 8 km. This decline is spatially

and temporally correlated with trends in sulphur dioxide emissions, suggesting a significant contribution of air-quality improvements, i.e. reduction in the aerosol sulphate loading which act as condensation nuclei for fog formation. Similar conclusions were reached by (van Oldenborgh et al., 2010), who restricted the study of (Vautard et al., 2009) to dense fog (visibility < 200 m). This study reported that the relative temporal trends of the number of days with dense fog are comparable to the trends of days with presence of haze and mist (2 km visibility and higher), although the scatter around the mean values is much larger in the former case. These studies address particularly the regions of eastern and central Europe, north of the Alps.

For the Po Valley area, (Mariani, 2009) reported a decreasing frequency of days with fog (in this case defined as visibility < 1 km) in the Milan area with a reduction of 73% within the city and of 52% at the Linate airport, 7 km from the city centre, over the decade 1991 - 2000 with respect to the decade 1960 - 1969. A reduction of fog frequency of about 50% over the period 1949 - 1990 was also documented by (Sachweh and Koepke, 1995) for the metropolitan area of Munich. These authors attribute this reduction to the urban heat island that increases the heating of the air and causes a moisture deficit.

Visibility data collected by the Regional Environmental Agency of Emilia Romagna in the area of Bologna airport are available since 1984. Assuming fog occurrence only during the fall-winter season (November - March), they show a statistically significant reduction of 47% of annual foggy hours in the period 2004/05-2012/13 with respect to the decade 1984/85 - 1993/94, with fog defined as visibility < 1 km. Visibility data at the field station of San Pietro Capofiume are available for a shorter period: fall-winter season 1986/87 - 1998/99. The trend is consistent with that of Bologna airport, even if the absolute values are higher, as expected for a rural site, not affected by the urban heat island effect. Both trends are reported in Fig.4.1. A reduction in fog occurrence is evident until the first half of the nineties. From then on, the percentage of foggy hours during the fall-winter season is slightly variable around the mean value of 10%. These data agree with the results of the studies presented above, where clear fog reduction is documented up to 2000, and few data are available for the last decade.

Due to instrumental limits (see chapter 2) only thick fog events (visibility < 200m) have been collected in San Pietro Capofiume and then analysed. For each event, start and end time have been registered, supplying information about the hours of dense fog occurred during each fall-

winter season at the field station. These data (reported in Fig. 4.2) show a high variability within the seasons but no significant temporal trend was observed, according to the Ordinary Least Squares (OLS) regression method (Hess et al., 2001). The highest value of fog occurrence was recorded in 1998/99 (17% of time was affected by dense fog episodes) and the lowest was in 2009/10 (only 3%).

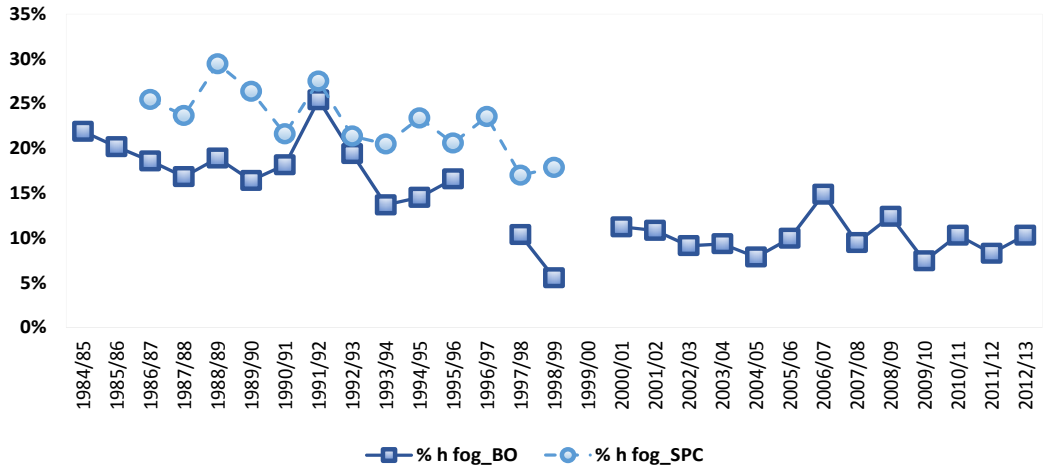

Fig. 4.1. *Time evolution of fog occurrence in Bologna airport (dark squares) and San Pietro Capofiume (light dots), expressed as percentage of foggy hours during the fall-winter season (November-March). In San Pietro Capofiume, visibility data recording stopped in 1999. Data referring to seasons 1996/97 and 1999/00 in Bologna have been rejected because measures covered less than 60% of time. (Time trends significance level > 99%).*

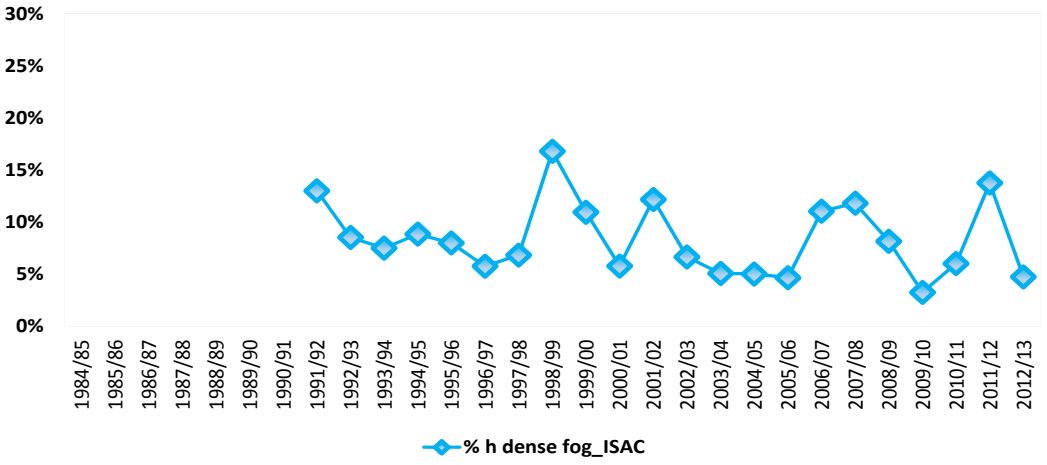

Fig. 4.2. *Time evolution of dense fog occurrence, expressed as percentage of foggy hours during the fall-winter season (November-March) registered in San Pietro Capofiume by the CNR-ISAC.*

4.2 Chemical composition of fog droplets

The first parameters taken into account were conductivity and ionic strength (IS). Conductivity has been measured directly (see Chapter 2), while IS has been calculated as a function of the concentration of all ions detected by ion chromatography, using the following equation:

$$IS = \frac{1}{2} \Sigma c_i z_i^2$$

where c_i is the molar concentration (mol l^{-1}) and z_i is the charge number of the ion i.

The two parameters are a function of the ionic content of fog water samples, so they both are indicative of the total pollution loading of the atmosphere where fog droplets form. The volume-weighted means of conductivity and IS have been calculated for each season (from November to March) from 1989/90 to 2010/11 and are reported in Fig.4.3. Panel A shows the volume weighted means of ionic strength and panel B refers to conductivity. Coloured areas on the plots represent the standard deviations of the calculated averages. Ion content from 1989/90 to 1992/93 was not available, so IS has not been calculated for those years.

Both IS and conductivity trends show a significant decrease: 82% and 80%, respectively (IS from 1993/94 to 2010/11 and conductivity from 1989/90 to 2010/11). The statistical significance of all the trends reported in this chapter has been calculated according to the Ordinary Least Square (OLS) regression method (Hess et al., 2001).

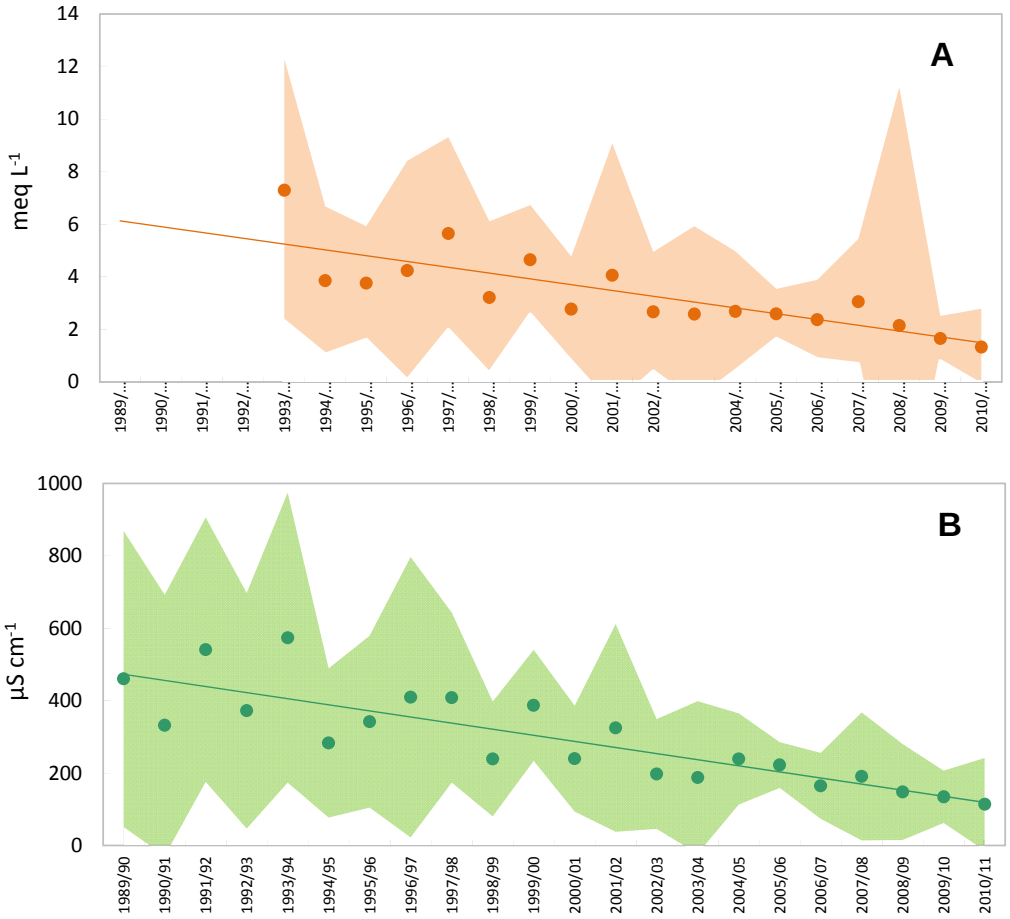

Figure 4.3. *Volume weighted averages of ionic strength (A) and conductivity (B). Coloured areas are standard deviation of the averages (represented by the dots). (Time trends significance level > 99%).*

Ionic composition of fog water samples have been determined by ion chromatography. The detected inorganic ions are: sodium (Na^+), ammonium (NH_4^+), potassium (K^+), magnesium (Mg^{2+}), calcium (Ca^{2+}), chloride (Cl^-), nitrate (NO_3^{2-}) and sulphate (SO_4^{2-}). A statistical summary of their concentration (mmol L^{-1}) is reported in Fig.4.4. Box plots indicate the 25th, median and 75th percentiles and whiskers the 10th and 90th percentiles. Data reported in plots refer to the period 1993/94 – 2010/11. Previous chromatographic data are not available, as already explained. It should be noticed that y axes scale (meq L^{-1}), is very different from species to species.

Medians, 10° percentile and 90° percentile of all ion concentrations are reported in detail in Table 4.1.

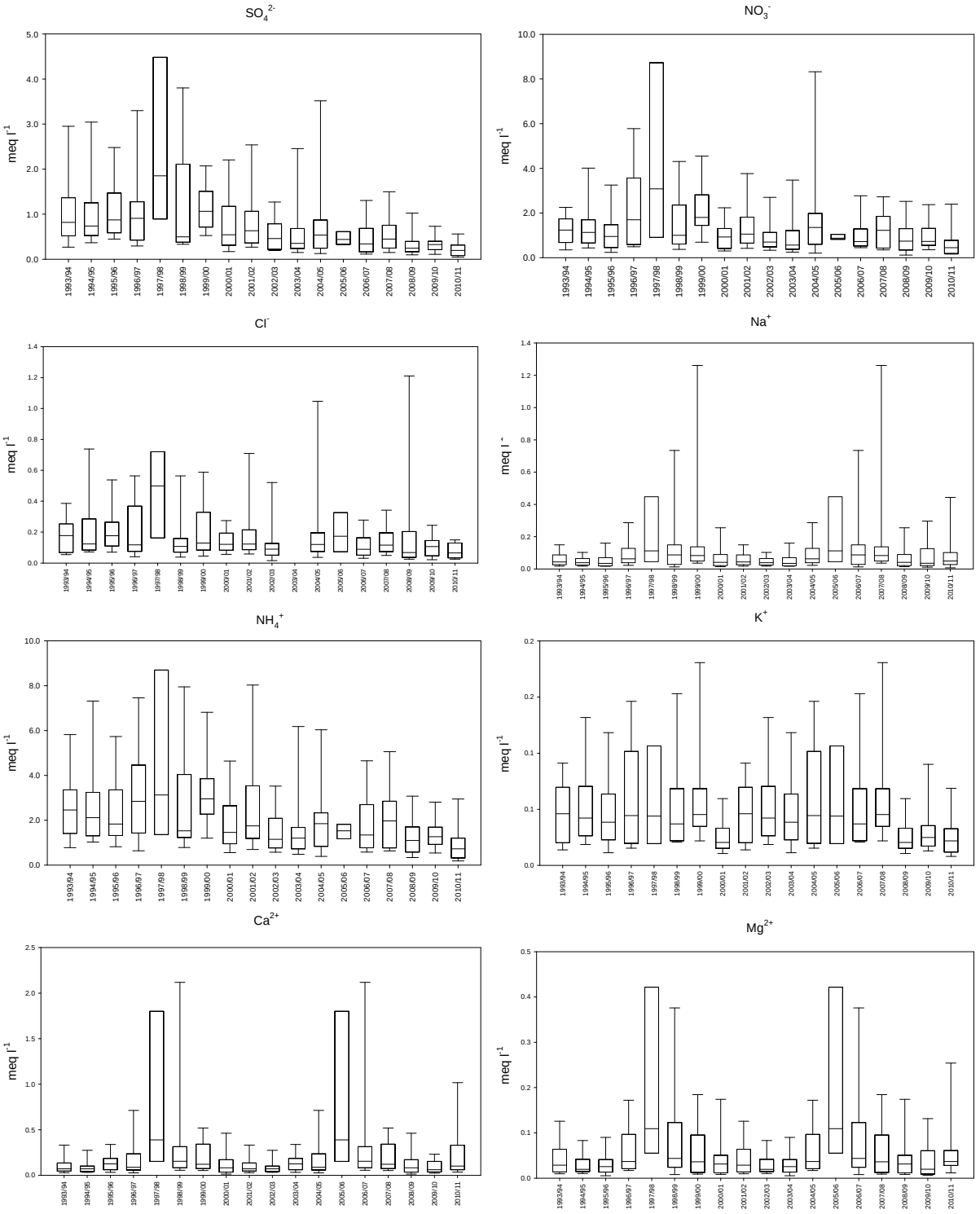

Figure 4.4. *Statistical summary of SO_4^{2-}, NO_3^-, Cl^-, Na^+, NH_4^+, K^+, Mg^{2+} and Ca^{2+} molar concentration (mmol L^{1}). Box plot indicate the 25th, median and 75th percentiles, whiskers the 10th and 90th percentiles.*

Table 4.1. *Median, 10° percentile and 90° percentile of inorganic ion concentrations (meq L^{-1}) in fog water from fall winter-season 1993/94 to fall-winter season 2010/11.*

	Cl^-			NO_3^-			SO_4^{2-}			Na^+		
meq L^{-1}	median	10° perc	90° perc	median	10° perc	90° perc	median	10° perc	90° perc	median	10° perc	90° perc
1993/94	0.18	0.06	0.35	1.2	0.38	2.2	0.82	0.30	2.2	0.04	0.02	0.14
1994/95	0.12	0.07	0.71	1.1	0.48	3.0	0.74	0.37	2.4	0.04	0.02	0.10
1995/96	0.18	0.08	0.42	0.95	0.29	2.9	0.87	0.53	2.2	0.03	0.02	0.13
1996/97	0.12	0.05	0.48	1.7	0.51	5.4	0.91	0.32	2.2	0.06	0.03	0.20
1997/98	0.50	0.13	5.0	3.1	0.60	15	1.9	0.72	7.9	0.11	0.04	4.4
1998/99	0.11	0.04	0.41	1.0	0.42	2.9	0.50	0.35	2.8	0.09	0.02	0.55
1999/00	0.13	0.05	0.48	1.8	0.83	3.7	1.1	0.60	1.7	0.08	0.04	0.38
2000/01	0.12	0.06	0.25	0.93	0.34	2.2	0.54	0.22	1.9	0.04	0.02	0.16
2001/02	0.12	0.06	0.35	1.1	0.47	3.0	0.63	0.28	2.2	0.04	0.01	0.29
2002/03	0.09	0.02	0.34	0.70	0.33	2.3	0.46	0.19	1.2	0.05	0.01	0.25
2003/04	0.00	0.00	0.00	0.57	0.30	1.5	0.35	0.17	1.3	0.10	0.03	0.15
2004/05	0.12	0.07	0.35	1.4	0.44	2.6	0.54	0.19	1.5	0.02	0.01	0.09
2005/06	0.17	0.06	0.48	0.88	0.64	1.2	0.44	0.29	0.6	0.07	0.01	0.41
2006/07	0.09	0.04	0.20	0.72	0.46	2.2	0.34	0.12	1.1	0.04	0.02	0.15
2007/08	0.12	0.05	0.28	1.23	0.39	2.3	0.45	0.16	1.2	0.06	0.02	0.29
2008/09	0.07	0.03	0.71	0.74	0.12	2.2	0.24	0.13	0.8	0.06	0.02	0.67
2009/10	0.11	0.02	0.21	0.73	0.43	2.2	0.33	0.15	0.5	0.07	0.04	0.13
2010/11	0.07	0.03	0.15	0.45	0.16	1.5	0.20	0.06	0.5	0.04	0.01	0.12
	NH_4^+			K^+			Mg^{2+}			Ca^{2+}		
meq L^{-1}	median	10° perc	90° perc	median	10° perc	90° perc	median	10° perc	90° perc	median	10° perc	90° perc
1993/94	2.5	0.84	5.2	0.05	0.02	0.08	0.03	0.01	0.10	0.07	0.03	0.21
1994/95	2.1	1.1	6.1	0.04	0.02	0.12	0.02	0.01	0.07	0.07	0.03	0.25
1995/96	1.8	0.93	5.2	0.04	0.01	0.10	0.03	0.01	0.07	0.13	0.04	0.28
1996/97	2.9	0.68	5.7	0.04	0.02	0.13	0.04	0.02	0.16	0.09	0.04	0.54
1997/98	3.1	1.1	11	0.04	0.02	0.39	0.11	0.05	2.84	0.39	0.12	6.40
1998/99	1.5	1.0	6.7	0.04	0.02	0.12	0.04	0.01	0.24	0.15	0.06	0.93
1999/00	3.0	1.3	5.3	0.05	0.02	0.15	0.04	0.01	0.15	0.12	0.05	0.44
2000/01	1.5	0.62	4.4	0.02	0.01	0.06	0.03	0.01	0.12	0.08	0.02	0.39
2001/02	1.8	0.71	5.9	0.02	0.01	0.07	0.02	0.01	0.11	0.06	0.03	0.22
2002/03	1.2	0.67	2.9	0.02	0.01	0.05	0.04	0.01	0.15	0.10	0.04	0.45
2003/04	1.2	0.59	3.0	0.01	0.01	0.03	0.04	0.02	0.08	0.11	0.06	0.27
2004/05	1.9	0.67	2.7	0.02	0.00	0.03	0.02	0.01	0.09	0.07	0.03	0.31
2005/06	1.5	0.88	2.0	0.01	0.00	0.02	0.04	0.01	0.16	0.12	0.08	0.22
2006/07	1.3	0.70	4.2	0.01	0.01	0.04	0.02	0.01	0.05	0.09	0.06	0.23
2007/08	2.0	0.69	4.3	0.02	0.01	0.04	0.04	0.01	0.10	0.10	0.04	0.31
2008/09	1.1	0.37	3.0	0.01	0.01	0.04	0.03	0.01	0.33	0.10	0.03	0.41
2009/10	1.3	0.67	2.6	0.01	0.01	0.03	0.03	0.01	0.06	0.04	0.02	0.13
2010/11	0.73	0.20	1.7	0.02	0.00	0.05	0.02	0.00	0.09	0.04	0.01	0.19

The major chemical constituents of fog water are NO_3^-, SO_4^{2-} and NH_4^+ that alone account for an average 86 (±12) % of total IS. The mean volume-weighted concentrations of the three ionic species are reported in Fig.4.5. NH_4^+, NO_3^- and SO_4^{2-} concentrations show a significant decreasing trend, as expected from the decrease of ionic strength and conductivity values over the considered period. Concentration of SO_4^{2-} in fog water decreased of 76%. NO_3^- and NH_4^+ underwent a smaller decrease: 43% and 55%, respectively. Ionic load reduction of these chemical species is explained by a parallel reduction of the atmospheric emission of fog droplets gas – phase precursors (SO_2, NO_x and NH_3). In order to verify this correlation, emission data, provided by the Italian Institute for the Environmental Protection and Research (ISPRA) (http://www.isprambiente.gov.it/banche-dati/aria-ed-emissioni-in-atmosfera), were analysed. The results are reported in Fig.4.6. Data refer to total emission in the region Emilia-Romagna from 1990 - 2010. They show a 90% reduction of SO_2 emission and smaller reductions for NOx emission (44%) and NH_3 (31%). These trends agree with those of fog chemical species, confirming the correlation between atmospheric emissions and ionic load in fog droplets composition.

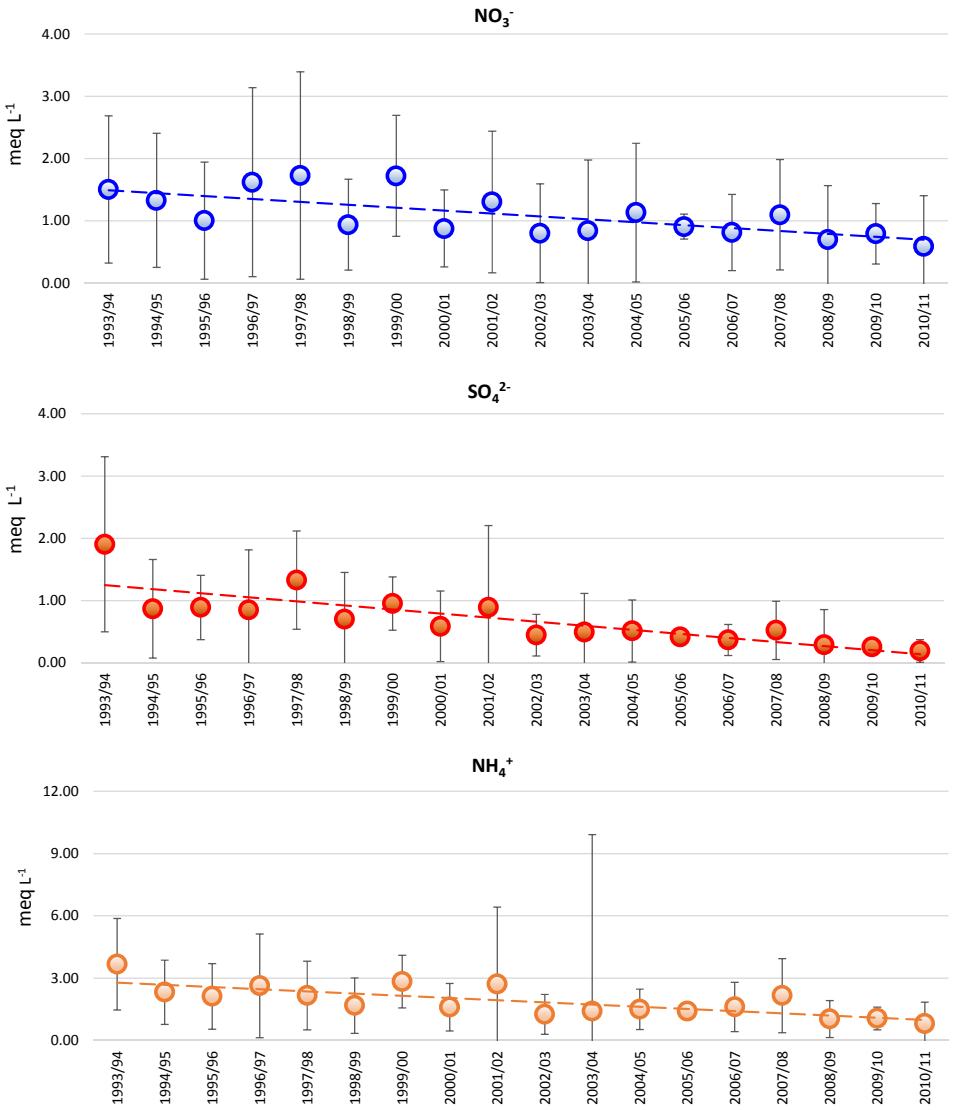

Figure 4.5. *Time trend of volume weighted means of nitrate, sulphate and ammonium concentrations (meq L^{-1}). (Time trends significance level > 99%).*

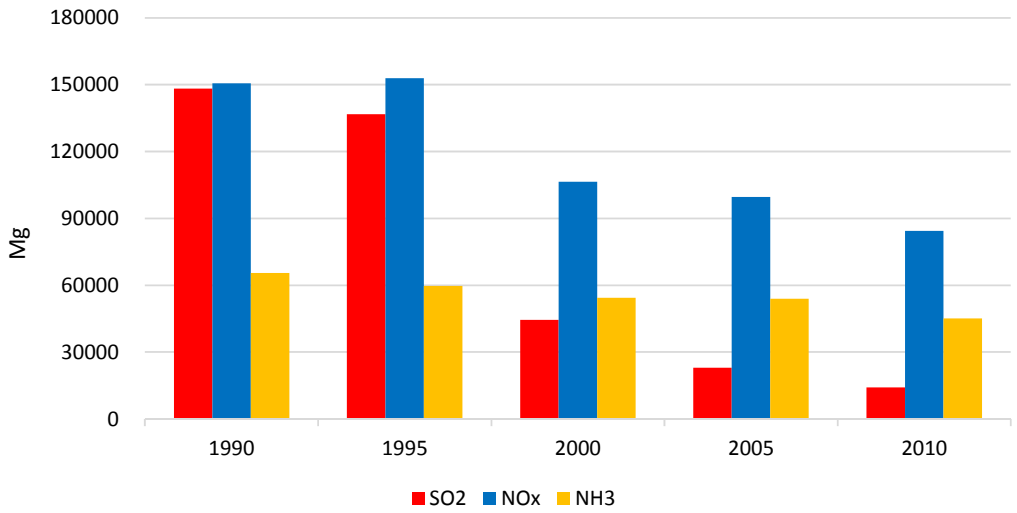

Figure 4.6. *Time trend of SO_2, NO_x and NH_3 emissions relative to Emilia Romagna region.*

Plotting the NO_3^-/SO_4^{2-} equivalent ratio over the considered period (Fig.4.7) an increase is observed, which confirms the higher decrease of sulphate compared to nitrate. NO_3^-/SO_4^{2-} ratio was close to 1 until the end of the nineties, then increased reaching the value of ~3.0 during the season 2010/11. The lower reduction achieved for NO_x emissions compared to SO_2 led to a fog composition where nitrate amount is twice, up to three times, that of sulphate. At the beginning of the nineties, the relative contribution of both nitrate and sulphate to the total ionic load was very similar, with values close to 20%. In the last years, nitrate become the main inorganic anion with a contribution to the total ionic amount of 34% in 2009/2010 and 32% in 2010/11. Conversely, sulphate contribution decreased, accounting for only 11% and 10% in 2009/2010 and in 2010/11, respectively.

Minor ions (Na^+, K^+, Mg^{2+}, Ca^{2+} and Cl^-) are the less concentrated ions. Together they account on average for 13 (±11) % of the total ionic content. Among the minor ions, only K^+ concentration shows a significative reduction, while the others do not show any significative trend. Water-soluble potassium has been used extensively as an inorganic tracer of the biomass burning contributions to ambient aerosol (Favez et al., 2010; Zhang et al., 2010). Its decreasing amount is attributable to changes in agricultural activity. A more severe legislation regulates the disposal of agricultural wastes, which previously were usually burned. Mean volume-weighted concentrations of K^+ on an equivalent basis is reported in Fig.4.8.

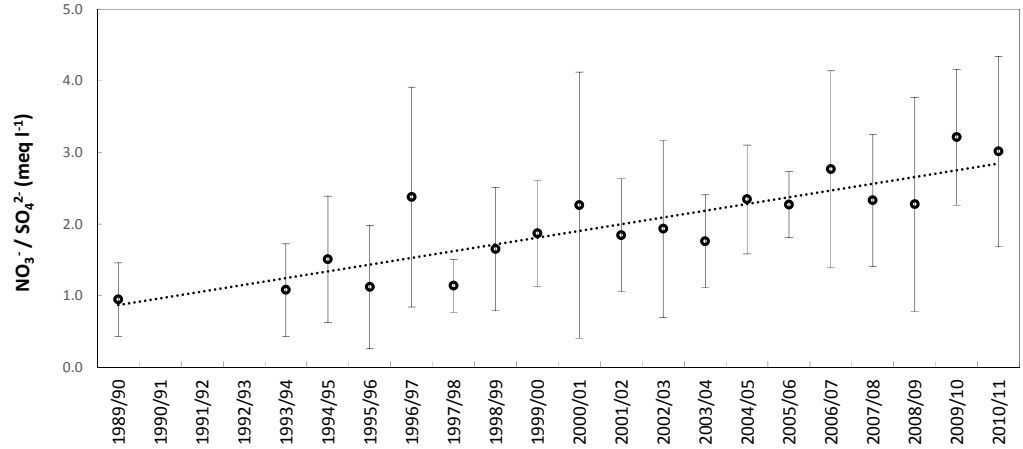

Figure 4.7. *Time trend of NO_3^-/SO_4^{2-} ratio. (Time trend significance level > 99%).*

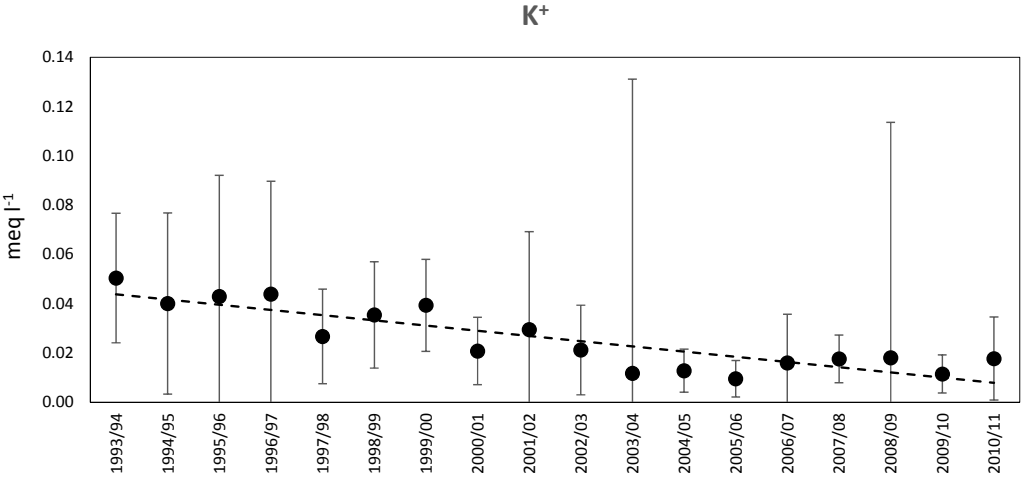

Figure 4.8. *Time trend of volume weighted means of potassium concentration (meq L^{-1}). (Time trend significance level > 99%).*

These results are in line with other studies carried out in Europe (Lange et al., 2003), where a reduction of ionic concentration in fog water was observed and attributed to an improvement of air quality pursued since the 1990s.

4.3 Liquid water content (LWC)

Another parameter systematically measured over the period of interest is liquid water content (LWC) of fog samples. It is expressed as grams of water per cubic metre (g m^{-3}) and it is measured in continuous by a Particulate Volume Monitor PVM-100, with a 1 minute time resolution (see Chapter 2). LWC values were averaged over the sampling time in order to have an average value of LWC for each fog sample. The statistical summary of LWC values from 1993/94 to 2010/11 is reported in Fig.4.9. Data are not available for the fall-winter season 2005/06. LWC values are variable within each season, with values ranging from 0.08 g m^{-3}, which is the lower threshold established for sampling starting, to 0.82 g m^{-3}. No significative trend is observed over the considered period.

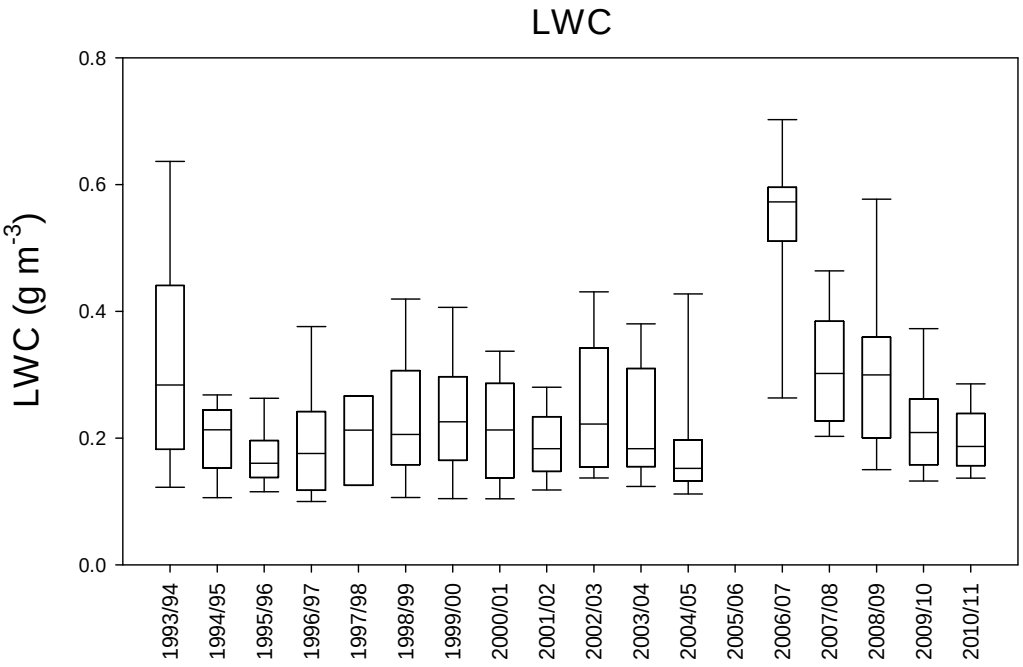

Figure 4.9. *Statistical summary of LWC values. Box plot indicate the 25th, median and 75th percentiles, whiskers the 10th and 90th percentiles.*

There are many studies in literature about the influence of LWC on soluble species concentration. An inverse relationship has been observed in previous studies between ion

concentrations and LWC, although with a different trends in different locations (Aleksic and Dukett, 2010; Elbert et al., 2000; Elbert et al., 2002; Kasper-Giebl, 2002; Straub et al., 2012). The plot in Fig.4.10 shows the sum of molalities of nitrate and sulphate as a function of LWC for the data recorded at San Pietro Capofiume from 1993/94 to 2010/11.

The best fit for the data was calculated using the following equation:

$$m = b\ L^{-1}$$

where m is the molality of a substance in fog water (µmol kg^{-1}), L the liquid water content (g m^{-3}) and b the regression slope obtained plotting measured m versus corresponding L^{-1}. This equation was chosen according to (Elbert et al., 2000), that suggested its suitability for samples of different origins, such as marine and polluted continental.

Best fit is represented by the thick solid line in the plot. Thin lines were calculated the same way, but slope values (b) derive from the 5^{th} and 95^{th} percentile molality values. Even if a decreasing anion molality with increasing LWC can be discerned, the power law best fit shows a very low correlation ($R^2 = 0.03$), indicating that variation in LWC values only minimally affect ions concentrations. This observation together with the fact that no statistically significant trend was found for LWC values, strengthen the hypothesis that the decreasing ionic load in fog water is not due to a “dilution” effect, but is connected with lower atmospheric emission of gaseous precursors.

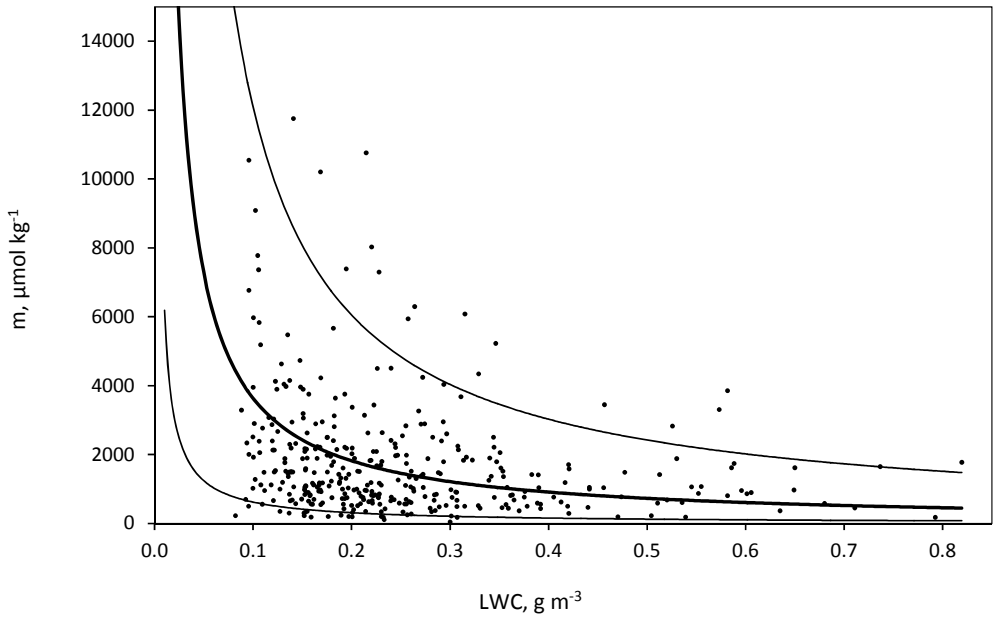

Figure 4.10. *Correlation between LWC and the sum of sulphate and nitrate molalities. Thick line is the power law best fit, while thin lines were calculated using the 5th and the 95th percentile values of molalities. No samples were collected at LWC < 0.08 g m^{-3} because of technical limitations (see chapter 2).*

4.4 Fog water acidity

Until the eighties, many studies were carried out about the acidity of cloud water, fog water, rain and snow, especially in the industrialized countries of the northern hemisphere, where increasing combustion processes caused the acidification of the atmospheric liquid water phase (Jacobson, 1984; Wisniewski, 1982) (Saxena and Lin, 1990). (Fuzzi et al., 1983) focused on the pH trend during the evolution of a fog event in the Po Valley, stressing the crucial role of NO_3^- and SO_4^{2-} in the determination of fog acidity. From then on, fog pH values have been regularly measured at the field station of San Pietro Capofiume. Fig.4.11 shows the statistical summary of pH value of each season from 1989/90 to 2010/11.

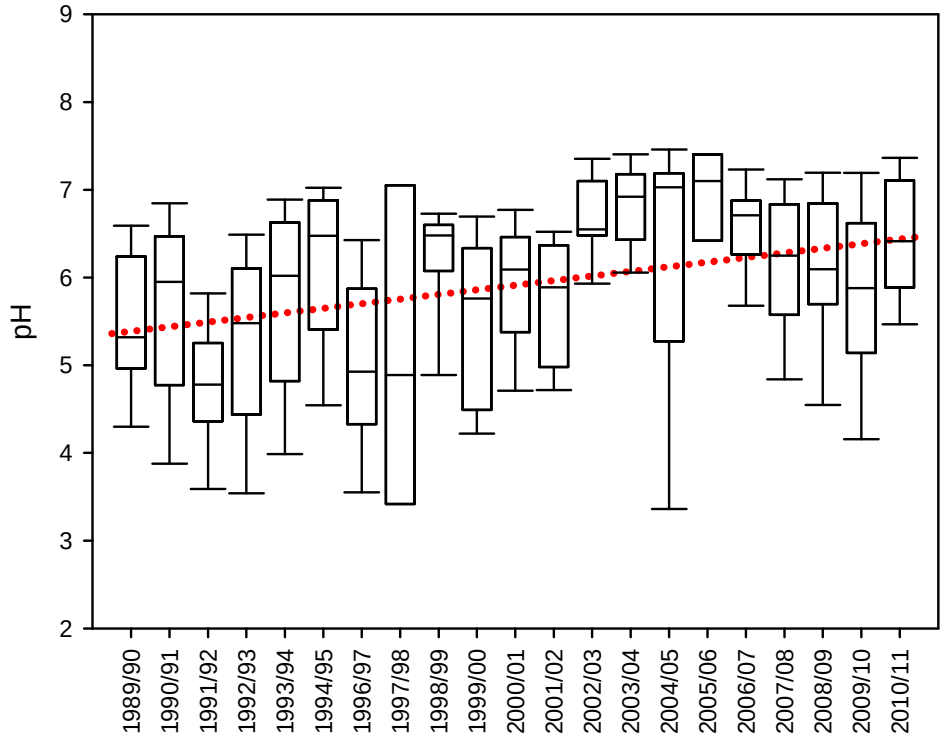

Figure 4.11. *Statistical summary of pH values. Box plot indicate the 25th, median and 75th percentiles, whiskers the 10th and 90th percentiles. Regression line (red dotted line) shows an increasing trend (significance level > 99%).*

Despite the variability of pH values within each season (in 2004/05 pH ranged from 3.4 to 7.5), pH shows an increasing trend, at a 99% confidence interval. The calculated volume weighted means show that during the 90s the mean pH values never exceeded 5, ranging from the lowest average pH in 1995/96 (3.6) to the highest in 1998/99 (4.7). In the last decade, the lowest average pH value was 4.1 in 2001/02 and the highest reached 6.9 in 2005/06 with values mostly exceeding 5. This reduction of fog acidity is what we expected from the observed decrease of NO_3^- and SO_4^{2-} concentrations in fog water.

The pH trend leads to a condition of neutrality in fog water presently collected, even though it should be taken into account that these pH values refer to bulk sample and not to single fog droplets. Anyway, the achievement of a pH neutral condition is linked to the lower decrease of ammonia emissions compared to those of SO_2 and NO_x that represent the precursors of the two major acidic species in solution.

4.5 Organic fraction of fog droplets

So far, only the inorganic components of fog water were taken into account. We saw that sulphate, nitrate and ammonium together account for near 90% of the total ionic strength of fog water. Besides these three main ionic species, the organic matter must also be evaluated, representing a significant fraction of the total mass of fog water, and playing a role in determining the physical - chemical characteristics of fog droplets and residual aerosol particles after water evaporation.

Starting from fall-winter season 1997/98, WSOC has been systematically measured with the purpose to implement the knowledge about the organic fraction of fog droplets. The average chemical composition of fog water over the period 1997/98 - 2010/11 is reported in Fig.4.12.

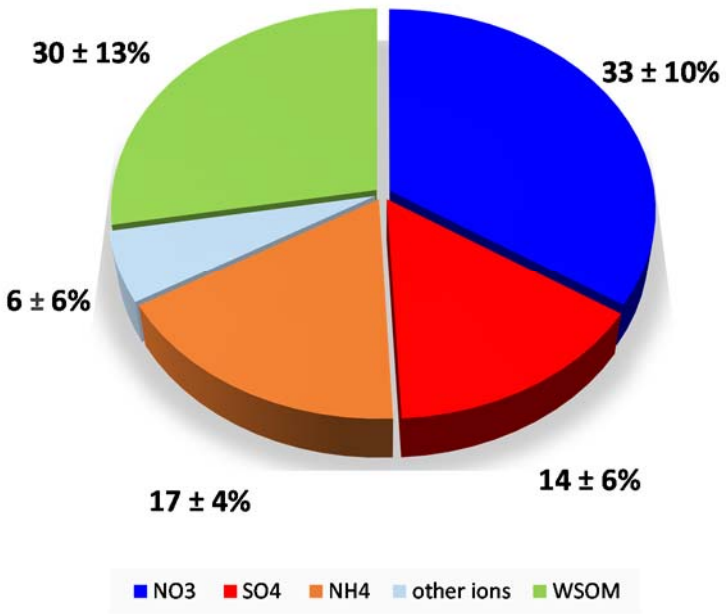

Figure 4.12. *Average chemical composition of fog water over the period 1997/98 - 2010/11.*

The three main ionic species together account on average for 67% of the total soluble mass and water-soluble organic matter (WSOM) for 28%. A factor of 1.8 was used to convert water-

soluble organic carbon (WSOC) to water-soluble organic matter (WSOM), according to the literature (Matta et al., 2003).

Fig.4.13 shows a statistical summary of WSOC concentration in fog water collected at San Pietro Capofiume. Concentrations can be very variable within each season and no significative trend is observed from 1997/98 to 2010/11. Values range from 3 mgC L^{-1} to 350 mgC L^{-1}. Seasonal median concentration range from 15 mgC L^{-1} in 2002/2003, to 49 mgC L^{1} in 1999/2000.

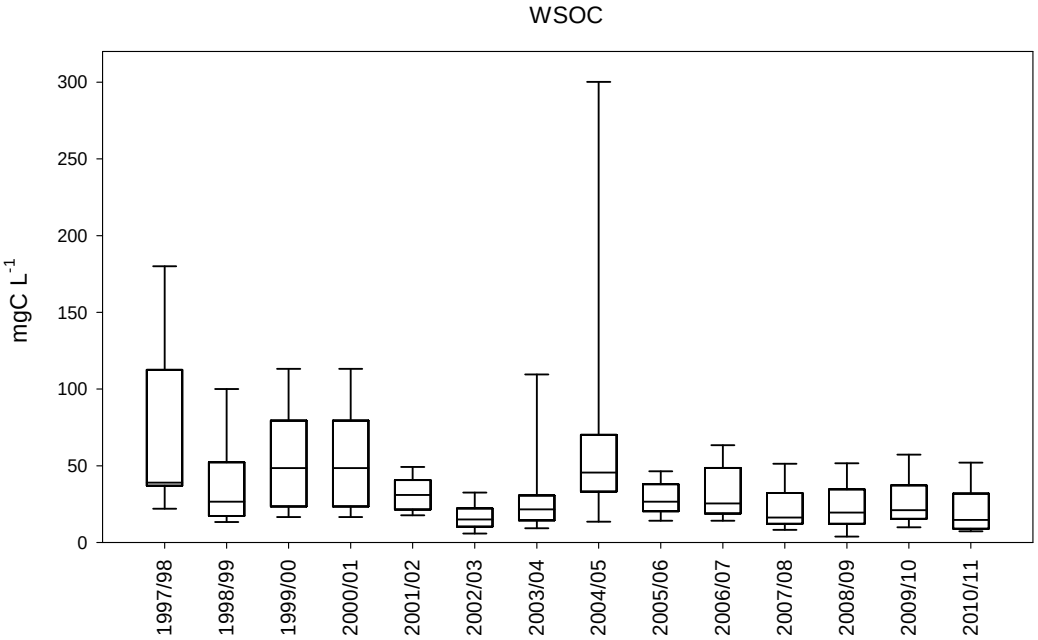

Figure 4.13. *Statistical summary of WSOC concentration (mgC L^{-1}). Box plot indicate the 25th, median and 75th percentiles, whiskers the 10th and 90th percentiles*.

Previous studies carried out at the field station of San Pietro Capofiume, showed that the absorption of gases contributes for about 3% to the fog droplets organic fraction, while the contribution of the coagulation of interstitial particles is negligible (Facchini et al., 1999). Nucleation scavenging has been found to be the most important source of soluble organic compounds in fog droplets in the Po Valley region.

Specific studies have been carried out to characterise the organic fraction of Po Valley fog samples. (Facchini et al., 1992), focused on the gas-liquid phase partitioning of carbonyl compounds, formaldehyde (HCHO), formic acid (HCOOH) and acetic acid (CH_3COOH), which in the Po Valley mainly originate from anthropogenic sources. Further efforts have been made to implement the characterization of the organic fraction. An analytical method was developed for this purpose, combining HPLC and HNMR techniques, and described in (Decesari et al., 2000). This methodology classifies WSOC into a few major classes of compounds, attempting a characterization and quantification of the functional groups, instead of a definition of individual molecular species. They found that 25% of soluble organic carbon derived from neutral and basic compounds, 35% from mono and dicarboxylic acids and 17% from polyacids, showing that the organic fraction was formed for more than 50% by acidic compounds. The unaccounted fraction (23%) was due to losses of material during the different phases of the analytical procedure. These results were confirmed in a later study reported in (Fuzzi et al., 2002), where a similar relative organic carbon content was determined. They also detected a class of polycarboxylic acids similar to fulvic acids. These studies showed that a significant fraction of WSOC in fog droplets is not volatile and cannot originate via condensation from the gas phase. The most plausible source of such non-volatile water-soluble organic matter is nucleation scavenging of aerosol particles, because polyacids are also found in submicron particles out of fog conditions (Decesari et al., 2000; Decesari et al., 2001). On the other hand, recent laboratory studies indicate that low-volatility compounds can form through aqueous phase reactions starting from volatile precursors (Ervens et al., 2011; Lim et al., 2013; Tan et al., 2012). These studies therefore suggest that complex, high-molecular water-soluble organic compounds in fog droplets can form as secondary compounds, along with the most common products such as pyruvic acid and oxalate.

Unfortunately, due to its time consuming nature, the analytical procedure described above was not applied to the whole series of available fog samples. Only low molecular weight carboxylic acids, acetic acid (CH_3COOH), formic acid (HCOOH), methanesulfonic acid (CH_3SO_3H) and oxalic acid ($C_2H_2O_4$), have been systematically detected and quantified by ion chromatography. Concentrations are very variable from sample to sample, ranging from a few to several hundreds $\mu mol\ L^{-1}$. A statistical summary of the data is reported in Table 4.2. The contribution of these low molecular weight organic acids to the total organic mass ranges from 1% to 68%, with median percentages ranging from 4%, in 2010/11, to 25%, in 1998/99.

Table 4.2. *Median, minimum and maximum of low molecular weight organic acids (µmol L^{-1}) in fog water from fall winter-season 1997/98 to fall-winter season 2010/11.*

	Concentration (µmol l^{-1})							
	Acetate		**Formate**		**Methanesulfonate**		**Oxalate**	
Season	**median**	**range**	**median**	**range**	**median**	**range**	**median**	**range**
1997/9	100	(43-163)	116	(43-314)	1.5	(0-31)	22	(7.9-106)
1998/9	98	(36-909)	91	(12-318)	n.a.	n.a.	8.0	(2.7-30)
1999/0	97	(17-290)	8.0	(0-174)	68	(0-191)	21	(3.8-82)
2000/0	36	(5.1-170)	6.8	(0-146)	47	(0-416)	12	(4.9-59)
2001/0	33	(0-239)	5.4	(0-152)	46	(0.2-358)	13	(4.9-70)
2002/0	n.a.	n.a.	n.a.	n.a.	n.a.	n.a.	8.5	(0-37)
2003/0	n.a.	n.a.	n.a.	n.a.	n.a.	n.a.	8.2	(0-60)
2004/0	59	(1.1-189)	57	(4.1-176)	0.5	(0-165)	14	(0.5-95)
2005/0	28	(6.3-125)	37	(4.2-67)	0	(0-4.3)	6.9	(0.7-13)
2006/0	4.6	(0.1-102)	18	(1.2-78)	0.1	(0-31)	5.2	(0-54)
2007/0	3.1	(0.3-60)	6.9	(0-46)	1.9	(0-13)	6.2	(0-58)
2008/0	13	(0.7-124)	18	(0-133)	0.4	(0-11)	3.6	(0-31)
2009/1	35	(7.9-184)	28	(1.6-79)	0	(0-35)	8.9	(0-30)
2010/1	14	(3.3-109)	1.7	(0.2-124)	0.7	(0-14)	0	(0-6.8)

5. Aerosol – fog interaction

In the frame of the Supersito project an intensive field campaign has been organized on November 2011, where aerosol samples were collected at the Meteorological station Giorgio Fea in San Pietro Capofiume, Bologna. A detailed description of the campaign has been provided in Chapter 3. The routine collection of fog samples at the measurement station in San Pietro Capofiume started in November 2011 and lasted until March 2012. The Supersito campaign started in 15/11/2011 and ended in 01/12/2011. The measurement period was characterized by very frequent fog episodes and 13 fog samples were collected. The list of fog samples is reported in Table 5.1.

Table 5.1. *List of fog samples collected during the Supersito field campaign at the meteorological station in San Pietro Capofiume (Bo).*

Sample name	Sample start	Sample stop	sampling time (min)
SPC141111	14/11/2011 19.30	15/11/2011 09.00	810
SPC151111	15/11/2011 09.00	15/11/2011 18.03	543
SPC151111_S	15/11/2011 18.03	16/11/2011 10.39	996
SPC161111	16/11/2011 18.00	17/11/2011 09.09	909
SPC171111	17/11/2011 17.23	18/11/2011 05.56	753
SPC181111	18/11/2011 18.20	19/11/2011 10.50	990
SPC191111	19/11/2011 17.30	20/11/2011 13.09	1179
SPC201111	20/11/2011 15.40	21/11/2011 12.30	1250
SPC211111	21/11/2011 19.00	21/11/2011 21.00	120
SPC251111	25/11/2011 19.00	25/11/2011 21.20	140
SPC261111	26/11/2011 19.00	26/11/2011 19.50	50
SPC271111	27/11/2011 19.40	28/11/2011 10.20	880
SPC281111	28/11/2011 17.10	28/11/2011 22.10	300
SPC291111	29/11/2011 18.10	30/11/2011 09.20	910

The campaign can be divided into three different periods:

- 15 - 20 November: fog occurred during the night and sometimes lasted also in the diurnal hours;
- 21 - 25 November: no fog;
- 26 November – 1 December: fog occurred during the night.

The overlap of aerosol and fog droplets sampling, supplied data both on aerosol and fog chemical composition. This combination of measurements was a precious tool to investigate the interactions between aerosol particles and fog droplets in the Po Valley and to elaborate an exhaustive description of the aerosol-fog system chemistry, which will be the topic of this chapter.

5.1 Fog scavenging

Fog droplets chemical composition is initially determined by the chemical composition of the aerosol particles that act as cloud condensation nuclei (CCN). Once fog formed, absorption of gases, aqueous phase reactions and particles uptake can change its composition as well as the composition of residual particles after water evaporation (Arends, 1996; Fuzzi et al., 1992b).

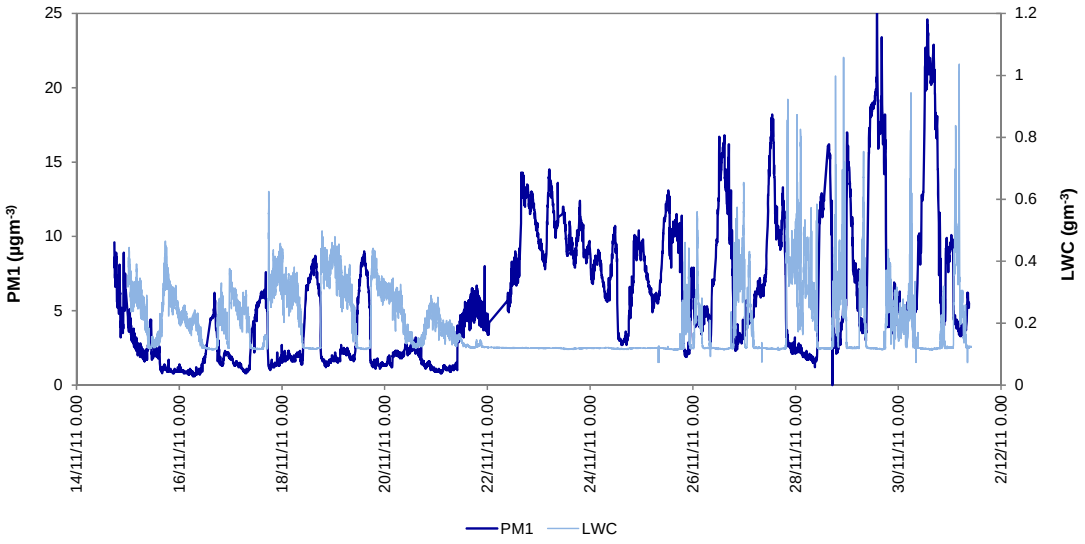

Figure 5.1. *PM1 concentration (µg m^{-3}) and LWC (g m^{-3}) during the Supersito field campaign in November 2011.*

PM1 concentration is controlled by the presence of fog, as observed in Fig.5.1, where trend of PM1 concentration (μg m^{-3}) and LWC values are showed. PM1 was quantified by HR-ToF-AMS. As LWC increases, and fog forms, PM1 particles undergo a sharp reduction. When fog dissipates and LWC reaches lower values, concentration raises again. This pattern was observed during the campaign, every foggy day. In clear sky conditions, PM1 average concentration is 32 (±14) μg m^{-3}. It decreases to an average 10 (±6) μg m^{-3} when fog occurs, corresponding to an average decrease of 60%.

5.1.1 Influence of fog on aerosol mass size distribution

Two aerosol samples per day were collected during the campaign on a diurnal – nocturnal basis: concerning the analysed samples, daytime samples are usually representative of out-of-fog conditions, while night-time samples represent in-fog conditions. Data presented on this paragraph are obtained from off-line analysis of Berner impactor samples (see chapter 2). Even though sampling was carried out on a five stages impactor, analysis of particles with 3.5 μm < D_a < 10 μm were not taken into account for the elaboration. This size range, corresponding to the fifth stage of Berner impactor, is the closest to the inlet. In high humidity conditions, it often gets flooded and most of the collected particles are washed out. Only a few daytime samples and no night-time samples were available for analysis, so we decided not to consider this size range. Therefore, the discussion on mass size distribution only regards particles with aerodynamic diameter between 0.05 and 3.5 μm.

Fig.5.2 shows the average aerosol mass size distribution of diurnal and nocturnal size segregated samples. The light blue area represents the average reconstructed mass of the analysed samples. Coloured lines show the average mass size distribution of every single chemical species detected by off-line analysis.

Mass size distribution is very different for diurnal and nocturnal samples. Diurnal mass size distribution shows a peak in the range 0.42 - 1.2 μm, representing on average 57 (±16) % of the total reconstructed mass. The remaining 43% is distributed among the other size ranges with smallest (0.05 μm < D_a < 0.14 μm) particles accounting for only 5 (±1) %. Diurnal mass size distribution is the typical size distribution of aerosol particles collected in fall-winter

season in urban continental environments, as reported in previous studies(Matta et al., 2003; Pennanen et al., 2007; Spindler et al., 2012).

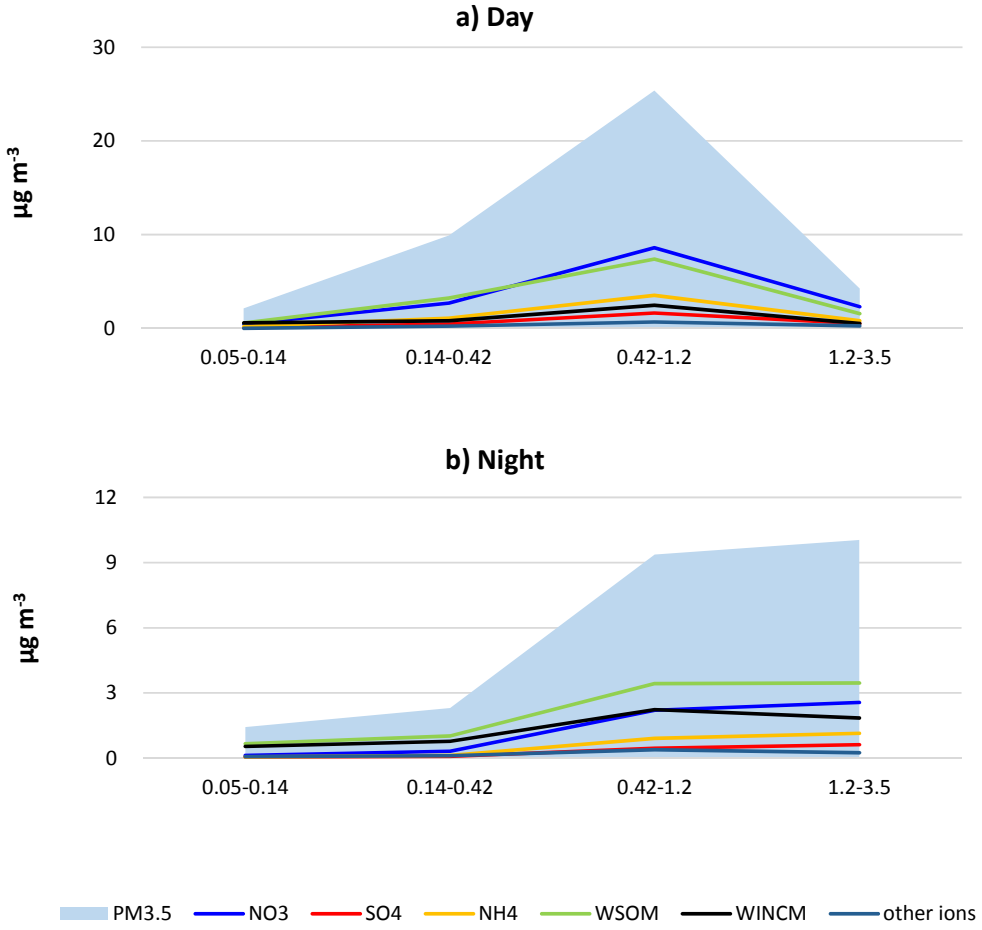

Figure 5.2. *Average aerosol total mass size distribution (µg m^{-3}) of diurnal (a) and nocturnal (b) samples and mass size distribution of the main chemical species.*

During the night, when fog occurs, mass size distribution differs significantly from the diurnal one, showing an intense decrease of particles with 0.42 µm < D_a < 1.2 µm, whose mass now accounts for 38 (±10) % of total reconstructed mass. Particles with 0.14 µm < D_a < 0.42 µm also show a sharp reduction, representing only 10 (±2) % of the total mass, compared to 23 (±4) % in daytime samples.

Compared to the diurnal conditions, there is an enrichment of particles with larger aerodynamic diameters (1.2 µm < D_a < 3.5 µm) that represents 46 (±12) % of mass, instead of 10 (±3) %. Smallest particles contribution is not affected by fog presence, accounting for 6 (±2) % of total mass in nocturnal samples.

Particles with aerodynamic diameter between 0.14 and 1.2 µm are those mostly efficiently removed by fog occurrence, as illustrated in Fig.5.3. The figure reports the relative contribution of soluble mass fraction in each stage and shows the comparison between daytime and night-time samples.

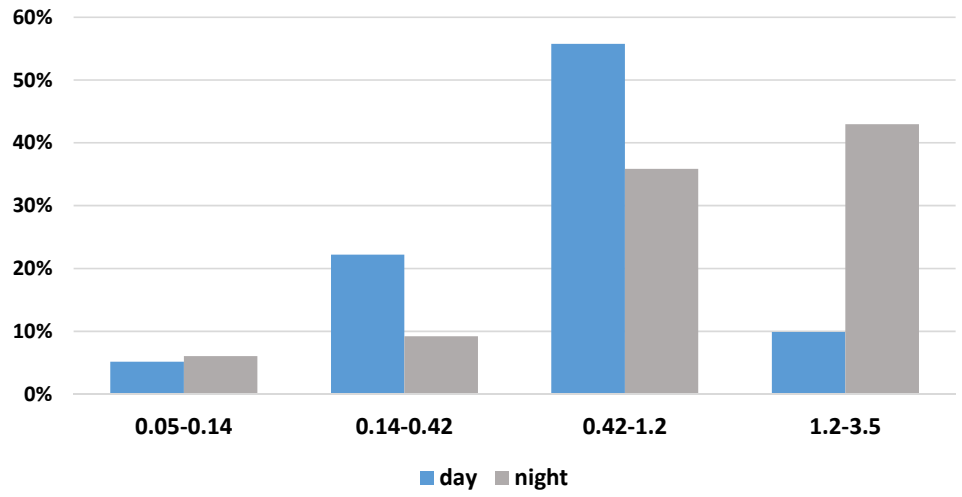

Figure 5.3. *Normalized mass contribution of each stage of Berner impactor in daytime and night-time conditions.*

The increasing mass concentration of particles larger than 1.2 µm is the result of two combined factors: the hygroscopic growth of smaller particles, not hygroscopic or large enough to be fully activated into fog droplets, and the collection of small fog droplets on the upper impactor stages (Fuzzi et al., 1992b).

Size controls particles ability to act as CCN (Dusek et al., 2006) and our data show that particles that most likely activate to form fog droplets are those included in the second and third stage of Berner impactor (0.14 µm < D_a < 1.2 µm). Particles in the size range between 0.05 and 0.14 µm are too small to act as CCN, therefore their contribution remain almost the same in

daytime and night-time conditions. These results are in agreement with previous observations reported in literature (McFiggans et al., 2006; Noone et al., 1992; Whiteaker et al., 2002).

Concerning the single chemical species considered, all of them show a peak at the size range 0.42 - 1.2 µm in daytime conditions. As fog occurs, inorganic species and water-soluble organic compounds show similar concentration both in the third and fourth stage (Fig.5.2b), while water-insoluble carbonaceous material still peaks at size range 0.42 - 1.2 µm. The behaviour of water-insoluble carbonaceous material (WINCM) is the same both in fog and out of fog, demonstrating that insoluble material is less effected by fog water scavenging than soluble species. The different behaviour between insoluble carbonaceous compounds and more soluble species indicates a certain degree of external mixing of the aerosol measured during the fall-winter season, even though the field station of San Pietro Capofiume represents a rural site, far from primary sources of particles.

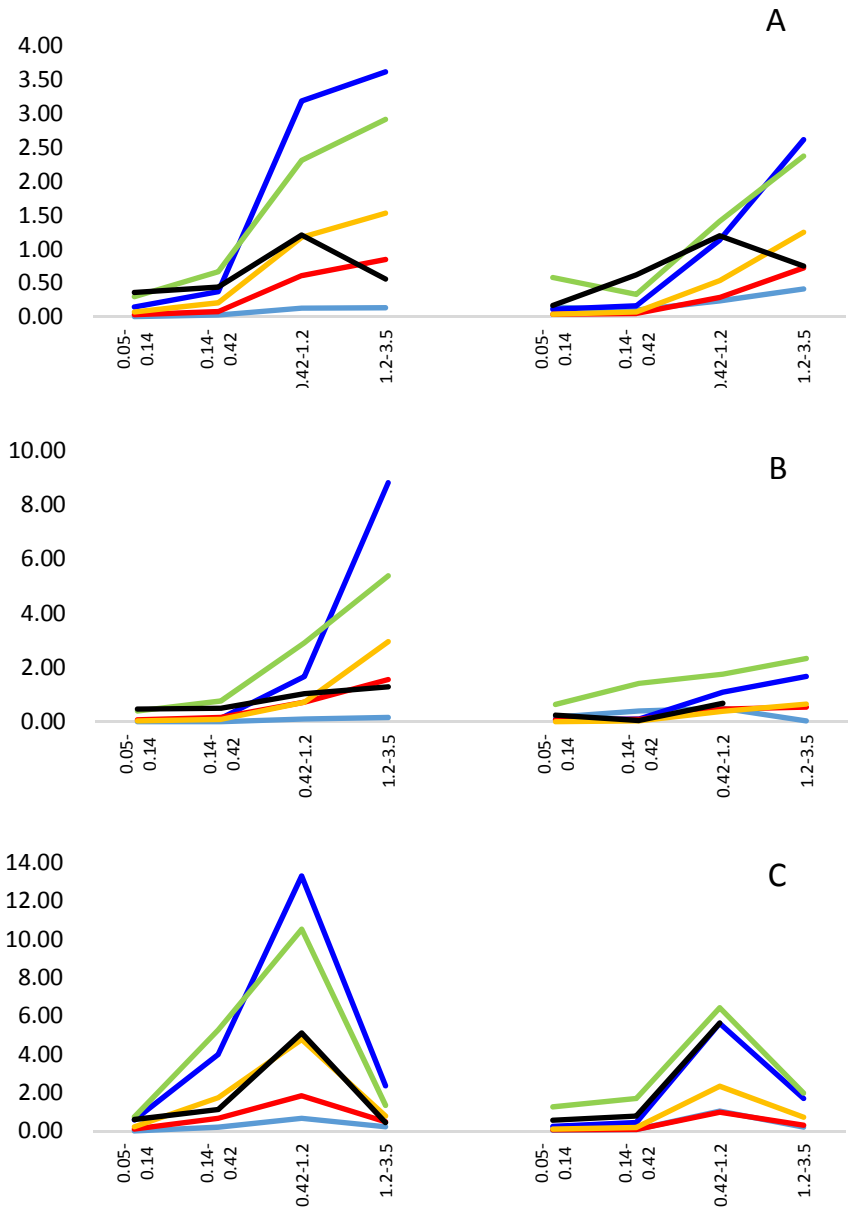

Figure 5.4. *Mass size distribution of main chemical species of daytime (left) and night-time (right) samples collected on 15/11/2011 (panel A), 20/11/2011 (panel B) and 28/11/2011 (panel C). WINCM data for the night-time samples of 20 and 28 November are missing because the aluminium substrate used to collect particles resulted flooded.*

Three couples of analysed samples show a different behaviour; their mass size distribution is reported in Fig.5.4. On 15/11/2011, panel A, fog was present also during diurnal hours, as well as in 20/11/2011, panel B. The mass size distribution is the same both in day and night samples and the profile is what we previously identified as the nocturnal one, with a maximum

concentration of soluble species in the fourth size range and the insoluble carbonaceous material still peaking at 0.42 µm < D_a < 1.2 µm. On the contrary, on 28/11/2011, panel C, fog lasted only a few hours during the night and the mass size distribution is typical of diurnal conditions for both samples. These examples confirm fog presence as the main factor driving the mass size distribution of aerosol particles in fall season in San Pietro Capofiume.

The above data show that the most interested size range by fog scavenging is that between 0.14 and 1.2 µm, while smaller and larger particles are only slightly affected. A focus on the scavenging effect on submicron aerosol chemical species was elaborated using the HR-ToF-AMS measurements, which produces data with higher size and time resolution. Fig.5.5 reports the average mass size distribution of nitrate, sulphate, ammonium, chloride and organic compounds in the two meteorological conditions: out-of-fog (left) and in-fog (right). Fine particles with vacuum aerodynamic diameter (D_{va}) larger than 200 nm shows the highest scavenging efficiency. All species show a reduction in concentration. Furthermore, peaks of nitrate (blue line) and organics (green line) shifted from 400 nm and 300 nm, respectively, to 200 nm. The peak of ammonium (yellow line) followed the same behaviour of nitrate and the broad sulphate peak (red line) at 400 - 500 nm in out-of-fog conditions smoothed over values around 200 nm.

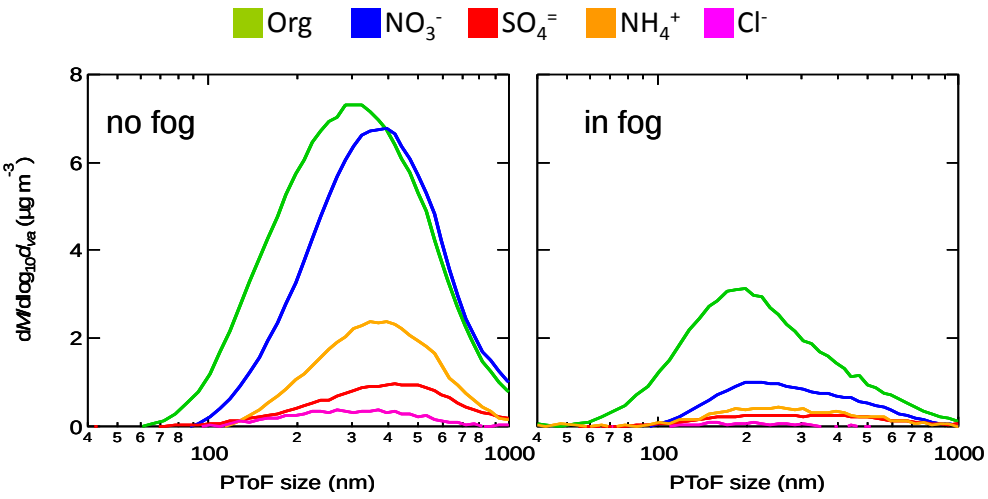

Figure 5.5. *Mass size distribution of the main chemical compounds of submicron particles out of fog (left) and in fog (right) measured by an HR-ToF-AMS and averaged over the entire campaign.*

5.1.2 Influence of fog on aerosol chemical composition

The parameters that contribute to determine the attitude of aerosol particles to be scavenged by fog droplets are both size and chemical composition (McFiggans et al., 2006). A full description of the size segregated chemical composition of aerosol particles is reported in Fig.5.6. The figure shows the relative contribution of the main chemical species to the total reconstructed mass of each sample, calculated as the sum of nitrate, sulphate, ammonium, other ions (potassium, magnesium, calcium and chloride), water-soluble organic matter (WSOM) and water-insoluble carbonaceous material (WINCM). A factor of 1.8 (Matta et al., 2003) and 1.2 (Zappoli et al., 1999) were used to convert, respectively, WSOC in WSOM and WINC in WINCM.

Comparison of daytime and night-time samples shows that water-soluble inorganic species are removed more efficiently than carbonaceous species during the night, when fog occurs: nitrate, sulphate and ammonium contribution is usually lower in nocturnal samples, while the contribution of carbonaceous material increases (particularly that of WINCM). Average percentage contributions of the main chemical species are reported in Table 5.2. The same trend is observed for all the four stages, even though to a lower extent for the largest particles (1. 2 μm < D_a < 3.5 μm).

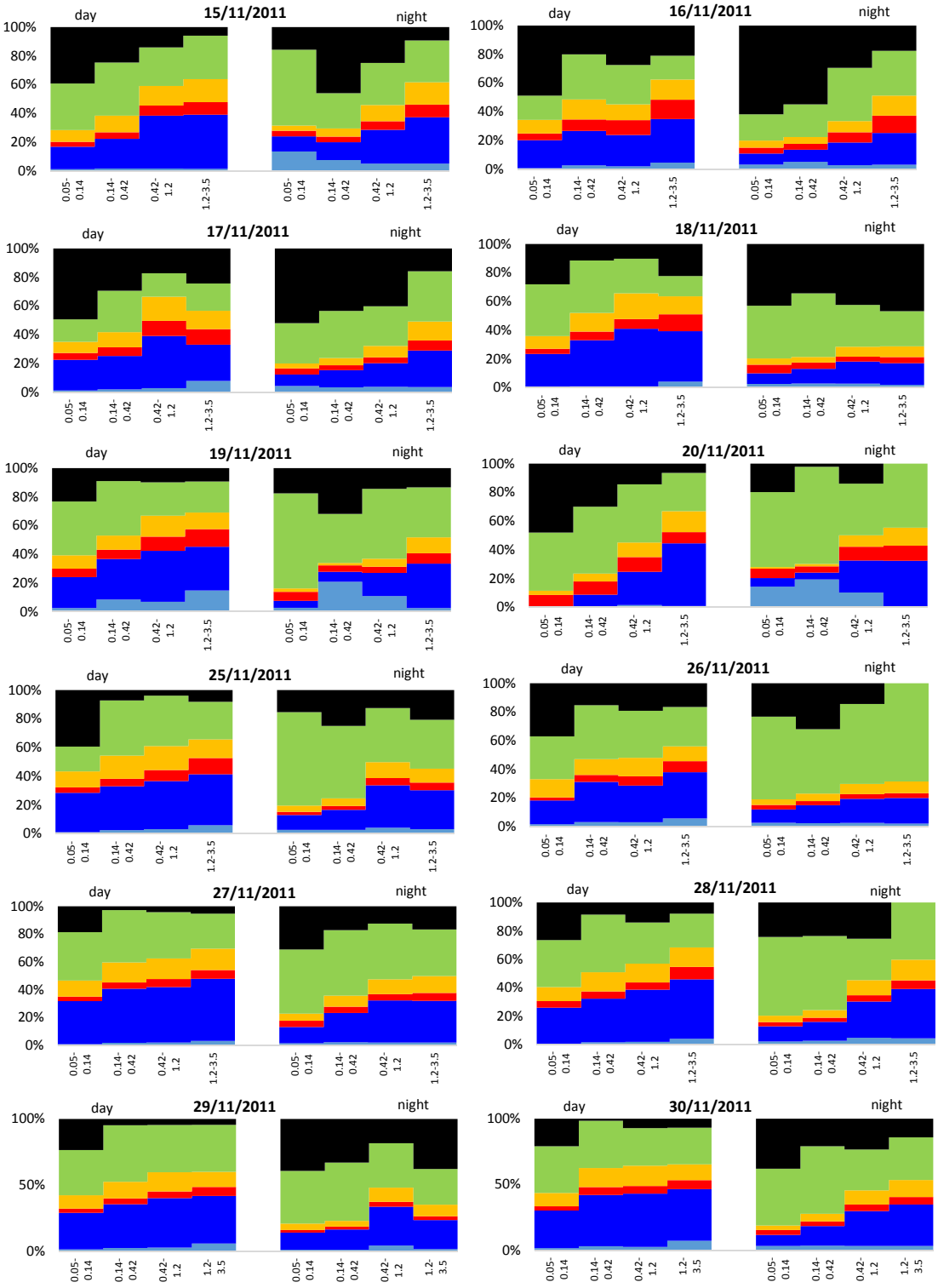

Figure 5.6. *Relative chemical composition of all the analysed aerosol size segregated samples.*

The percentage contribution of nitrate to the total mass in the first three stages of the nocturnal samples decreases from 24 (±4) % to 9 (±4) %, 31 (±5) % to 12 (±5) % and 35 (±6) %

to 23 (±7) %, respectively. The percentage contribution of sulphate and ammonium also shows a depletion with the occurrence of fog, while carbonaceous material, considered as the sum of soluble and insoluble carbonaceous compounds, increases its contribution, accounting for more than 70% of the total reconstructed mass of the finest particles (first and second stage) at night.

Table 5.2. *Size segregated average relative contribution of the main chemical species to the total reconstructed mass of aerosol samples.*

		other ions	NO_3^-	SO_4^{2-}	NH_4^+	WSOM	WINCM
0.05 – 0.14 µm	day	1% ± 1%	24% ± 4%	4% ± 1%	10% ± 1%	29% ± 9%	32% ± 11%
	night	4% ± 4%	9% ± 4%	4% ± 2%	4% ± 2%	45% ± 14%	33% ± 15%
0.14 – 0.42 µm	day	3% ± 2%	31% ± 5%	6% ± 1%	13% ± 2%	37% ± 4%	11% ± 9%
	night	5% ± 6%	12% ± 5%	4% ± 2%	5% ± 2%	43% ± 12%	30% ± 13%
0.42 – 1.2 µm	day	3% ± 2%	35% ± 6%	7% ± 2%	15% ± 2%	29% ± 6%	12% ± 8%
	night	4% ± 3%	23% ± 7%	6% ± 2%	9% ± 2%	36% ± 8%	21% ± 10%
1.2 – 3.5 µm	day	6% ± 3%	35% ± 6%	10% ± 3%	13% ± 1%	24% ± 6%	13% ± 8%
	night	3% ± 1%	29% ± 8%	7% ± 3%	12% ± 3%	35% ± 11%	15% ± 14%

The scavenging efficiency (η) can be calculated to determine the attitude of chemical species to be scavenged by fog droplets. During the November 2011 field campaign, online measurements were carried out using an HR-ToF-AMS that supplies high time resolution data of submicron aerosol chemical composition. In Gilardoni et al. (2014) we used the available chemical data to calculate η, according to the definition given by (Collett et al., 2008):

$$\eta = 1 - [X]_{interstitial}/[X]_{before\ fog}$$

Concentration of before-fog and interstitial species X was calculated from HR-ToF-AMS measurements, averaged over 30 minutes before fog formation and over 30 minutes after fog formation. Scavenging efficiency is found to be related to the water solubility of the considered chemical species. The highest scavenging efficiencies were observed for ammonium and nitrate, the most soluble components (on average 71% and 68%, respectively). Black carbon, the most hydrophobic compound, showed the lowest η value (on average 45%). Organic aerosol showed the largest η variability (20 - 60%), as suggested by its highly variable composition, including soluble molecules and more hydrophobic compounds. (Gilardoni et al., 2014) supported the idea that the observed differences among the scavenging efficiencies depend on a joined effect of both solubility and size distribution of chemical species. According to Köhler theory, activation of particles larger than 300 - 400 nm D_{va} is more likely than activation of smaller particles especially at supersaturation values typical of fog events (0.01 - 0.03%). Nitrate and ammonium size distribution peaks around 400 - 500 nm, while black carbon, besides to be the most insoluble compound, usually dominates smaller particles (D_{va} < 150 nm) (Seinfeld and Pandis, 1998).

5.2 Organic fraction of aerosol particles and fog droplets

So far, the study regarded the observation of how chemical and physical characteristics of aerosol particles are affected by fog occurrence. This paragraph, instead, will compare particles chemical composition with that of fog droplets, with a particular interest for the organic fraction.

Carbonaceous compounds account for a significant fraction of total mass composition of both fog droplets and aerosol particles (Fuzzi et al., 2002). Fig.5.7 shows the average relative chemical composition of fog and PM10 collected in San Pietro Capofiume over the entire campaign in November 2011: the carbonaceous material (intended as the sum of soluble and insoluble material) accounts on average for 33 (±8) % and 50 (±12) % of total reconstructed mass for fog droplets and aerosol particles (PM10), respectively.

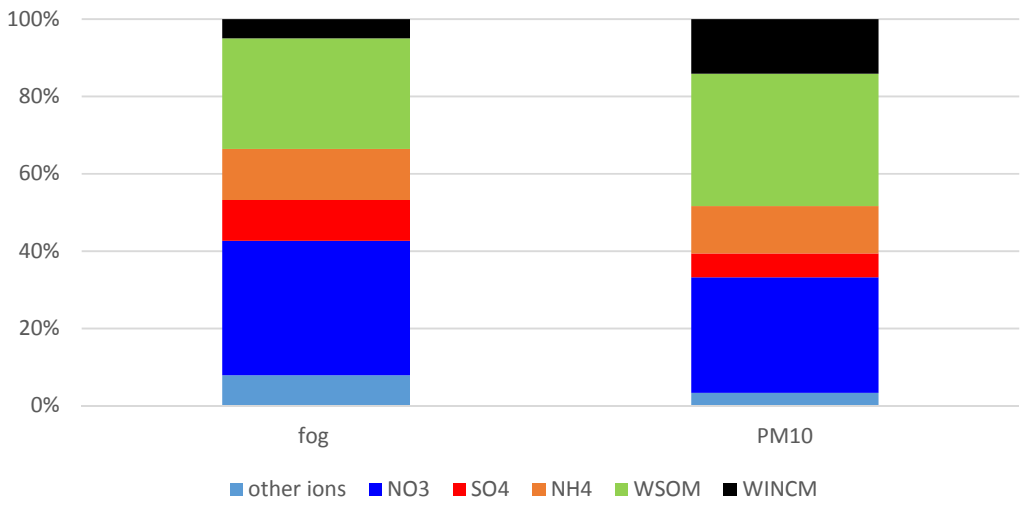

Figure 5.7. *Relative chemical composition of fog droplets and PM10 averaged over the entire campaign.*

Except for the contribution of the insoluble carbonaceous fraction, which will be discussed later in this paragraph, the percentage composition of both aerosol and fog is very similar. It indicates that fog composition is mainly determined by aerosol particles that act as condensation nuclei. Studies carried out in the Po Valley in the last decades, reported the negligible contribution of the coagulation of interstitial particles with fog droplets to the mass of fog droplets, leading to a major role of nucleation scavenging in determining the organic composition (Facchini et al., 1999). Further studies reported high similarity between the organic chemical composition of fog droplets and aerosol particles collected during the cold season at the field station of San Pietro Capofiume, confirming the nucleation scavenging as the main source of organic compounds in fog water (Fuzzi et al., 2002).

In Fig.5.8 relative contribution of WSOC and WINC to the total carbon content is reported for fog water, PM10 out of fog and PM10 in fog conditions (interstitial aerosol). In fog droplets, water-soluble carbon accounts on average for 77 (±6) % and insoluble carbon for 24 (±7) %. The partitioning of carbon between soluble and insoluble species is similar in PM10 out of fog: soluble C accounts for 62 (±16) %. In interstitial aerosol samples the contribution of insoluble carbon increases, reaching 45 (±16) % of total carbon mass, because of the scavenging of part of the soluble carbonaceous species in fog water.

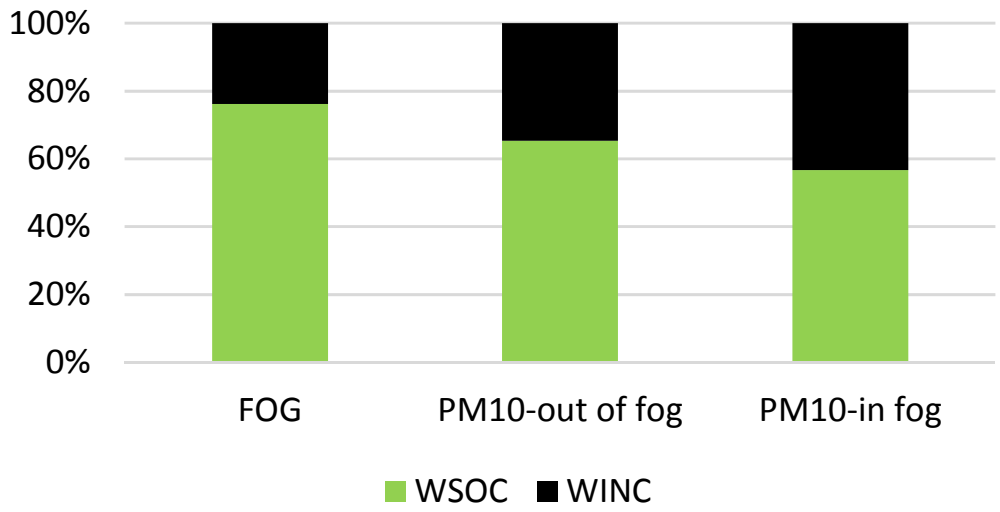

Figure 5.8. *Average relative contribution of WSOC and WINC to the total carbon content of fog water, PM10 out-of-fog and PM10 in-fog conditions.*

The water-soluble carbonaceous fraction of both aerosol and fog droplets has been further analysed, to reach a better characterization. By ion chromatography some low molecular weight carboxylic acids can been detected and quantified. Acetic acid (CH_3COOH), formic acid (HCOOH), methanesulfonic acid (CH_3SO_3H) and oxalic acid ($C_2H_2O_4$) have been measured. Their carbon contribution to the total WSOC is small and variable from sample to sample. They accounts on average only for 0.7 (±1.9) %, 1.2 (±1.8) %, 1.5 (±0.6) % and 2.5 (±2.0) % of the total WSOC in the four size stages of size segregated aerosol samples, respectively. Low molecular weight carboxylic acids contribute for 4.3 (±2.1) % to the water-soluble organic carbon of the fog droplets.

Using an individual compound approach to determine the chemical composition of aerosol organic fraction, the speciation usually produces a list of individual compounds which together account only for a few percent of the OC composition (Fuzzi et al., 2001). A different approach aimed to a more general characterization, based on determination of type and concentration of functional groups, instead of individual compounds, is more affordable. This strategy was pursued using ^{1}H-NMR spectroscopy (Decesari et al., 2000; Decesari et al., 2001). For these analysis aerosol particles were sampled on quartz fibre filter by a dichotomous sampler, with

a size segregation between fine particles (PM1) and coarse particles (PM1-10). In this study only PM1 fraction was analysed.

The soluble carbonaceous fraction chemical composition for in-fog, out-of-fog and fog droplets samples is shown in Fig.5.9. Functional groups detected by ^{1}H-NMR are aromatics (Ar-H), anomeric or vynilic groups (O-CH-O), alcohols, ethers and esters (H-C-O) and aliphatics (H-C-C= and H-C). Average water-soluble organic carbon concentration is higher for fog droplets and decrease in aerosol samples affected by fog presence.

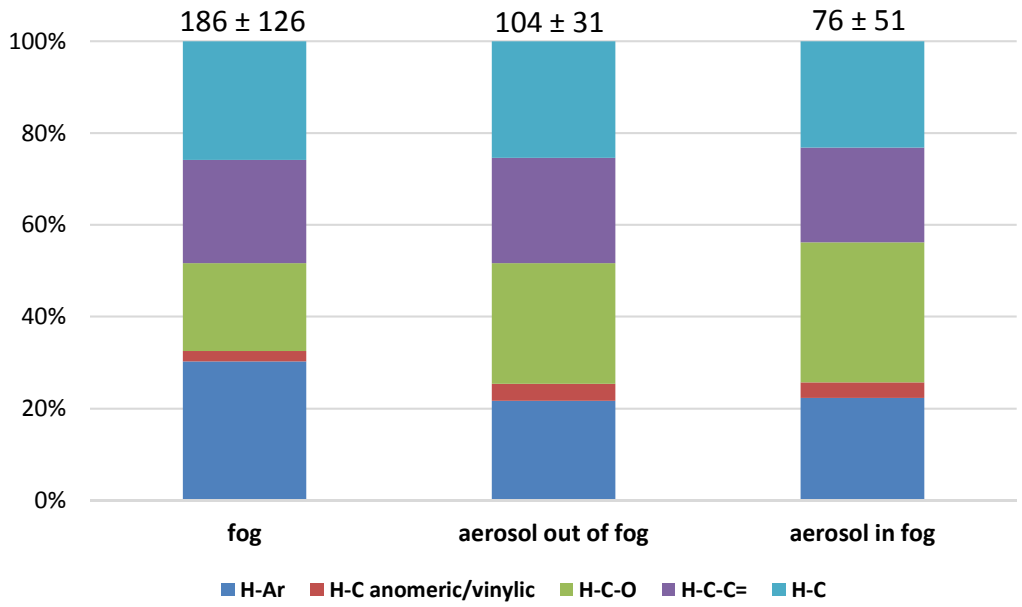

Figure 5.9. *Average contribution of functional groups detected by ^{1}H-NMR in fog droplets and fine aerosol particles. Numbers on top of each bar indicate the average atmospheric concentration (nmolC m^{-3}).*

A synthetic graphical representation of the functional groups distribution is reported in Fig.5.10, indicating the fraction of aliphatic carbon accounted for by hydroxyl groups in the horizontal axis, and the aliphatic fraction accounted for by carbonylic/carboxylic groups in the vertical axis. Aromatic fraction is represented by the size of the dots. Concentration units are moles of organic carbon, estimated by the measured ^{1}H-NMR concentrations in hydrogen moles using group-specific H/C ratios. This graph was used in (Decesari et al., 2007) to provide

source identification for water-soluble organic aerosol based on ^{1}H-NMR functional group composition. Comparing our results to those reported in the paper, we found that our samples are positioned in the area assigned to samples affected by biomass burning (black border rectangle in Fig.5.10). This result agrees with previous studies indicating that organic aerosol in the rural Po Valley in fall is usually dominated by wood burning emissions from residential heating and fossil fuel burning from traffic and residential heating (Gilardoni et al., 2011). The figure shows that the compositions of the three sample subsets object of this study (fog, aerosol in-fog and aerosol out-of-fog), beside falling approximately in the same region of the functional group diagram, they tend to scatter out in different directions. In particular, the composition of interstitial aerosol (blue dots) is enriched in aromatic and hydroxyl groups and depleted in carbonyls/carboxyls with respect to that of out-of-fog aerosol (in green). This finding indicates that interstitial aerosols retain the original ("primary") constituents of wood burning products (e.g., anhydrosugars, phenols) while they are depleted of the secondary species (e.g., carboxylic acids). This in turn can be explained by the fact that local sources from domestic heating directly impact the composition of aerosol particles in the small size range which is less efficiently scavenged by fog than larger particles (where biomass burning products are more aged and enriched in secondary species). Conversely, the ^{1}H-NMR composition of fog WSOC is depleted of primary biomass burning products (hydroxyl groups from anhydrosugars), but, unexpectedly, they exhibit a greater aromatic content than out-of-fog aerosols. To explain this last finding, additional sources of aromatic compounds in fog droplets must be hypothesized, like scavenging of aromatic aldehydes (e.g., benzoaldehyde) and acids from the gas phase, or formation of heteroaromatic compounds from the reaction of low-molecular weight carbonyls and ammonia (e.g., Yu et al., 2011). These additional mechanisms involving aqueous phase chemical reactions cannot be fully explained based on the available set of data and require further attempts for chemical speciation.

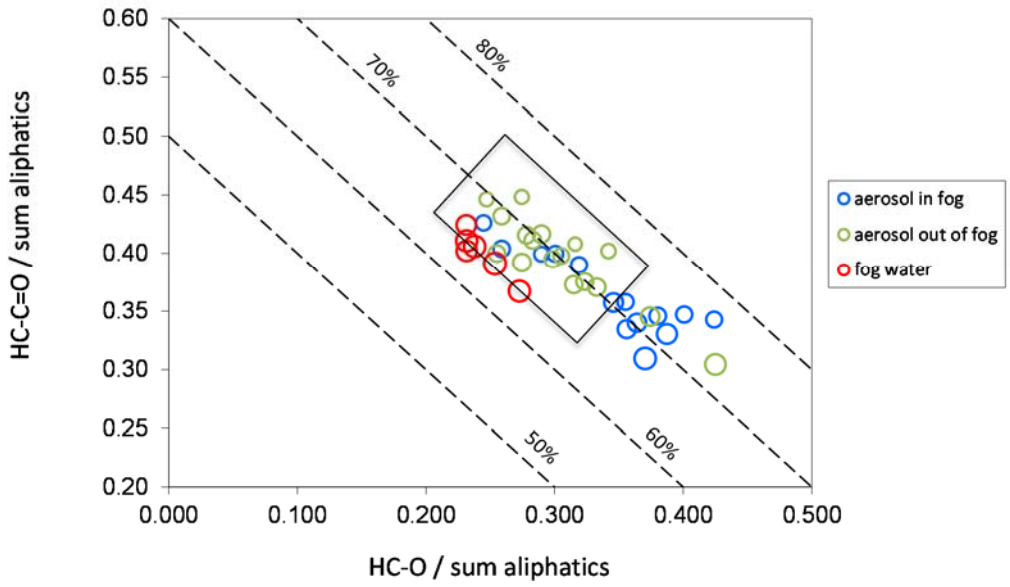

Figure 5.10. *Functional group distribution of water-soluble organic fraction in fog and aerosol samples.*

5.3 High time resolution characterization of a nocturnal fog episode

Due to the presence of very dense fog on the first day of the campaign, a special fog and aerosol sampling was set up on 15/11/2011. Starting from 18:00, fog samples were collected every hour and aerosol samples were collected every four hours using a Berner impactor, until the fog dissipation on the following morning (sampling stopped on 16/11/2011 at 11:18). The purpose was to collect samples with a higher time resolution in order to observe how both aerosol and fog water change during a unique fog event.

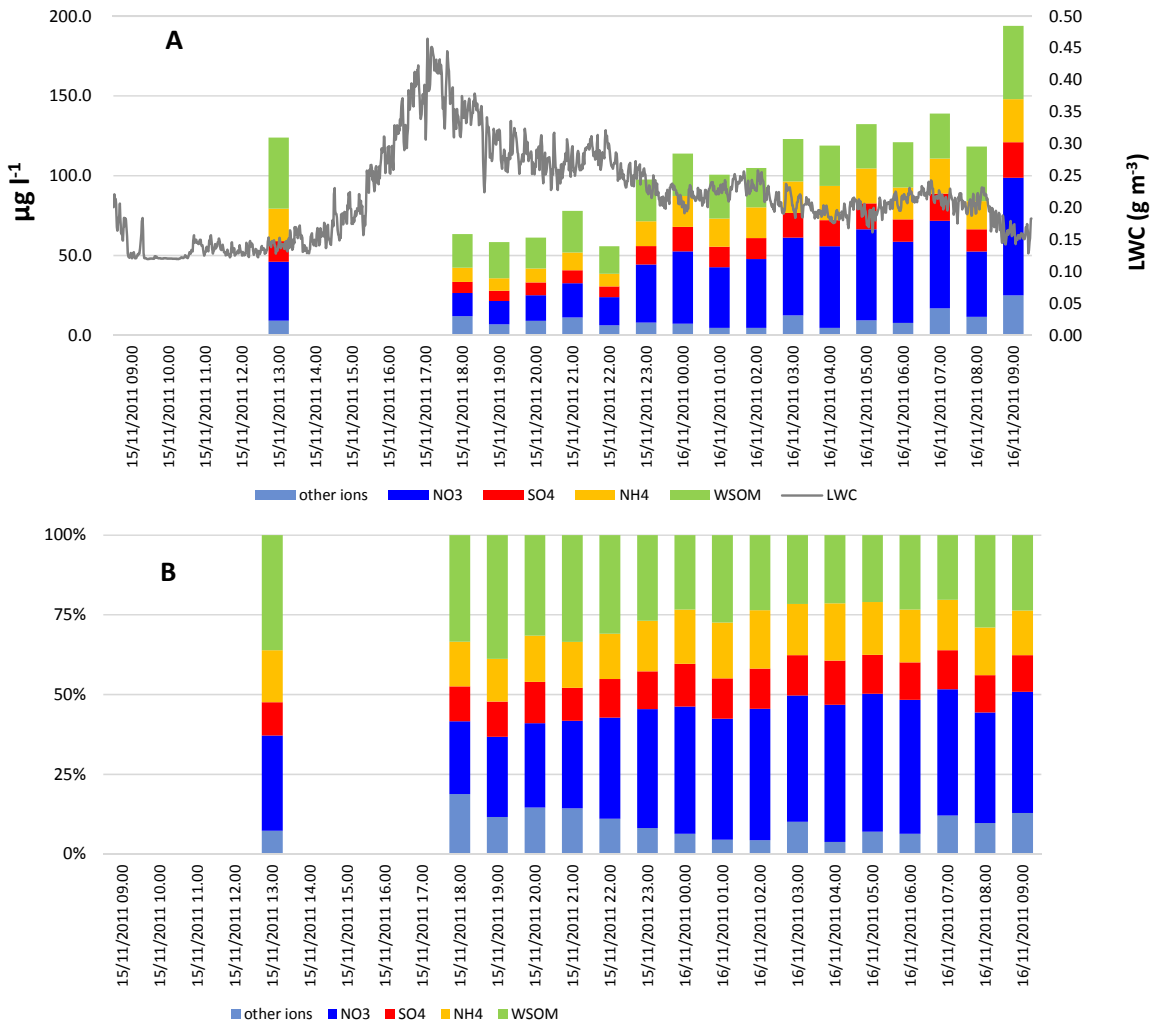

Figure 5.11. *A: concentration of the main chemical species of fog water (µg L^{-1}) and LWC values (g m^{-3}, grey line). B: percentage contribution of the main chemical species to the total reconstructed soluble mass of fog samples.*

Fig.5.11 shows the chemical composition of the bulk fog sample collected on 15/11/2011 from 9:00 to 18:00 and of the 16 fog samples collected during the night between 15 and 16 November at higher time resolution. Histograms in panel A show the concentration of the main chemical species of fog water, expressed as µg L^{-1}, and the grey line represents the LWC values (g m^{-3}). Panel B shows the percentage contribution of the main species to the total reconstructed soluble mass. The absolute concentration of soluble species is inversely proportional to the LWC values: an increase of the liquid water content determines a dilution effect (Elbert et al., 2000) so that concentrations are lower in the late afternoon, when LWC values have a maximum. Fog water becomes enriched in nitrate during the night, with nitrate

accounting for 23% of the total mass at 18:00 and 43% at 5:00. WSOC trend is the opposite, showing the highest contribution at 19:00 (39%) and the minimum at 5:00 (21%).

The absolute concentration of all the main chemical species measured in fog water shows an increasing profile during the night. Regression lines of the increment of nitrate, sulphate, ammonium and WSOC are reported in (Fig.5.12). Sulphate and ammonium behave the same, with slopes value of 3. The slope of nitrate is steeper, with a value of 5.5, indicating a higher increase in concentration of this species compared to sulphate and ammonium. Another process, in addition to the decreasing of LWC, must have affected the concentration of nitrate in fog water.

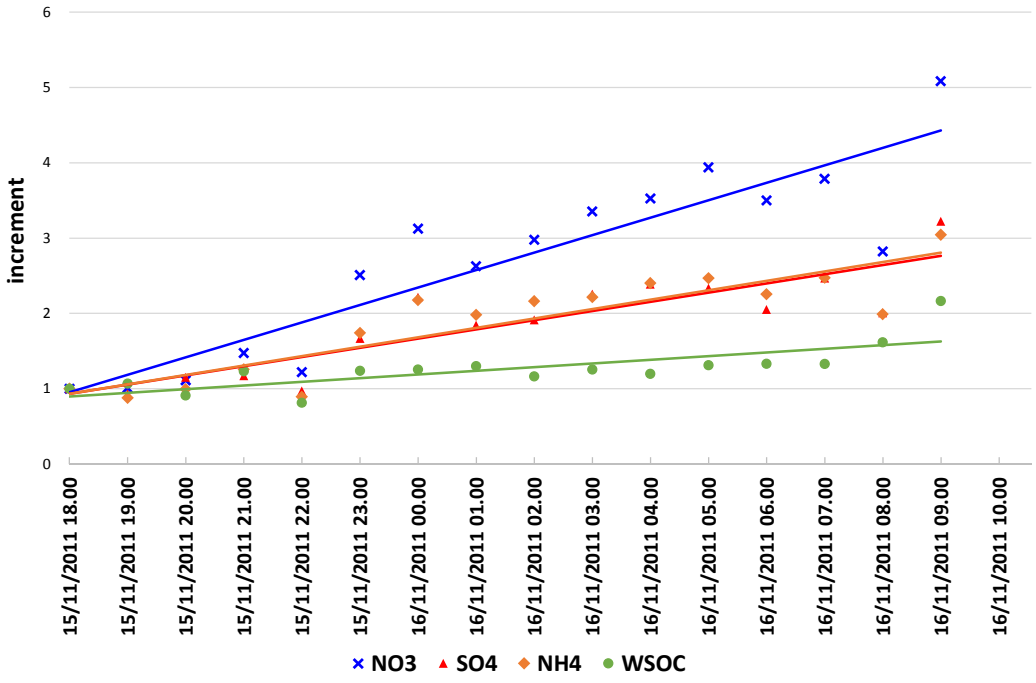

Figure 5.12. *Soluble species increment as a function of time and corresponding regression lines.*

A possible explanation for the observed nitrate trend is the following. During the night, nitrogen dioxide (NO_2) reacts with ozone to form nitrate radical ($NO_3^{\bullet}$) (Seinfeld and Pandis, 1998). Because of the lack of photolytic processes, nitrate radical accumulates. Once accumulated this equilibrium is established:

$$NO_3^{\bullet} + NO_2 \leftrightarrow N_2O_5$$

Dinitrogen pentoxide (N_2O_5) is very soluble and quickly dissolves in fog water producing nitric acid (HNO_3). Through this mechanism nitrate is produced directly in the aqueous phase and contributes to the accumulation of this ion in fog droplets throughout the night.

The above data demonstrate that fog chemistry occurring during the night can be responsible for the formation of important amounts of aerosol nitrate in the Po Valley, in addition to the most common process of NO_X oxidation by the OH radical, occurring during the day. Conversely, the concentration of WSOC shows a lower increment compared to the other species. This behaviour is due to the semivolatile nature of a fraction of soluble organic compounds that likely passes into the gas phase with decreasing water content.

Fig.5.13 shows the soluble fraction chemical composition of the aerosol particles with 0.14 µm < D_a < 0.42 µm and 0.42 µm < D_a < 1.2 µm collected from 15/11/2011 at 9:00 to 16/11/2011 at 11:00. We previously observed that these particles are the most affected by fog scavenging. This statement is confirmed by the results shown on the left side of Fig.5.13, where the absolute mass concentration of each sample is reported. When LWC values start to increase, around 18:00, and fog become denser, a reduction of particles occurs. Concentrations remain stationary until the early hours in the morning of 16/11/2011 when fog begins to dissipate. At 11:30, when fog is completely dissipated, aerosol particles accumulate again. Concentrations of total soluble mass and of each chemical species are reported in detail in Table 5.3. In size range 0.42 µm < D_a < 1.2 µm, nitrate is the most scavenged species by fog water. Its contribution to the total mass decreases contemporary to its increase in fog water samples (compare with Fig.5.11 panel B), passing from 43% in the first sample to 30% in the last one.

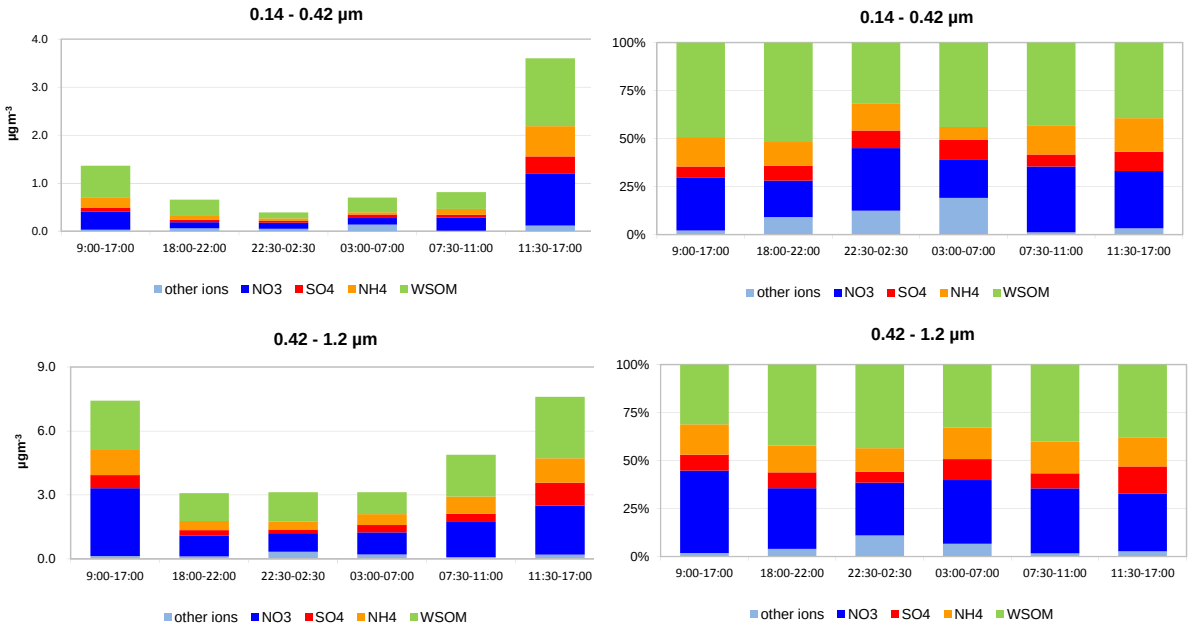

Figure 5.13. *Histograms on the left show the chemical composition of aerosol particles collected on 15-16 November 2011, in the size range 0.14 - 0.42 µm (up) and 0.42 - 1.2 µm (down). Histograms on the right show their relative chemical composition.*

In the interstitial aerosol, the contribution of "other ions" increases throughout the night, mainly because of an increase of potassium amount, which is considered a marker of biomass burning (Favez et al., 2010; Lee et al., 2008; Liu et al., 2005; Zhang et al., 2010). In the evening the activity linked to domestic heating reaches a maximum leading to an accumulation of biomass burning aerosol within the shallow nocturnal boundary layer.

This data elaboration was made also for the other size range samples collected by Berner impactor, but no similar behaviour has been observed. This confirms the hypothesis explained previously in the chapter, that fog scavenging affects mostly submicron particles with D_a > 200 µm.

Table 5.3. *Concentrations of chemical species in aerosol particles collected on 15 - 16 November 2011, in the size range 0.14 - 0.42 µm and 0.42 - 1.2 µm.*

		µg m^{-3}					
ID Sample	sampling time	total mass	NO_3^-	SO_4^{2-}	NH_4^+	other ions	WSOM
Size: 0.14-0.42µm							
SPC151111_D2	9:00-17:00	1.4	0.37	0.08	0.21	0.67	0.03
SPC151111_NA2	18:00-22:00	0.66	0.13	0.05	0.08	0.34	0.06
SPC151111_NB2	22:30-02:30	0.39	0.13	0.04	0.05	0.12	0.05
SPC151111_NC2	03:00-07:00	0.70	0.14	0.07	0.05	0.31	0.13
SPC151111_ND2	07:30-11:00	0.81	0.28	0.05	0.12	0.35	0.01
SPC161111_D2	11:30-17:00	3.6	1.1	0.36	0.63	1.4	0.12
Size: 0.42-1.2 µm							
SPC151111_D3	9:00-17:00	7.4	3.2	0.61	1.2	2.3	0.14
SPC151111_NA3	18:00-22:00	3.1	0.98	0.25	0.43	1.3	0.12
SPC151111_NB3	22:30-02:30	3.1	0.86	0.18	0.39	1.4	0.34
SPC151111_NC3	03:00-07:00	3.1	1.0	0.34	0.52	1.03	0.21
SPC151111_ND3	07:30-11:00	4.9	1.7	0.38	0.81	2.0	0.08
SPC161111_D3	11:30-17:00	7.6	2.3	1.1	1.2	2.9	0.20

6. Conclusions

Air pollution is believed to be responsible for more than 400,000 premature deaths in Europe (Brunekreef, 2013). The impact on human health is exacerbated in so-called pollution "hot spots": environments in which anthropogenic sources are concentrated and dispersion of pollutants is limited. One of these environments, the Po Valley, normally experiences exceedances of PM10 and PM2.5 daily concentration limits, especially in the cold season when the ventilation of the lower layers of the atmosphere is reduced. Traditionally, air pollution studies in the cold season have focused on primary combustion emission sources (traffic, residential heating) and atmospheric dispersion, while the role of photochemical (secondary) processes has been investigated mainly in the summer. In this study we were able to show that secondary processes are responsible for the formation of the largest fraction of PM10 in the Po Valley also in winter, when photochemistry is reduced, and that fog aqueous chemistry can play a key role in such processes.

Size-segregated aerosol samples (5 size classes between 0.05 and 10 µm) were collected simultaneously in two different sites (Bologna, urban site, and San Pietro Capofiume, rural site) during two different campaigns (November 2011 and February 2013). The total concentrations of the reconstructed PM10 mass and the size-distributions were similar between the urban and the rural site, confirming the importance of the regional background aerosol contribution in determining the concentrations at the urban scale in the Po Valley. Most importantly, our results from the analysis of the water-soluble inorganic and organic fraction show that the chemical composition is dominated by ammonium nitrate and ammonium sulphate, which are known secondary components of the aerosol. This finding indicates that not only the limited atmospheric dispersion is the cause for the build-up of the regional background aerosol, but also atmospheric reactions occurring in the gas and in the particulate phase across the Po Valley. Soluble organic compounds are also relevant, accounting for more than 80% of the finest particles (size range between 0.05 and 0.14 µm). Water-soluble organic matter (WSOM) is homogeneously distributed between BO and SPC, analogously to ammonium nitrate and sulphate, indicating that secondary processes also contributed to WSOM over the Po Valley during the investigated period.

The role of fog formation and fog chemistry in the formation, processing and deposition of PM10 in the Po Valley has been studied during the field campaign of November 2011 in San Pietro Capofiume. Our results show that particles with aerodynamic diameter between 0.14 and 1.2 μm, where most of the PM1 mass is found, are efficiently scavenged by fog occurrence. Therefore, during fog events, the ambient concentration of the finest particles, with the highest capacity to penetrate in the human respiratory system, is strongly reduced because of fog scavenging (up to 60%). The presence of fog in the Po Valley thus represents a relevant mechanism of control of the aerosol load in the atmosphere, with relevant implications on the air quality of the region.

Other potential impacts of aerosol-fog interaction that have been evaluated in the present study are the role of fog droplets in absorbing trace gases like nitric acid, sulphur dioxide and ammonia, which can result in increased concentrations of PM10 upon fog evaporation, or, in case of an excess of acidic gases, in wet deposition of fogs with low pH, with harmful effects on the vegetation and buildings. Time-resolved measurements of fog composition highlighted the formation of particulate nitrate through an in-fog aqueous phase reaction: gaseous dinitrogen pentoxide (N_2O_5) is absorbed into the droplets and then hydrolysed and neutralized by ammonia to form ammonium nitrate (NH_4NO_3). After evaporation of fog droplets, aerosol particles result enriched in NH_4NO_3. This aqueous secondary aerosol formation mechanism is very important in wintertime, when the photochemical activity is reduced, and so the formation of nitric acid (HNO_3) in the gaseous phase is slow. These results indicate that fog processing can be responsible for the enrichment of ammonium nitrate in PM10 in the Po Valley in wintertime, and that these reactions contribute to the build-up of the regional background aerosol concentrations in the region.

During the 2011 field campaign, the absorption of ammonia neutralized the production of nitric acid from the N_2O_5 channel. The fog water pH during the full 2011/12 season remained close to neutrality, in conflict with first observations at the site dating back the 80s and showing frequent episodes of acidic pH. In fact, the composition of fog water has evolved continuously over the last decades following the changes in atmospheric composition, which in turn were dictated by several processes, including the introduction of anthropogenic emission controls. We present here for the first time the results of the analysis of fog water composition from a 20 years record of measurements in San Pietro Capofiume. This long time

series showed a clear decreasing trend of ionic strength and conductivity of fog water, indicating a reduction of its ionic load. The ionic species that exhibited the highest decrease was sulphate (SO_4^{2-}). The gradual decrease of sulphates, lead to an increased relative contribution of organic compounds and nitrates, which suffered a less drastic reduction. The low correlation between ion concentrations and LWC, and the lack of a statistically significant trend for LWC, excluded that the observed decreasing concentrations were due to a "dilution effect". The negative trend of fog water ionic load is mainly due to the reduction in SO_2 and NO_X atmospheric emissions (emission data are reported by the Italian Institute for the Environmental Protection and Research –ISPRA), in agreement with other studies carried out in Europe (Lange et al., 2003). These results reflect the impact of the implemented air quality policies in determining the concentrations of atmospheric constituents. As a consequence of the lower content of the two main acidic species (NO_3^- and SO_4^{2-}) pH values showed an increase over the last two decades, reaching values close to neutrality. In the today-atmosphere, the ammonia concentrations are large enough to neutralize the production/absorption of acidic compounds in fog water, excluding the formation of acidic fogs. On the other hand, the neutralization of nitric acid leads to the production of particulate ammonium nitrate, which, upon fog evaporation, leads to an increase of PM10 concentrations in the region. Introducing a regulation on the emissions of ammonia (mainly from agricultural activities, animal husbandry, and waste treatment) can be an agreeable strategy to decrease the particulate matter concentrations, but with the possible side effect of making the fog depositions more acidic.

Even though the results presented in this doctoral thesis refer to data collected in Bologna and San Pietro Capofiume, they can be extended to the whole Po Valley basin that has been classified as a unique megacity (see chapter 1). Therefore, these results could be a valuable tool to support integrated future policy actions in the whole region.

Acknowledgments

The research work reported in this PhD thesis was carried out at the Institute of Atmospheric Sciences and Climate, National Research Council (ISAC-CNR), Bologna, within the Atmospheric Chemistry group headed by Dr. Sandro Fuzzi and Dr. Maria Cristina Facchini.

Financial supports was provided by the Emilia-Romagna Region "SUPERSITO" Project, the Atmospheric Composition Change European Network of Excellence (ACCENT-Plus) and the European project PEGASOS.

I would like to express, first of all, my gratitude to Dr. Fuzzi e Dr. Facchini for having given me this opportunity. I owe to them most of all I learned in these years.

I gratefully acknowledge Prof. Emilio Tagliavini (University of Bologna) for having supported this doctoral project.

My special thanks to my friend and colleague Dr. Matteo Rinaldi for his supervision and most of all for his support during the whole period of the PhD. My work would not have been successful without his help.

My special thanks also to Dr. Stefano Decesari for his precious and fundamental suggestions and supervision during the preparation of the thesis.

I warmly thank Dr. Marco Paglione, Dr. Stefania Gilardoni, Dr. Claudio Carbone, Dr. Silvia Sandrini and Dr. Leone Tarozzi, which all contributed to this work with their constant human and professional support.

Bibliography

Aleksic, N. and Dukett, J. E. (2010). Probabilistic relationship between liquid water content and ion concentrations in cloud water. *Atmospheric Research* 98, 400-405.

Alves, C., Vicente, A., Pio, C., Kiss, G., Hoffer, A., Decesari, S., Prevot, A. S. H., Cruz Minguillon, M., Querol, X., Hillamo, R., Spindler, G. and Swietlicki, E. (2012). Organic compounds in aerosols from selected European sites - Biogenic versus anthropogenic sources. *Atmospheric Environment* 59, 243-255.

Andreae, M. O. and Gelencser, A. (2006). Black carbon or brown carbon? The nature of light-absorbing carbonaceous aerosols. *Atmospheric Chemistry and Physics* 6, 3131-3148.

Andreae, M. O. and Rosenfeld, D. (2008). Aerosol-cloud-precipitation interactions. Part 1. The nature and sources of cloud-active aerosols. *Earth-Science Reviews* 89, 13-41.

Arends, B. G. (1996). *Aerosol and Cloud Microphysics, Measurements and Interpretations*.

Barrie, L. A. (1985). Features of the Atmospheric Cycle of Aerosol Trace-Elements and Sulfur Dioxide revealed-by Baseline Observations in Canada. *Journal of Atmospheric Chemistry* 3, 139-152.

Blanchard, D. (1983). *The Production, distribution, and bacterial enrichment of the sea-salt aerosol, in Air-Sea Exchange of Gases and Particles*. D Reidel: Norwell, Mass.

Braun, S., Kalinowski, H. O. and Berber, S. (1998). *150 and more basic NMR Experiments*. Wiley-VHC: Weinheim, Germany.

Brunekreef, B. (2013). Air Quality and Health In Union, E. (Ed), *Air Quality - Research Findings in support of the EU*: Luxembourg, pp. 20 - 30.

Calvert, J. G., Heikes, B. G., Stockwell, W. R., Mohnen, V. A. and Kerr, J. A. (1986). Some considerations of the important chemical processes in acid deposition In Ed., W. J. (Ed), *Chemistry of Multiphase Atmospheric Systems*, Springer Verlag, berlin: City, pp. 615-647.

Carbone, C., Decesari, S., Mircea, M., Giulianelli, L., Finessi, E., Rinaldi, M., Fuzzi, S., Marinoni, A., Duchi, R., Perrino, C., Sargolini, T., Varde, M., Sprovieri, F., Gobbi, G. P., Angelini, F. and Facchini, M. C. (2010). Size-resolved aerosol chemical composition over the Italian Peninsula during typical summer and winter conditions. *Atmospheric Environment* 44, 5269-5278.

Casareto, B. E., Suzuki, Y., Okada, K. and Morita, M. (1996). Biological micro-particles in rain water. *Geophysical Research Letters* 23, 173-176.

Caseiro, A., Bauer, H., Schmidl, C., Pio, C. A. and Puxbaum, H. (2009). Wood burning impact on PM10 in three Austrian regions. *Atmospheric Environment* 43, 2186-2195.

Chen, J., Ying, Q. and Kleeman, M. J. (2010). Source apportionment of wintertime secondary organic aerosol during the California regional PM10/PM2.5 air quality study. *Atmospheric Environment* 44, 1331-1340.

Collett, J. L., Jr., Herckes, P., Youngster, S. and Lee, T. (2008). Processing of atmospheric organic matter by California radiation fogs. *Atmospheric Research* 87, 232-241.

Collett, J. L., Oberholzer, B., Mosimann, L., Staehelin, J. and Waldvogel, A. (1993). Contributions of Cloud Processes to Precipitation Chemistry in Mixed-phase Clouds. *Water Air and Soil Pollution* 68, 43-57.

DeCarlo, P. F., Kimmel, J. R., Trimborn, A., Northway, M. J., Jayne, J. T., Aiken, A. C., Gonin, M., Fuhrer, K., Horvath, T., Docherty, K. S., Worsnop, D. R. and Jimenez, J. L. (2006). Field-deployable, high-resolution, time-of-flight aerosol mass spectrometer. *Analytical Chemistry* 78, 8281-8289.

Decesari, S., Facchini, M. C., Fuzzi, S. and Tagliavini, E. (2000). Characterization of water-soluble organic compounds in atmospheric aerosol: A new approach. *Journal of Geophysical Research-Atmospheres* 105, 1481-1489.

Decesari, S., Facchini, M. C., Matta, E., Lettini, F., Mircea, M., Fuzzi, S., Tagliavini, E. and Putaud, J. P. (2001). Chemical features and seasonal variation of fine aerosol water-soluble organic compounds in the Po Valley, Italy. *Atmospheric Environment* 35, 3691-3699.

Decesari, S., Mircea, M., Cavalli, F., Fuzzi, S., Moretti, F., Tagliavini, E. and Facchini, M. C. (2007). Source attribution of water-soluble organic aerosol by nuclear magnetic resonance spectroscopy. *Environmental Science & Technology* 41, 2479-2484.

Derome, A. E. (1987). *Modern NMR Techniques for Chemistry Research*. Pergamon Press: Oxford, UK.

Deserti, M., Cacciamani, C., Golinelli, M., Kerschbaumer, A., Leoncini, G., Savoia, E., Selvini, A., Paccagnella, T. and Tibaldi, S. (2001). Operational meteorological pre-processing at Emilia-Romagna ARPA Meteorological Service as a part of a decision support system for air quality management. *International Journal of Environment and Pollution* 16, 571-582.

Dollard, G. J., Unsworth, M. H. and Harve, M. J. (1983). Pollutant tranfer in Upland Regions by Occult Precipitation. *Nature* 302, 241-243.

Dusek, U., Frank, G. P., Hildebrandt, L., Curtius, J., Schneider, J., Walter, S., Chand, D., Drewnick, F., Hings, S., Jung, D., Borrmann, S. and Andreae, M. O. (2006). Size matters more than chemistry for cloud-nucleating ability of aerosol particles. *Science* 312, 1375-1378.

Elbert, W., Hoffmann, M. R., Kramer, M., Schmitt, G. and Andreae, M. O. (2000). Control of solute concentrations in cloud and fog water by liquid water content. *Atmospheric Environment* 34, 1109-1122.

Elbert, W., Kramer, M. and Andreae, M. O. (2002). Reply to discussion on "Control of solute concentrations in cloud and fog water by liquid water content". *Atmospheric Environment* 36, 1909-1910.

Ervens, B., Turpin, B. J. and Weber, R. J. (2011). Secondary organic aerosol formation in cloud droplets and aqueous particles (aqSOA): a review of laboratory, field and model studies. *Atmospheric Chemistry and Physics* 11, 11069-11102.

Facchini, M. C., Fuzzi, S., Lind, J. A., Fierlingeroberlinninger, H., Kalina, M., Puxbaum, H., Winiwarter, W., Arends, B. G., Wobrock, W., Jaeschke, W., Berner, A. and Kruisz, C. (1992). Phase Partitioning and Chemical Reactions of Low Molecular Weight Organic Compounds in Fog. *Tellus Series B-Chemical and Physical Meteorology* 44, 533-544.

Facchini, M. C., Fuzzi, S., Zappoli, S., Andracchio, A., Gelencser, A., Kiss, G., Krivacsy, Z., Meszaros, E., Hansson, H. C., Alsberg, T. and Zebuhr, Y. (1999). Partitioning of the organic aerosol component between fog droplets and interstitial air. *Journal of Geophysical Research-Atmospheres* 104, 26821-26832.

Favez, O., El Haddad, I., Piot, C., Boreave, A., Abidi, E., Marchand, N., Jaffrezo, J. L., Besombes, J. L., Personnaz, M. B., Sciare, J., Wortham, H., George, C. and D'Anna, B. (2010). Inter-comparison of source apportionment models for the estimation of wood burning aerosols during wintertime in an Alpine city (Grenoble, France). *Atmospheric Chemistry and Physics* 10, 5295-5314.

Flossmann, A. I., Hall, W. D. and Pruppacher, H. R. (1985). A Theoretical Study of the Wet Removal of Atmospheric Pollutants.1. The Redistribution of Aerosol-particles Captured through Nucleationa and Impaction Scavenging by Growing Cloud Drops. *Journal of the Atmospheric Sciences* 42, 583-606.

Fowler, D., Pilegaard, K., Sutton, M. A., Ambus, P., Raivonen, M., Duyzer, J., Simpson, D., Fagerli, H., Fuzzi, S., Schjoerring, J. K., Granier, C., Neftel, A., Isaksen, I. S. A., Laj, P., Maione, M., Monks, P. S., Burkhardt, J., Daemmgen, U., Neirynck, J., Personne, E., Wichink-Kruit, R., Butterbach-Bahl, K., Flechard, C., Tuovinen, J. P., Coyle, M., Gerosa, G., Loubet, B., Altimir, N., Gruenhage, L., Ammann, C., Cieslik, S., Paoletti, E., Mikkelsen, T. N., Ro-Poulsen, H., Cellier, P., Cape, J. N., Horvath, L., Loreto, F., Niinemets, U., Palmer, P. I., Rinne, J., Misztal, P., Nemitz, E., Nilsson, D., Pryor, S., Gallagher, M. W., Vesala, T., Skiba, U., Brueggemann, N., Zechmeister-Boltenstern, S., Williams, J., O'Dowd, C., Facchini, M. C., de Leeuw, G., Flossman, A., Chaumerliac, N. and Erisman, J. W. (2009). Atmospheric composition change: Ecosystems-Atmosphere interactions. *Atmospheric Environment* 43, 5193-5267.

Fuzzi, S. (1994). Clouds in Troposphere In Boutron, C. F. (Ed), *Topics in Atmospheric and Interstellar Physics and Chemistry*, Les Editions de Physique: France, pp. 291-308.

Fuzzi, S., Andreae, M. O., Huebert, B. J., Kulmala, M., Bond, T. C., Boy, M., Doherty, S. J., Guenther, A., Kanakidou, M., Kawamura, K., Kerminen, V. M., Lohmann, U., Russell, L. M. and Poschl, U. (2006). Critical assessment of the current state of scientific knowledge, terminology, and research needs concerning the role of organic aerosols in the atmosphere, climate, and global change. *Atmospheric Chemistry and Physics* 6, 2017-2038.

Fuzzi, S., Decesari, S., Facchini, M. C., Matta, E., Mircea, M. and Tagliavini, E. (2001). A simplified model of the water soluble organic component of atmospheric aerosols. *Geophysical Research Letters* 28, 4079-4082.

Fuzzi, S., Facchini, M. C., Decesari, S., Matta, E. and Mircea, M. (2002). Soluble organic compounds in fog and cloud droplets: what have we learned over the past few years? *Atmospheric Research* 64, 89-98.

Fuzzi, S., Facchini, M. C., Orsi, G. and Ferri, D. (1992a). Seasonal Trend of Fog Water Chemical Composition in the Po Valley. *Environmental Pollution* 75, 75-80.

Fuzzi, S., Facchini, M. C., Orsi, G., Lind, J. A., Wobrock, W., Kessel, M., Maser, R., Jaeschke, W., Enderle, K. H., Arends, B. G., Berner, A., Solly, I., Kruisz, C., Reischl, G., Pahl, S., Kaminski, U., Winkler, P., Ogren, J. A., Noone, K. J., Hallberg, A., Fierlingeroberlinninger, H., Puxbaum, H., Marzorati, A., Hansson, H. C., Wiedensohler, A., Svenningsson, I. B., Martinsson, B. G., Schell, D. and Georgii, H. W. (1992b). The Po Valley Fog Experiment 1989 - AN OVERVIEW. *Tellus Series B-Chemical and Physical Meteorology* 44, 448-468.

Fuzzi, S. and Gilardoni, S. (2013). Particulate Matter In Union, E. (Ed), *Air Quality - Research Findings in support of the EU*: Luxembourg, pp. 31 - 42.

Fuzzi, S., Mandrioli, P. and Perfetto, A. (1997a). Fog droplets - An atmospheric source of secondary biological aerosol particles. *Atmospheric Environment* 31, 287-290.

Fuzzi, S., Orsi, G., Bonforte, G., Zardini, B. and Franchini, P. L. (1997b). An automated fog water collector suitable for deposition networks: Design, operation and field tests. *Water Air and Soil Pollution* 93, 383-394.

Fuzzi, S., Orsi, G. and Mariotti, M. (1983). Radiation Fog Liquid Water Acidity at a Field Station in the Po Valley. *Journal of Aerosol Science* 14, 135-138.

Fuzzi, S., Orsi, G. and Mariotti, M. (1985). Wet Deposition Due to Fog in the Po Valley, Italy. *Journal of Atmospheric Chemistry* 3, 289-296.

Ge, X., Setyan, A., Sun, Y. and Zhang, Q. (2012). Primary and secondary organic aerosols in Fresno, California during wintertime: Results from high resolution aerosol mass spectrometry. *Journal of Geophysical Research-Atmospheres* 117.

Gilardoni, S., Massoli, P., Giulianelli, L., Rinaldi, M., Paglione, M., Pollini, F., Lanconelli, C., Poluzzi, V., Carbone, S., Hillamo, R., Russell, L. M., Facchini, M. C. and Fuzzi, S. (2014). Fog Scavenging of Organic and Inorganic Aerosol in the Po Valley. *Atmospheric Chemistry and Physics Discussion* 14, 4787-4826.

Gilardoni, S., Vignati, E., Cavalli, F., Putaud, J. P., Larsen, B. R., Karl, M., Stenstrom, K., Genberg, J., Henne, S. and Dentener, F. (2011). Better constraints on sources of carbonaceous aerosols using a combined C-14 - macro tracer analysis in a European rural background site. *Atmospheric Chemistry and Physics* 11, 5685-5700.

Hallberg, A., Ogren, J. A., Noone, K. J., Heintzenberg, J., Berner, A., Solly, I., Kruisz, C., Reischl, G., Fuzzi, S., Facchini, M. C., Hansson, H. C., Wiedensohler, A. and Svenningsson, I. B. (1992). Phase Partitioning for Differernt Aerosol Species in Fog. *Tellus Series B-Chemical and Physical Meteorology* 44, 545-555.

Herckes, P., Valsaraj, K. T. and Collett, J. L., Jr. (2013). A review of observations of organic matter in fogs and clouds: Origin, processing and fate. *Atmospheric Research* 132, 434-449.

Hess, A., Iyer, H. and Malm, W. (2001). Linear trend analysis: a comparison of methods. *Atmospheric Environment* 35, 5211-5222.

Hileman, B. (1983). ACID FOG. *Environmental Science & Technology* 17, A117-A120.

Hoffmann, M. R. (1986). Laboratory studies of the Kinetics and Mechanisms of Reactions Important in Clouds and Fogs. *Abstracts of Papers of the American Chemical Society* 192, 4-CHED.

Houghton, H. G. (1955). On the Chemical Composition of Fog and Cloud Water. *Journal of Meteorology* 12, 355-357.

Isaksen, I. S. A., Granier, C., Myhre, G., Berntsen, T. K., Dalsoren, S. B., Gauss, M., Klimont, Z., Benestad, R., Bousquet, P., Collins, W., Cox, T., Eyring, V., Fowler, D., Fuzzi, S., Joeckel, P., Laj, P., Lohmann, U., Maione, M., Monks, P., Prevot, A. S. H., Raes, F., Richter, A., Rognerud, B., Schulz, M., Shindell, D., Stevenson, D. S., Storelvmo, T., Wang, W. C., van Weele, M., Wild, M. and Wuebbles, D.

(2009). Atmospheric composition change: Climate-Chemistry interactions. *Atmospheric Environment* 43, 5138-5192.

Jacobson, J. S. (1984). Effects of Acidic Aerosol, Fog, Mist and Rain on Crops and Trees. *Philosophical Transactions of the Royal Society of London Series B-Biological Sciences* 305, 327-338.

Jaenicke, R. (2005). Abundance of cellular material and proteins in the atmosphere. *Science* 308, 73-73.

Kanakidou, M., Seinfeld, J. H., Pandis, S. N., Barnes, I., Dentener, F. J., Facchini, M. C., Van Dingenen, R., Ervens, B., Nenes, A., Nielsen, C. J., Swietlicki, E., Putaud, J. P., Balkanski, Y., Fuzzi, S., Horth, J., Moortgat, G. K., Winterhalter, R., Myhre, C. E. L., Tsigaridis, K., Vignati, E., Stephanou, E. G. and Wilson, J. (2005). Organic aerosol and global climate modelling: a review. *Atmospheric Chemistry and Physics* 5, 1053-1123.

Kasper-Giebl, A. (2002). Control of solute concentrations in cloud and fog water by liquid water content. *Atmospheric Environment* 36, 1907-1908.

Kaufman, Y. J. and Koren, I. (2006). Smoke and pollution aerosol effect on cloud cover. *Science* 313, 655-658.

Keene, W. C., Pszenny, A. A. P., Galloway, J. N. and Hawley, M. E. (1986). Sea-salt Corrections and Interpretations of Constituent Ratios in Marine Precipitation. *Journal of Geophysical Research-Atmospheres* 91, 6647-6658.

Kroll, J. H. and Seinfeld, J. H. (2008). Chemistry of secondary organic aerosol: Formation and evolution of low-volatility organics in the atmosphere. *Atmospheric Environment* 42, 3593-3624.

Kulmala, M., Asmi, A., Lappalainen, H. K., Baltensperger, U., Brenguier, J. L., Facchini, M. C., Hansson, H. C., Hov, O., O'Dowd, C. D., Poeschl, U., Wiedensohler, A., Boers, R., Boucher, O., de Leeuw, G., van der Gon, H. A. C. D., Feichter, J., Krejci, R., Laj, P., Lihavainen, H., Lohmann, U., McFiggans, G., Mentel, T., Pilinis, C., Riipinen, I., Schulz, M., Stohl, A., Swietlicki, E., Vignati, E., Alves, C., Amann, M., Ammann, M., Arabas, S., Artaxo, P., Baars, H., Beddows, D. C. S., Bergstrom, R., Beukes, J. P., Bilde, M., Burkhart, J. F., Canonaco, F., Clegg, S. L., Coe, H., Crumeyrolle, S., D'Anna, B., Decesari, S., Gilardoni, S., Fischer, M., Fjaeraa, A. M., Fountoukis, C., George, C., Gomes, L.,

Halloran, P., Hamburger, T., Harrison, R. M., Herrmann, H., Hoffmann, T., Hoose, C., Hu, M., Hyvarinen, A., Horrak, U., Iinuma, Y., Iversen, T., Josipovic, M., Kanakidou, M., Kiendler-Scharr, A., Kirkevag, A., Kiss, G., Klimont, Z., Kolmonen, P., Komppula, M., Kristjansson, J. E., Laakso, L., Laaksonen, A., Labonnote, L., Lanz, V. A., Lehtinen, K. E. J., Rizzo, L. V., Makkonen, R., Manninen, H. E., McMeeking, G., Merikanto, J., Minikin, A., Mirme, S., Morgan, W. T., Nemitz, E., O'Donnell, D., Panwar, T. S., Pawlowska, H., Petzold, A., Pienaar, J. J., Pio, C., Plass-Duelmer, C., Prevot, A. S. H., Pryor, S., Reddington, C. L., Roberts, G., Rosenfeld, D., Schwarz, J., Seland, O., Sellegri, K., et al. (2011). General overview: European Integrated project on Aerosol Cloud Climate and Air Quality interactions (EUCAARI) - integrating aerosol research from nano to global scales. *Atmospheric Chemistry and Physics* 11, 13061-13143.

Köhler, H. (1936). The Nucleus in and the Growth of Hygroscopic Particles. *Transactions of the Faraday Society* 32, 1152-1162.

Laj, P., Fuzzi, S., Facchini, M. C., Orsi, G., Berner, A., Kruisz, C., Wobrock, W., Hallberg, A., Bower, K. N., Gallagher, M. W., Beswick, K. M., Colvile, R. N., Choularton, T. W., Nason, P. and Jones, B. (1997). Experimental evidence for in-cloud production of aerosol sulphate. *Atmospheric Environment* 31, 2503-2514.

Lange, C. A., Matschullat, J., Zimmermann, F., Sterzik, G. and Wienhaus, O. (2003). Fog frequency and chemical composition of fog water - a relevant contribution to atmospheric deposition in the eastern Erzgebirge, Germany. *Atmospheric Environment* 37, 3731-3739.

Lee, S., Liu, W., Wang, Y., Russell, A. G. and Edgerton, E. S. (2008). Source apportionment of PM2.5: Comparing PMF and CMB results for four ambient monitoriniz sites in the southeastern United States. *Atmospheric Environment* 42, 4126-4137.

Lewtas, J. (2007). Air pollution combustion emissions: Characterization of causative agents and mechanisms associated with cancer, reproductive, and cardiovascular effects. *Mutation Research-Reviews in Mutation Research* 636, 95-133.

Lim, Y. B., Tan, Y. and Turpin, B. J. (2013). Chemical insights, explicit chemistry, and yields of secondary organic aerosol from OH radical oxidation of methylglyoxal and glyoxal in the aqueous phase. *Atmospheric Chemistry and Physics* 13, 8651-8667.

Liu, W., Wang, Y. H., Russell, A. and Edgerton, E. S. (2005). Atmospheric aerosol over two urban-rural pairs in the southeastern United States: Chemical composition and possible sources. *Atmospheric Environment* 39, 4453-4470.

Lonati, G., Ozgen, S. and Giugliano, M. (2007). Primary and secondary carbonaceous species in PM2.5 samples in Milan (Italy). *Atmospheric Environment* 41, 4599-4610.

Lovett, G. M. (1984). Rates and Mechanisms of Cloud Water Deposition to a Subalpine Balsam Fir Forest. *Atmospheric Environment* 18, 361-371.

Mariani, L. (2009). Fog in the Po Valley:some meteo-climatic aspects. *Italian Journal of Agrometeorology* 3, 35-44.

Matta, E., Facchini, M. C., Decesari, S., Mircea, M., Cavalli, F., Fuzzi, S., Putaud, J. P. and Dell'Acqua, A. (2003). Mass closure on the chemical species in size-segregated atmospheric aerosol collected in an urban area of the Po Valley, Italy. *Atmospheric Chemistry and Physics* 3, 623-637.

Maurizi, A., Russo, F. and Tampieri, F. (2013). Local vs. external contribution to the budget of pollutants in the Po Valley (Italy) hot spot. *Science of the Total Environment* 458, 459-465.

McFiggans, G., Artaxo, P., Baltensperger, U., Coe, H., Facchini, M. C., Feingold, G., Fuzzi, S., Gysel, M., Laaksonen, A., Lohmann, U., Mentel, T. F., Murphy, D. M., O'Dowd, C. D., Snider, J. R. and Weingartner, E. (2006). The effect of physical and chemical aerosol properties on warm cloud droplet activation. *Atmospheric Chemistry and Physics* 6, 2593-2649.

Munger, J. W., Jacob, D. J., Waldman, J. M. and Hoffmann, M. R. (1983). Fogwater chemistry in an Urban Atmosphere. *Journal of Geophysical Research-Oceans and Atmospheres* 88, 5109-5121.

Noone, K. J., Ogren, J. A., Hallberg, A., Heintzenberg, J., Strom, J., Hansson, H. C., Svenningsson, B., Wiedensohler, A., Fuzzi, S., Facchini, M. C., Arends, B. G. and Berner, A. (1992). CHANGES IN AEerosol Size and Phase Distributions Due to Physical and Chemical Processes in Fog. *Tellus Series B-Chemical and Physical Meteorology* 44, 489-504.

Onasch, T. B., Trimborn, A., Fortner, E. C., Jayne, J. T., Kok, G. L., Williams, L. R., Davidovits, P. and Worsnop, D. R. (2012). Soot Particle Aerosol Mass Spectrometer: Development, Validation, and Initial Application. *Aerosol Science and Technology* 46, 804-817.

Pandis, S. N., Seinfeld, J. H. and Pilinis, C. (1990). The Smog-Fog_Smog Cycle and Acid Deposition. *Journal of Geophysical Research-Atmospheres* 95, 18489-18500.

Pennanen, A. S., Sillanpaa, M., Hillamo, R., Quass, U., John, A. C., Branis, M., Hunova, I., Meliefste, K., Janssen, N. A. H., Koskentalo, T., Castano-Vinyals, G., Bouso, L., Chalbot, M. C., Kavouras, I. G. and Salonen, R. O. (2007). Performance of a high-volume cascade impactor in six European urban environments: Mass measurement and chemical characterization of size-segregated particulate samples. *Science of the Total Environment* 374, 297-310.

Pernigotti, D., Georgieva, E., Thunis, P. and Bessagnet, B. (2012). Impact of meteorology on air quality modeling over the Po valley in northern Italy. *Atmospheric Environment* 51, 303-310.

Pope, C. A. and Dockery, D. W. (2006). Health effects of fine particulate air pollution: Lines that connect. *Journal of the Air & Waste Management Association* 56, 709-742.

Putaud, J. P., Raes, F., Van Dingenen, R., Bruggemann, E., Facchini, M. C., Decesari, S., Fuzzi, S., Gehrig, R., Huglin, C., Laj, P., Lorbeer, G., Maenhaut, W., Mihalopoulos, N., Mullller, K., Querol, X., Rodriguez, S., Schneider, J., Spindler, G., ten Brink, H., Torseth, K. and Wiedensohler, A. (2004). European aerosol phenomenology-2: chemical characteristics of particulate matter at kerbside, urban, rural and background sites in Europe. *Atmospheric Environment* 38, 2579-2595.

Puxbaum, H., Caseiro, A., Sanchez-Ochoa, A., Kasper-Giebl, A., Claeys, M., Gelencser, A., Legrand, M., Preunkert, S. and Pio, C. (2007). Levoglucosan levels at background sites in Europe for assessing the impact of biomass combustion on the European aerosol background. *Journal of Geophysical Research-Atmospheres* 112.

Rinaldi, M., Emblico, L., Decesari, S., Fuzzi, S., Facchini, M. C. and Librando, V. (2007). Chemical characterization and source apportionment of size-segregated aerosol collected at an urban site in sicily. *Water Air and Soil Pollution* 185, 311-321.

Rodriguez, S., Van Dingenen, R., Putaud, J. P., Dell'Acqua, A., Pey, J., Querol, X., Alastuey, A., Chenery, S., Ho, K. F., Harrison, R. M., Tardivo, R., Scarnato, B. and Gemelli, V. (2007). A study on the relationship between mass concentrations, chemistry and number size distribution of urban fine aerosols in Milan, Barcelona and London. *Atmospheric Chemistry and Physics* 7, 2217-2232.

Rosenfeld, D., Lohmann, U., Raga, G. B., O'Dowd, C. D., Kulmala, M., Fuzzi, S., Reissell, A. and Andreae, M. O. (2008). Flood or drought: How do aerosols affect precipitation? *Science* 321, 1309-1313.

Sachweh, M. and Koepke, P. (1995). Radiation Fog and Urban Climate. *Geophysical Research Letters* 22, 1073-1076.

Saxena, V. K. and Lin, N. H. (1990). Cloud Chemistry Measurements and Estimates of Acidic Deposition on an Above Cloudbase Coniferous Forest. *Atmospheric Environment Part a-General Topics* 24, 329-352.

Schemenauer, R. S. (1986). Acidic Deposition to Forests: The 1985 Chemistry of High Elevation Fog (CHEF) Project. *Atmosphere-Ocean* 24, 303-328.

Seinfeld, J. and Pandis, S. (1998). *Atmospheric Chemistry and Physics*. John Wiley & Sons: New York, USA.

Spindler, G., Gnauk, T., Gruener, A., Iinuma, Y., Mueller, K., Scheinhardt, S. and Herrmann, H. (2012). Size-segregated characterization of PM10 at the EMEP site Melpitz (Germany) using a five-stage impactor: a six year study. *Journal of Atmospheric Chemistry* 69, 127-157.

Straub, D. J., Hutchings, J. W. and Herckes, P. (2012). Measurements of fog composition at a rural site. *Atmospheric Environment* 47, 195-205.

Svenningsson, I. B., Hansson, H. C., Wiedensohler, A., Ogren, J. A., Noone, K. J. and Hallberg, A. (1992). Hygroscopic Growth of Aerosol Particles in the Po Valley. *Tellus Series B-Chemical and Physical Meteorology* 44, 556-569.

Szidat, S., Jenk, T. M., Synal, H. A., Kalberer, M., Wacker, L., Hajdas, I., Kasper-Giebl, A. and Baltensperger, U. (2006). Contributions of fossil fuel, biomass-burning, and biogenic emissions to carbonaceous aerosols in Zurich as traced by C-14. *Journal of Geophysical Research-Atmospheres* 111.

Tan, Y., Lim, Y. B., Altieri, K. E., Seitzinger, S. P. and Turpin, B. J. (2012). Mechanisms leading to oligomers and SOA through aqueous photooxidation: insights from OH radical oxidation of acetic acid and methylglyoxal. *Atmospheric Chemistry and Physics* 12, 801-813.

van Oldenborgh, G. J., Yiou, P. and Vautard, R. (2010). On the roles of circulation and aerosols in the decline of mist and dense fog in Europe over the last 30 years. *Atmospheric Chemistry and Physics* 10, 4597-4609.

Vautard, R., Yiou, P. and van Oldenborgh, G. J. (2009). Decline of fog, mist and haze in Europe over the past 30 years. *Nature Geoscience* 2, 115-119.

Waldman, J. M. and Hoffmann, M. R. (1987). Depositional Aspects of Pollutant Behavior in Fog and Intercepted Clouds. *Advances in Chemistry Series*, 79-129.

Waldman, J. M., Munger, J. W., Jacob, D. J., Flagan, R. C., Morgan, J. J. and Hoffmann, M. R. (1982). CHEMICAL-COMPOSITION OF ACID FOG. *Science* 218, 677-680.

Waldman, J. M., Munger, J. W., Jacob, D. J. and Hoffmann, M. R. (1985). Chemical Characterization of Stratus Cloudwater and its Role as a Vector for Pollutant Deposition in a Los Angeles Pine Forest. *Tellus Series B-Chemical and Physical Meteorology* 37, 91-108.

Watson, J. G. and Chow, J. C. (2002). A wintertime PM2.5 episode at the fresno, CA, supersite. *Atmospheric Environment* 36, 465-475.

Weimer, S., Mohr, C., Richter, R., Keller, J., Mohr, M., Prevot, A. S. H. and Baltensperger, U. (2009). Mobile measurements of aerosol number and volume size distributions in an Alpine valley: Influence of traffic versus wood burning. *Atmospheric Environment* 43, 624-630.

Whiteaker, J. R., Suess, D. T. and Prather, K. A. (2002). Effects of meteorological conditions on aerosol composition and mixing state in Bakersfield, CA. *Environmental Science & Technology* 36, 2345-2353.

Wisniewski, J. (1982). The Potential Acidity Associated with Dews, Frosts and Fogs. *Water Air and Soil Pollution* 17, 361-377.

Wobrock, W., Schell, D., Maser, R., Jaeschke, W., Georgii, H. W., Wieprecht, W., Arends, B. G., Mols, J. J., Kos, G. P. A., Fuzzi, S., Facchini, M. C., Orsi, G., Berner, A., Solly, I., Kruisz, C., Svenningsson, I. B., Wiedensohler, A., Hansson, H. C., Ogren, J. A., Noone, K. J., Hallberg, A., Pahl, S., Schneider, T., Winkler, P., Winiwarter, W., Colvile, R. N., Choularton, T. W., Flossmann, A. I. and Borrmann, S. (1994). The Kleiner-Feldberg Cloud Experiment 1990 - an Overview. *Journal of Atmospheric Chemistry* 19, 3-35.

Yttri, K. E., Dye, C., Braathen, O. A., Simpson, D. and Steinnes, E. (2009). Carbonaceous aerosols in Norwegian urban areas. *Atmospheric Chemistry and Physics* 9, 2007-2020.

Yu, G., Bayer, A. R., Galloway, M. M., Korshavn, K. J., Fry, C. G. and Keutsch, F. N. (2011). Glyoxal in Aqueous Ammonium Sulfate Solutions: Products, Kinetics and Hydration Effects. *Environmental Science & Technology* 45, 6336-6342.

Zappoli, S., Andracchio, A., Fuzzi, S., Facchini, M. C., Gelencser, A., Kiss, G., Krivacsy, Z., Molnar, A., Meszaros, E., Hansson, H. C., Rosman, K. and Zebuhr, Y. (1999). Inorganic, organic and macromolecular components of fine aerosol in different areas of Europe in relation to their water solubility. *Atmospheric Environment* 33, 2733-2743.

Zhang, L., Vet, R., Wiebe, A., Mihele, C., Sukloff, B., Chan, E., Moran, M. D. and Iqbal, S. (2008). Characterization of the size-segregated water-soluble inorganic ions at eight Canadian rural sites. *Atmospheric Chemistry and Physics* 8, 7133-7151.

Zhang, Q., Jimenez, J. L., Canagaratna, M. R., Allan, J. D., Coe, H., Ulbrich, I., Alfarra, M. R., Takami, A., Middlebrook, A. M., Sun, Y. L., Dzepina, K., Dunlea, E., Docherty, K., DeCarlo, P. F., Salcedo, D., Onasch, T., Jayne, J. T., Miyoshi, T., Shimono, A., Hatakeyama, S., Takegawa, N., Kondo, Y., Schneider, J., Drewnick, F., Borrmann, S., Weimer, S., Demerjian, K., Williams, P., Bower, K., Bahreini, R., Cottrell, L., Griffin, R. J., Rautiainen, J., Sun, J. Y., Zhang, Y. M. and Worsnop, D. R. (2007). Ubiquity and dominance of oxygenated species in organic aerosols in anthropogenically-influenced Northern Hemisphere midlatitudes. *Geophysical Research Letters* 34.

Zhang, X., Hecobian, A., Zheng, M., Frank, N. H. and Weber, R. J. (2010). Biomass burning impact on PM2.5 over the southeastern US during 2007: integrating chemically speciated FRM filter

measurements, MODIS fire counts and PMF analysis. *Atmospheric Chemistry and Physics* 10, 6839-6853.

Zhang, X. F., Smith, K. A., Worsnop, D. R., Jimenez, J., Jayne, J. T. and Kolb, C. E. (2002). A numerical characterization of particle beam collimation by an aerodynamic lens-nozzle system: Part I. An individual lens or nozzle. *Aerosol Science and Technology* 36, 617-631.

Zhang, X. F., Smith, K. A., Worsnop, D. R., Jimenez, J. L., Jayne, J. T., Kolb, C. E., Morris, J. and Davidovits, P. (2004). Numerical characterization of particle beam collimation: Part II - Integrated aerodynamic-lens-nozzle system. *Aerosol Science and Technology* 38, 619-638.

List of frequently used abbreviations

^{1}H-NMR = Proton-Nuclear Magnetic Resonance Spectroscopy

BC = Black Carbon

BO = Bologna

CCN = Cloud Condensation Nuclei

D_a = Aerodynamic Diameter

D_{va} = Vacuum Aerodynamic Diameter

EC = Elemental Carbon

HR-ToF-AMS = High Resolution Time of Flight Aerosol Mass Spectrometer

IC = Ion Chromatography

IS = Ionic Strenght

LWC = Liquid Water Content

MSA = Methane Sulfonic Acid

OA = Organic Aerosol

OM = Organic Matter

PBL = Planet Boundary Layer

PM1 = Particulate Matter with D_a<1µm

PM1.2 = Particulate Matter with D_a<1.2µm

PM10 = Particulate Matter with D_a<10µm

POA = Primary Organic Aerosol

RH = Relative Humidity

SOA = Secondary Organic Aerosol

SPC = San Pietro Capofiume

TC = Total Carbon

VOC = Volatile Organic Compound

WINC = Water Insoluble Carbon

WINCM = Water Insoluble Carbonaceous Matter

WSOC = Water Soluble Organic Carbon

WSOM = Water Soluble Organic Matter